# Basics of Ion Traps

G. Werth
Johannes Gutenberg University
Mainz

# Why trapping?

„A single trapped particle floating forever at rest in free space would be the ideal object for precision measurements“

(H.Dehmelt)

Ion traps provide the closest approximation to this ideal

# Pioneers of ion trapping: Hans Dehmelt and Wolfgang Paul (Nobel price 1989)

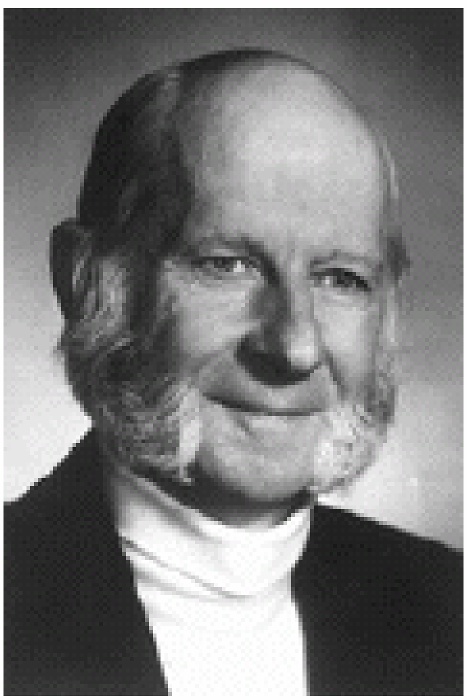 

# Trapping of charged particles by electromagnetic fields

***Required*: 3-dimensional force towards center**

$$F = -e \text{ grad } U$$

***Convenience:* harmonic force** $F \propto x,y,z$

$\rightarrow$ $$U = ax^2 + by^2 + cz^2$$

***Laplace equ.:*** $\Delta(eU) = 0$

$\rightarrow$ **a,b,c can not be all positive**

***Convenience:* rotational symmetry**

$\rightarrow$ $$\boxed{U = (U_0/r_0^2)(x^2+y^2-2z^2)}$$

**Quadrupole potential**

**Equipotentials: Hyperboloids of revolution**

Problem:
No 3-dimensional potential minimum because of different sign of the coefficients in the quadrupole potential

Solutions:

- Application of r.f. voltage: dynamical trapping

  Paul trap

- d.c. voltage + magnetic field in z-direction:

  Penning trap

# The ideal 3-dimensional Paul trap

**Potential: $U=(U_0+V_0\cos\Omega t)(r^2-2z^2)/d_0^2$**

**Using dimensionless parameters a, q**

$$a_z = \frac{8eU_o}{md_0^2\Omega^2} = -2a_r$$

$$q_z = \frac{4eV_0}{md_0^2\Omega^2} = 2q_r$$

$$u = r, z$$

$$\tau = \Omega t / 2$$

U: DC

V: RF

m: mass of particle

e: charge of particle

d: distance between el

$$d = \sqrt{\frac{1}{2}r_0^2 + z_0^2}$$

Ω: RF frequency

We can write the equation of motion from F=Δ(eU) and obtain

$$\frac{d^2u}{dt^2} + (a - 2q\cos 2\tau)u = 0$$

*Mathieu differential equation*

# Electrode configuration for Paul traps

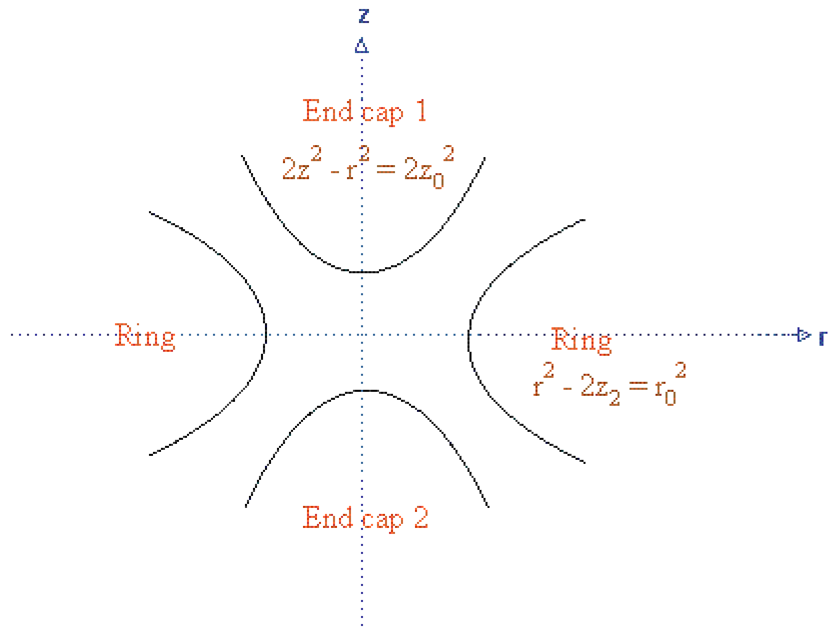


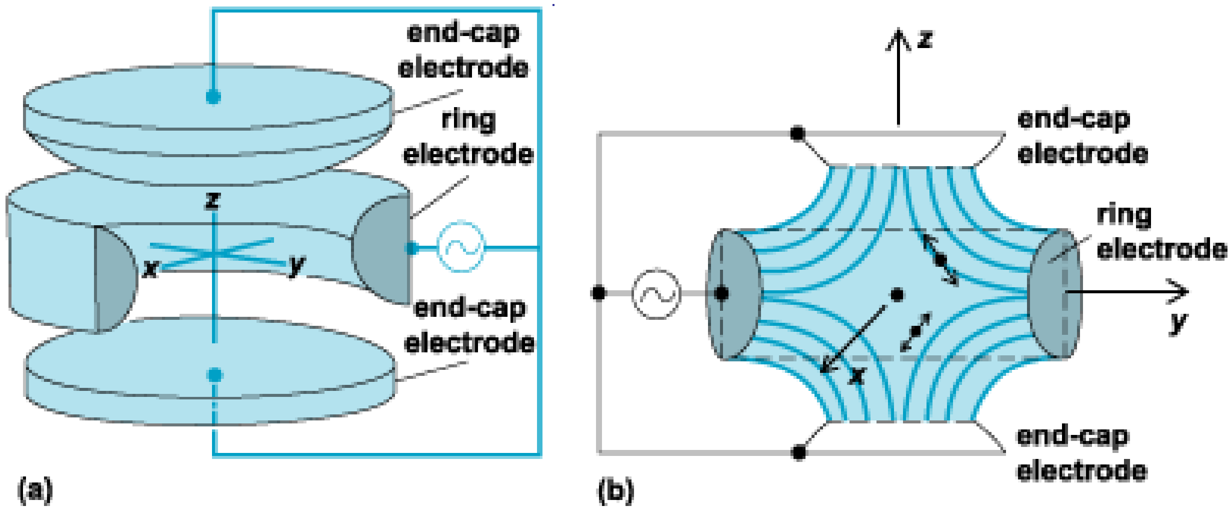


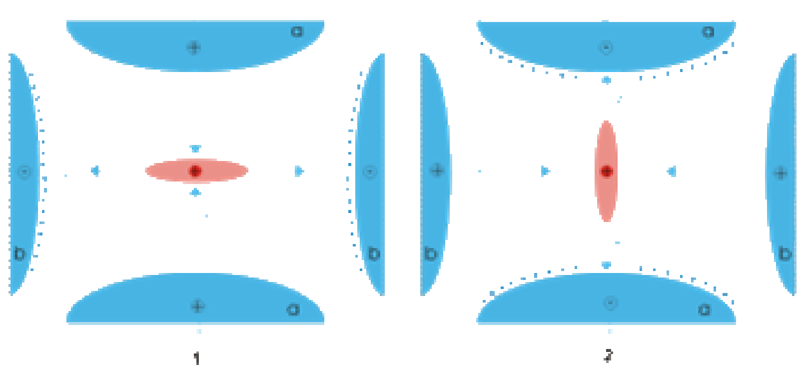

# Paul trap of 1 cm diameter (Univ. of Mainz)

# Wire trap with transparent electrodes

**(UBC Vancouver)**

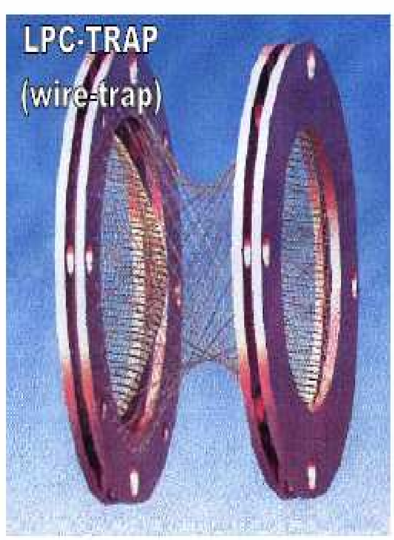

## Mathieu differential equation:

**The solutions are well known. Depending on the size of the parameters *a* and *q*, the amplitude *u* remains finite in time or goes to infinity.**

**When *u* remains finite :stable solutions**
**When *u* goes to infinity: unstable solutions**

**Areas of stable confinement (shaded) for stable confinement in axial direction of a Paul trap**

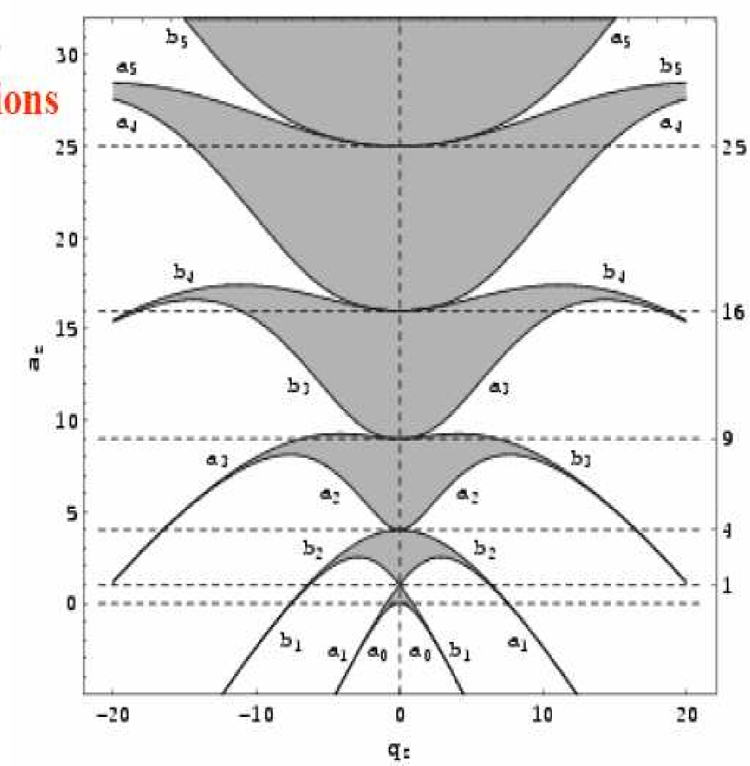


Similar for the radial direction
(with opposite sign of a)

# Stability in 3 dimension
# when radial and axial  domains overlap

Overlapping areas of stable confinemt in axial and radial direction for a Paul trap.

Defines operational parameter for stable trapping.

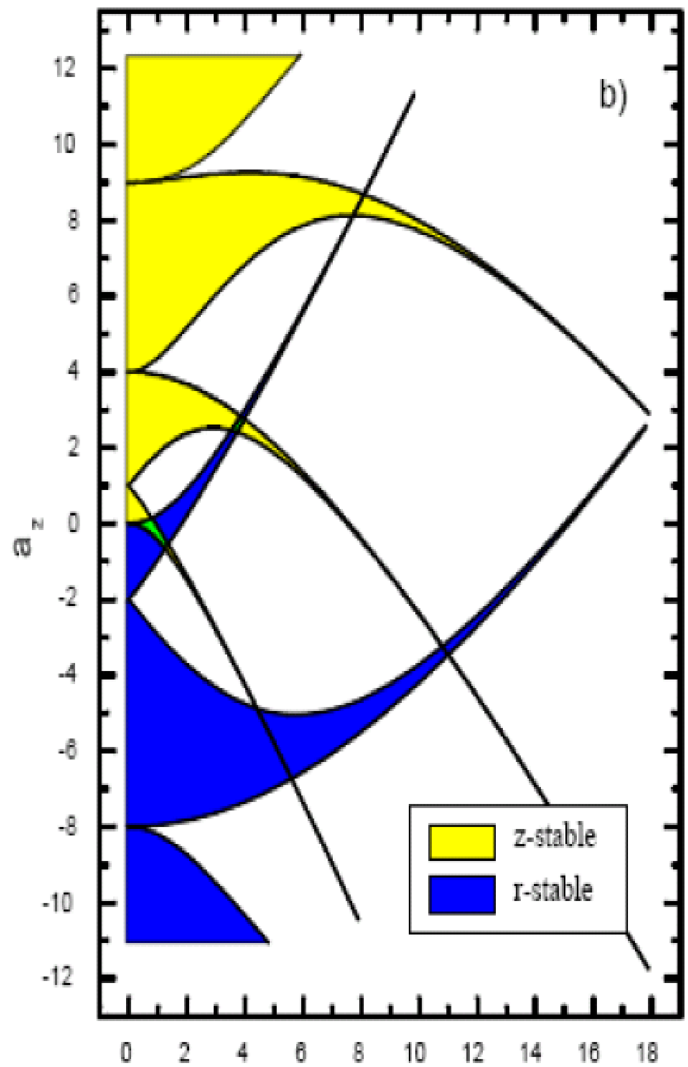

# First stable region of a Paul trap

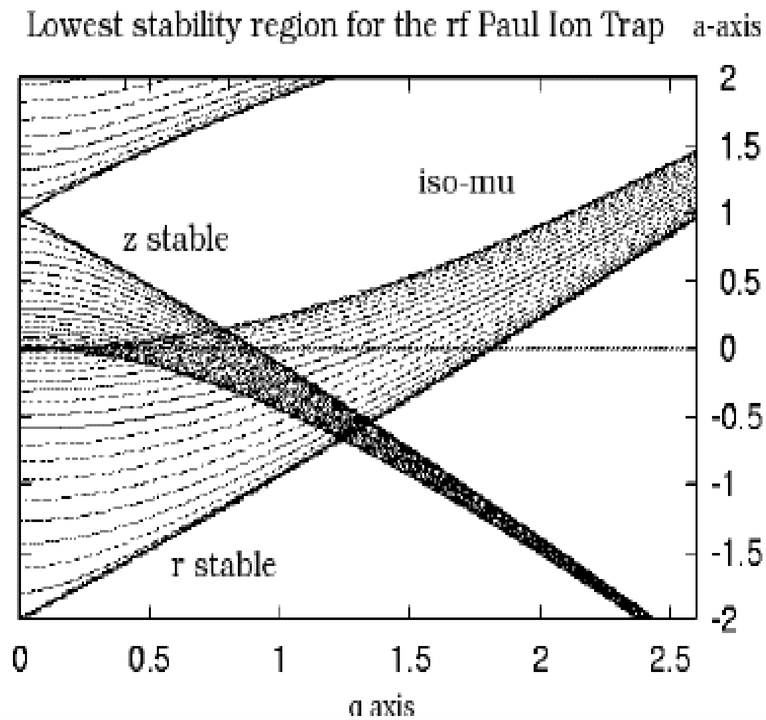


First region of stability of the Paul trap.

The ○ shows a stable parameter set in RF-only mode (hence with no DC off-set)

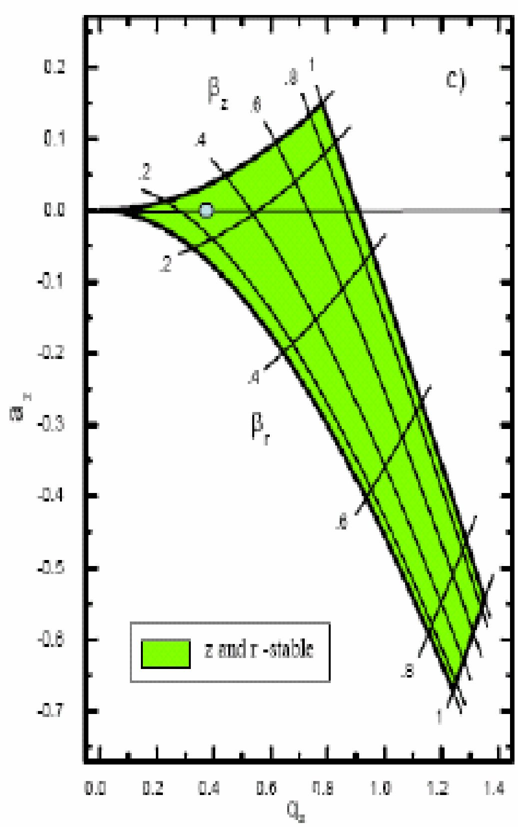

**solution of the equation of motion:**

$$u(t) = A\sum_{n=0}^{\infty} c_{2n} \cos(\beta + 2n)(\Omega t / 2)$$

$$\beta = \beta(a, q)$$

$$c_{2n} = f(a, q)$$

**Approximate solution for a,q<<1:**

$$u(t) = A[1 - (q/2)\cos \omega t]\cos \Omega t$$

$\omega = \beta/2\Omega$ $\beta^2 = a + q^2/2$

**This is a harmonic oscillation at frequency Ω (micromotion) modulated by an oscillation at frequency ω (macromotion)**

# Time averaged potential depth:

$$\overline{D_i} = \frac{m}{8}\Omega^2 r_0^2 \beta_i^2$$

**<u>Numerical example:</u>**

**m=50**

**$\Omega/2\pi$=1 MHz**

**$r_0$=1 cm**

**ß=0.3**

**D = 25 eV**

**Maximum ion density, when space charge potential equals trapping potential depth**

**$n_{max}$≈1o$^6$ cm$^{-3}$**

# Ion oscillation frequencies in a Paul Trap

$$\omega_z \approx (a_z + \frac{q_z^2}{2})\Omega$$

$$\omega_x = \omega_y = \omega_r \approx (a_r + \frac{q_r^2}{2})\Omega$$

$$\omega_{z,r} = m\Omega \pm n\,\omega_{z,r}$$

$$m, n = 0,1,2\ldots$$

# Mechanical analogon:
# Rotating saddle

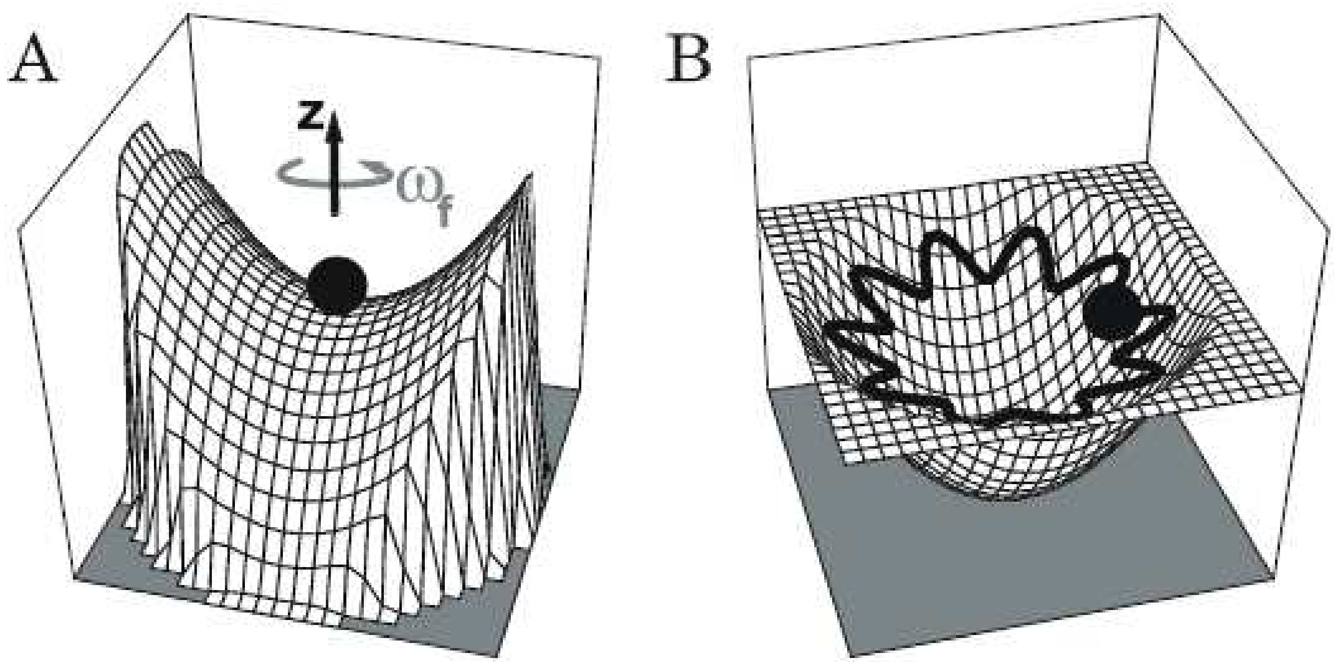


**Figure 1.1:** The effect of rotating the potential in part A, is a pseudopotential well which is illustrated in part B. The particle motion in the pseudopotential is indicated by the black line. The motion is a combination of a secular motion in the pseudopotential and a small amplitude micromotion at the frequency of rotation $\omega_f$.

# Ion motion at different operating conditions

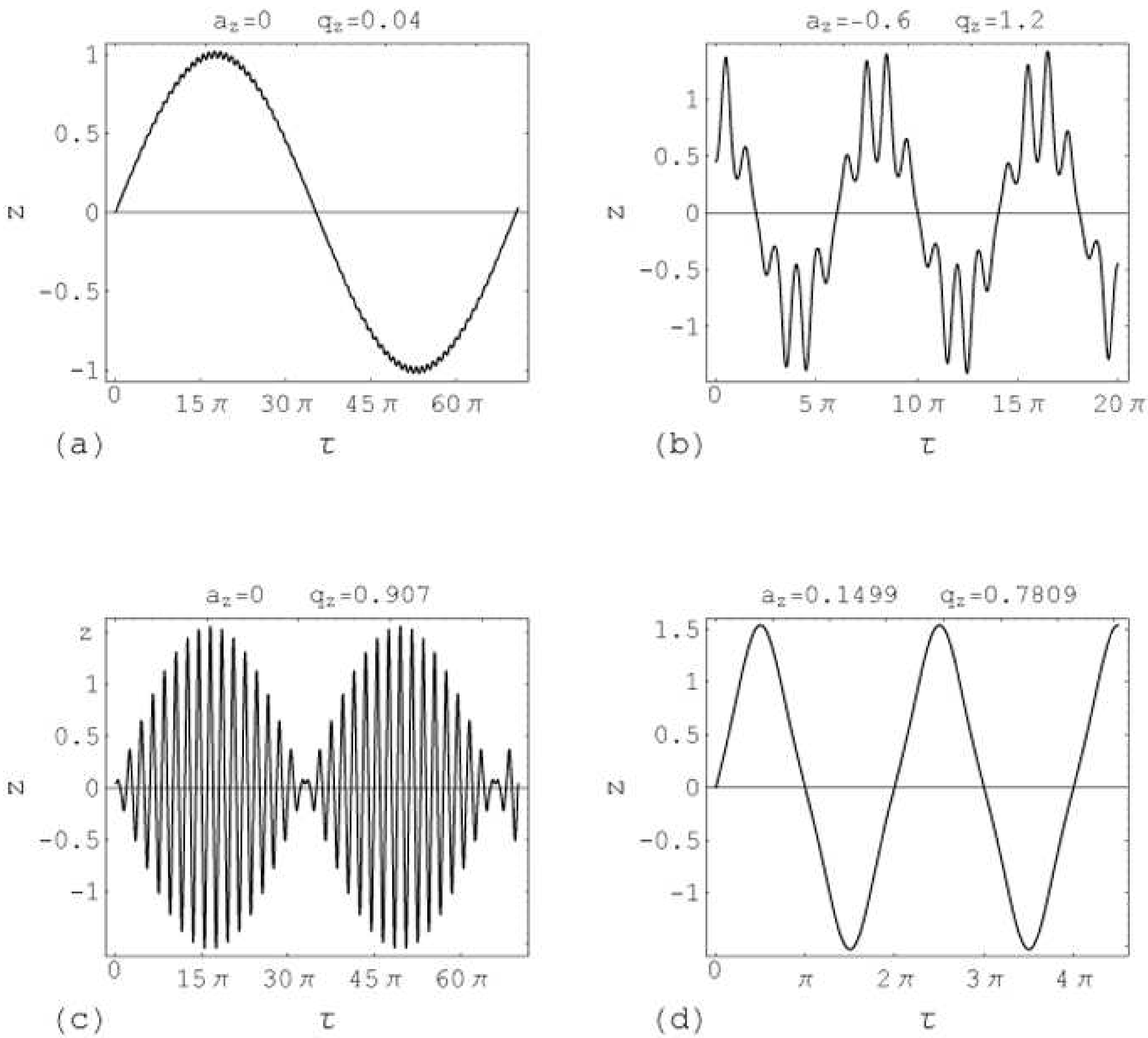

**Trajectory of a single microscopic particle**

(Wuerker 1959)

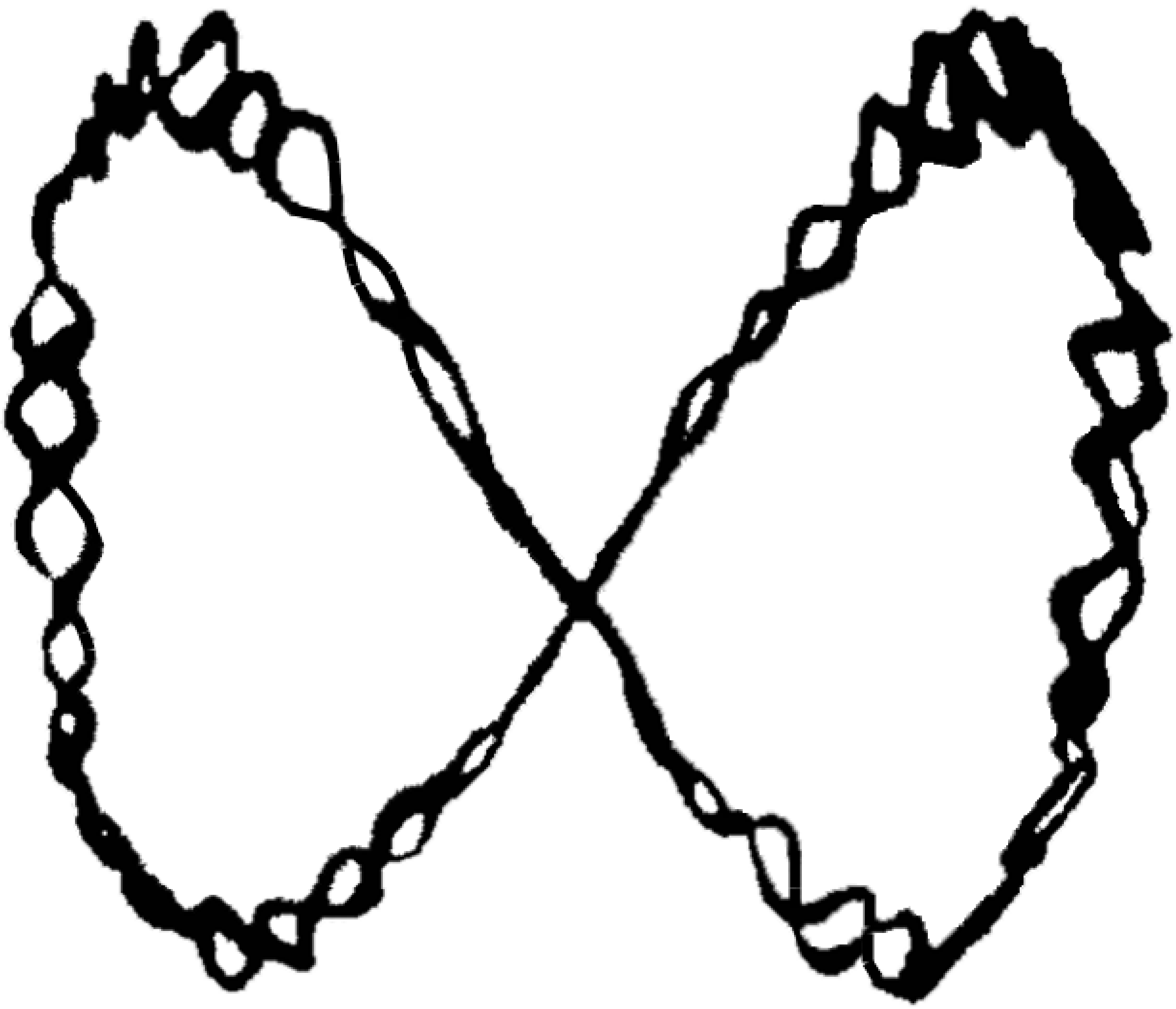

**Observed ion oscillation frequencies**

Excitation of motion by an additional weak rf field leads to ion loss at resonances

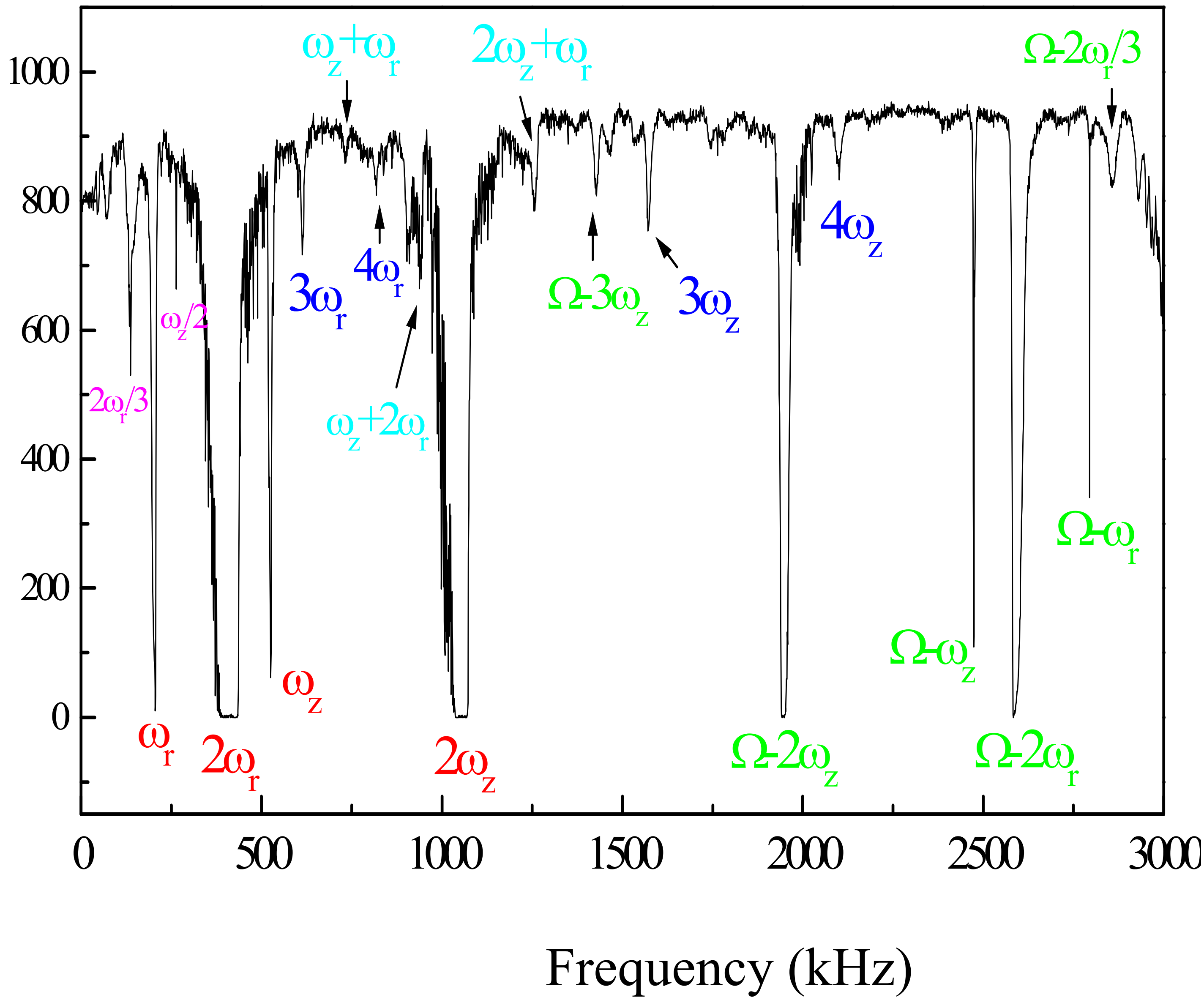

# Excitation of a motional frequency with different rf amplitudes

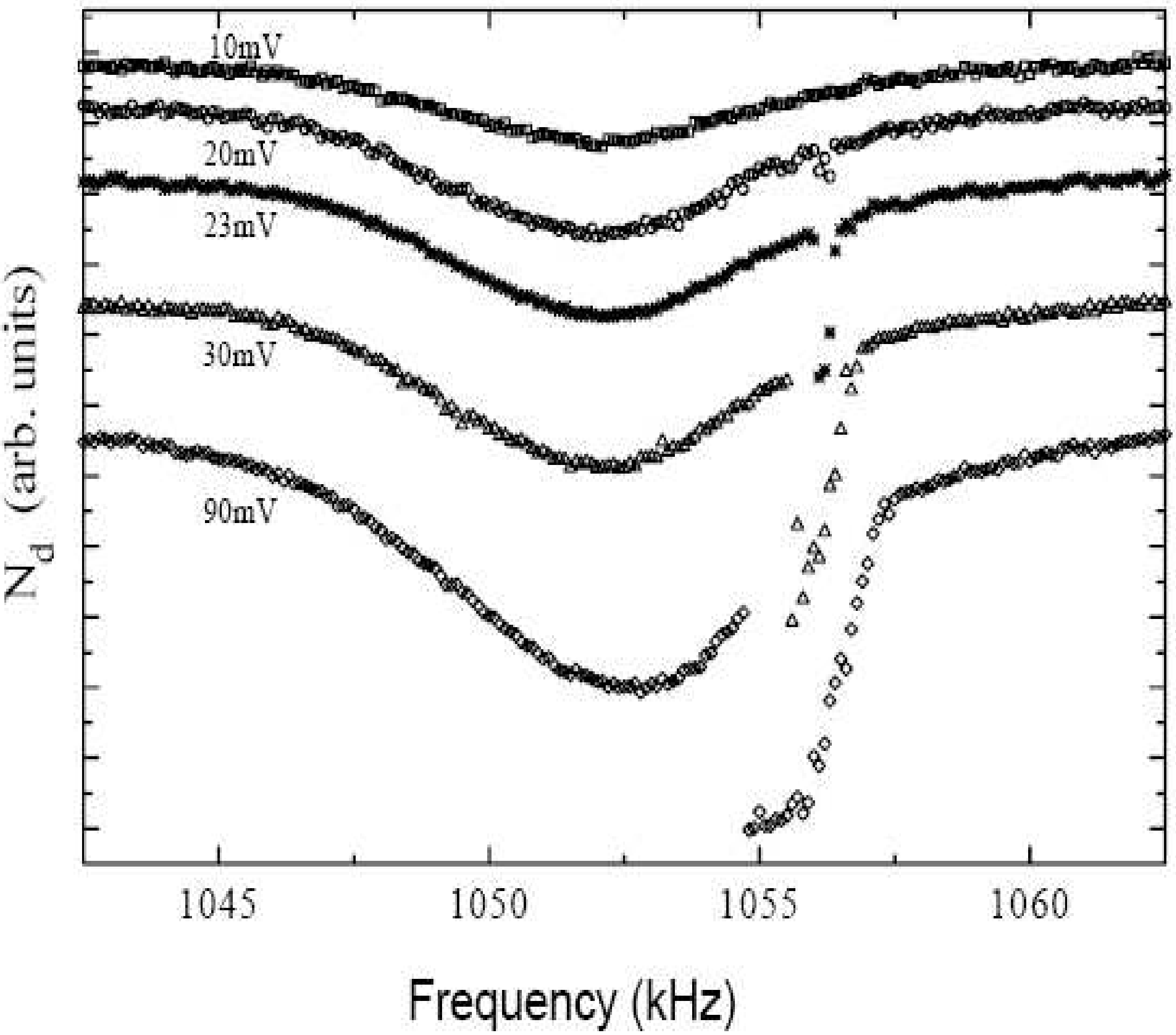

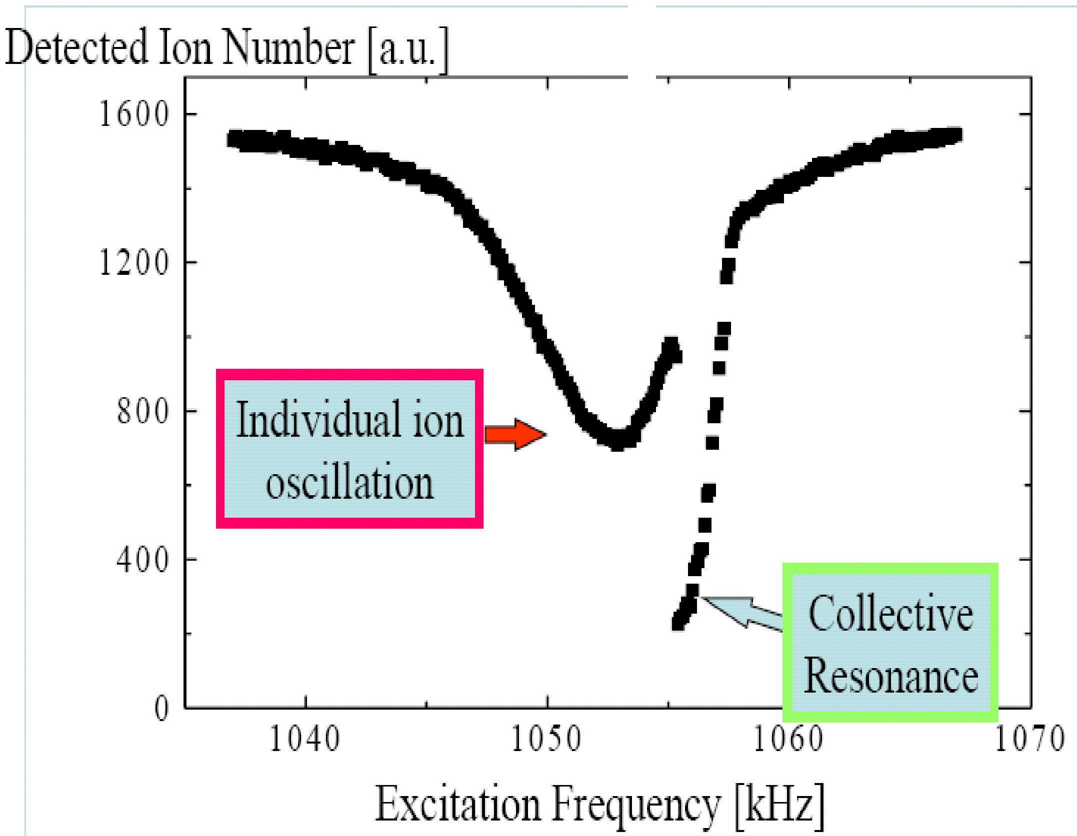
Detected Ion Number [a.u.]
1600
1200
800
400
0
1040
1050
1060
1070
Excitation Frequency [kHz]
Individual ion oscillation
Collective Resonance

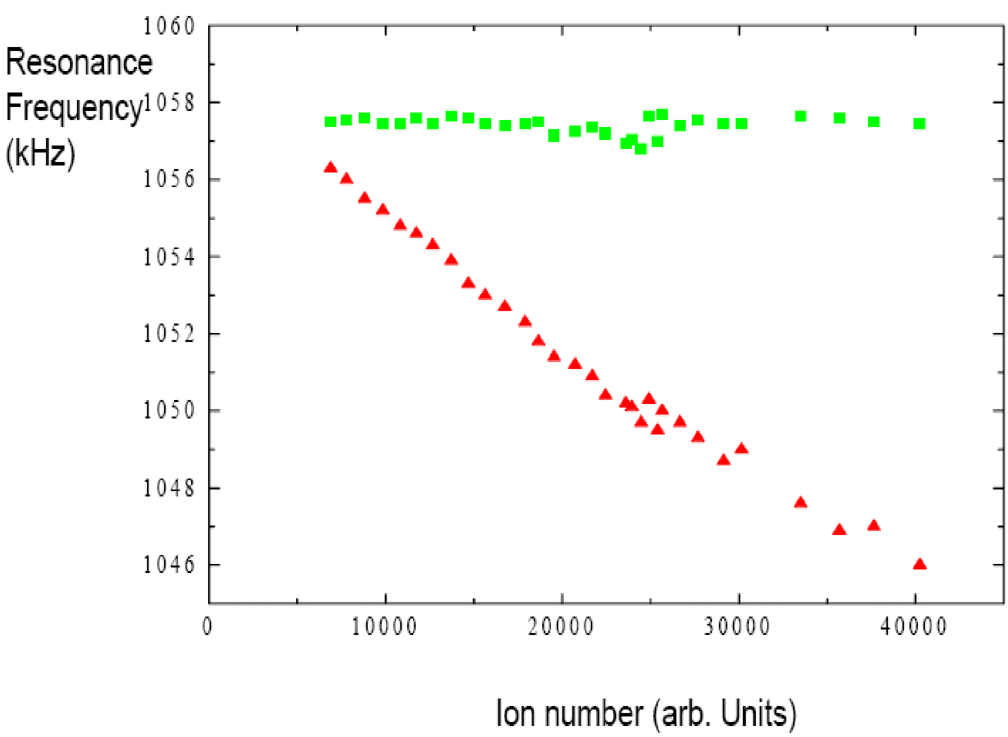
Resonance Frequency (kHz)
1060
1058
1056
1054
1052
1050
1048
1046
0
10000
20000
30000
40000
Ion number (arb. Units)

Interaction in ion cloud characterized by plasma parameter

$$\boxed{\Gamma = \frac{1}{4\pi\varepsilon_0}\frac{q^2/r}{k_B T}}$$

**Γ<1:** gaseous behaviour→ Individual particles model with small perturbation

**Γ>1:** liquid like behaviour

**Γ>176:** strong interaction regime: crystallization

# Calculated spatial distribution of an ion cloud at different temperatures

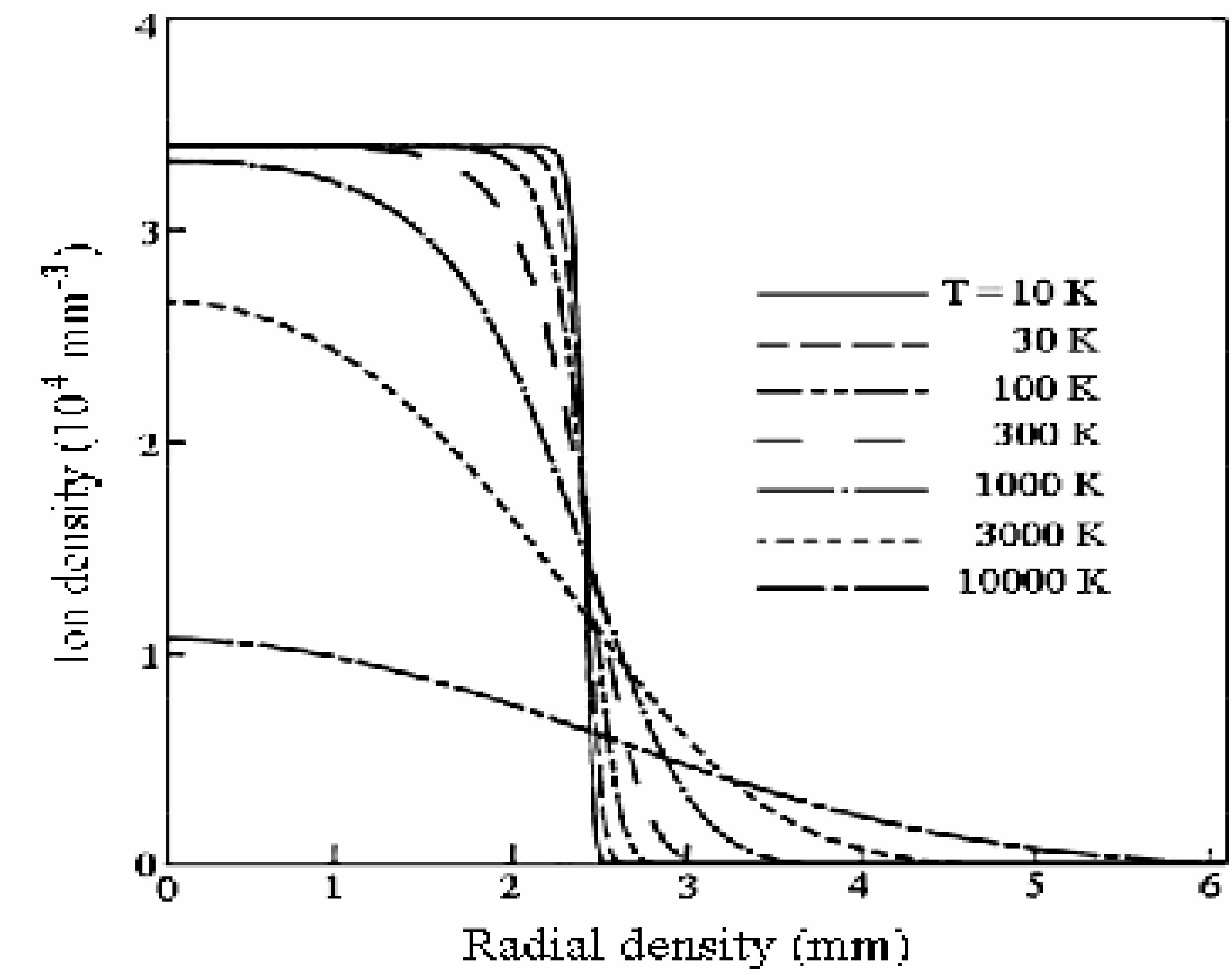

# Measured density distribution of trapped ion cloud

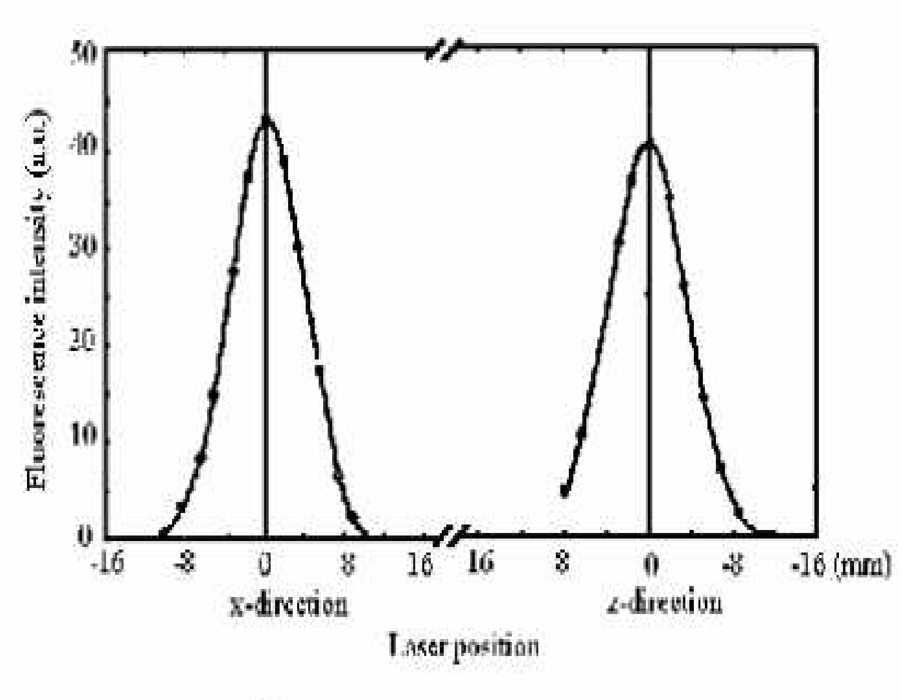


Uncooled ion cloud

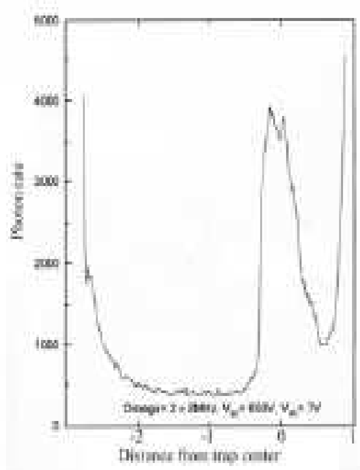


Laser cooled ion cloud

Maximum density limited by space charge to ~ $10^6$ $cm^{-3}$

# Influence of trap imperfections

**expansion of the trapping potential in spherical harmonics**

$$\Phi(|r|) = U_0 \sum_{k=1}^{\infty} C_k \left(\frac{r}{r_0}\right)^k P_k(\cos\theta)$$

## Consequence:
## Asymmetry of motional resonances

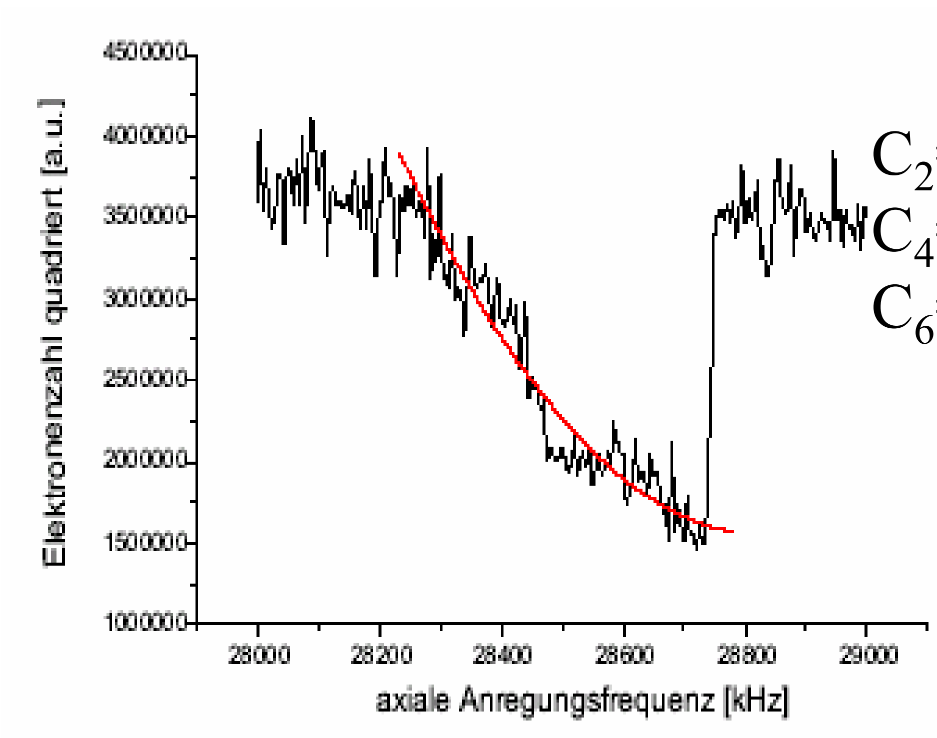


$C_2 = 1$
$C_4 = -7.5\ 10^{-2}$
$C_6 = -8\ 10^{-4}$

# Instability of ion motion

**Ion trajectories become unstable**
**when the axial and radial macromotion frequencies $\omega_r$, $\omega_z$**
**and the micromotion frequency $\Omega$ are related as**

$$n_r\omega_r + n_z\omega_z = m\Omega$$

**$n_r$, $n_z$, m integer,**
**$n_r + n_z = k$,      2k=order of perturbing potential**

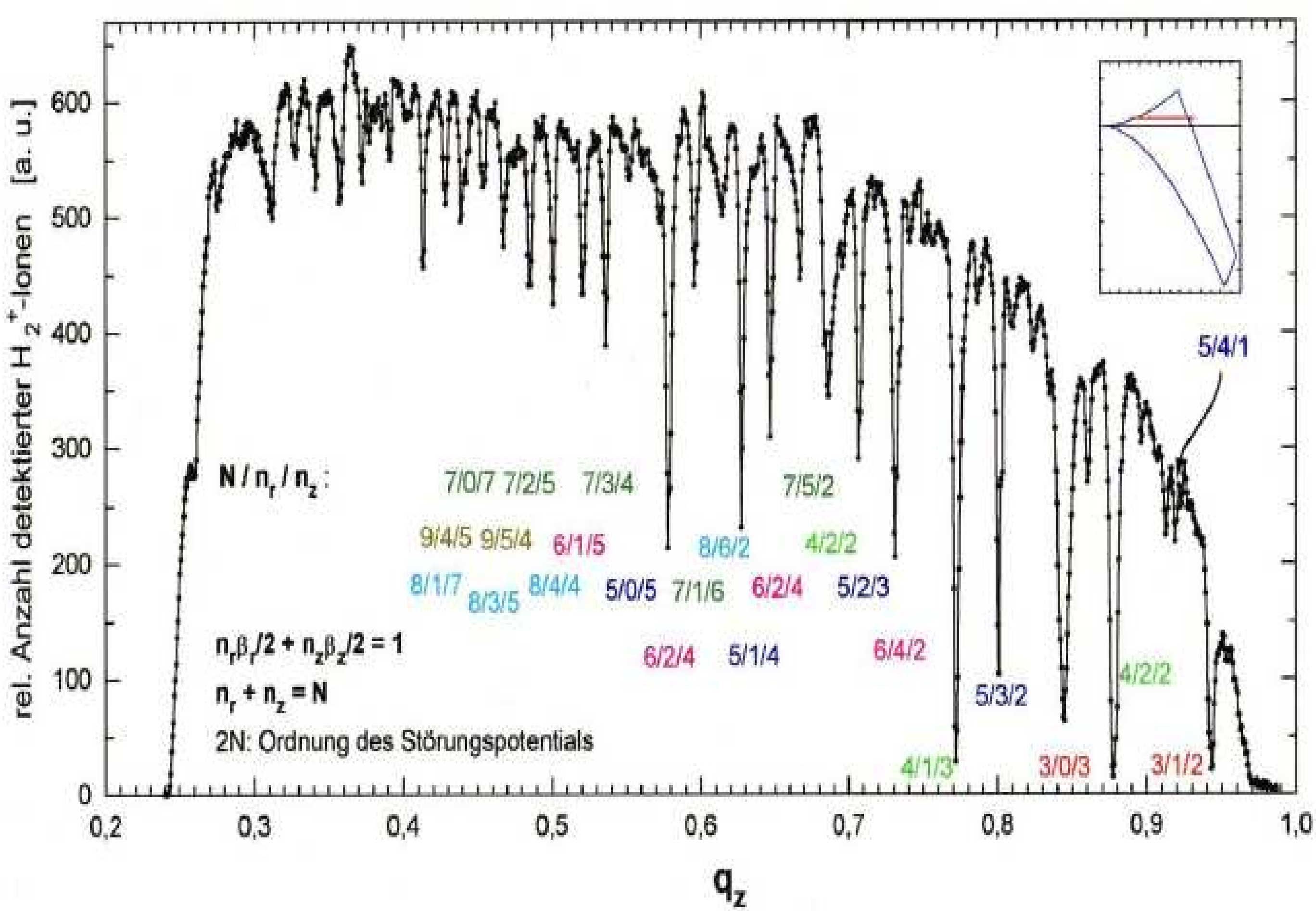


Instabilities occur when $n_r\omega_r + n_z\omega_z = \Omega$,
caused by higher order contributions to the quadrupolar trap poten

# Measured ion density in a real Paul trap

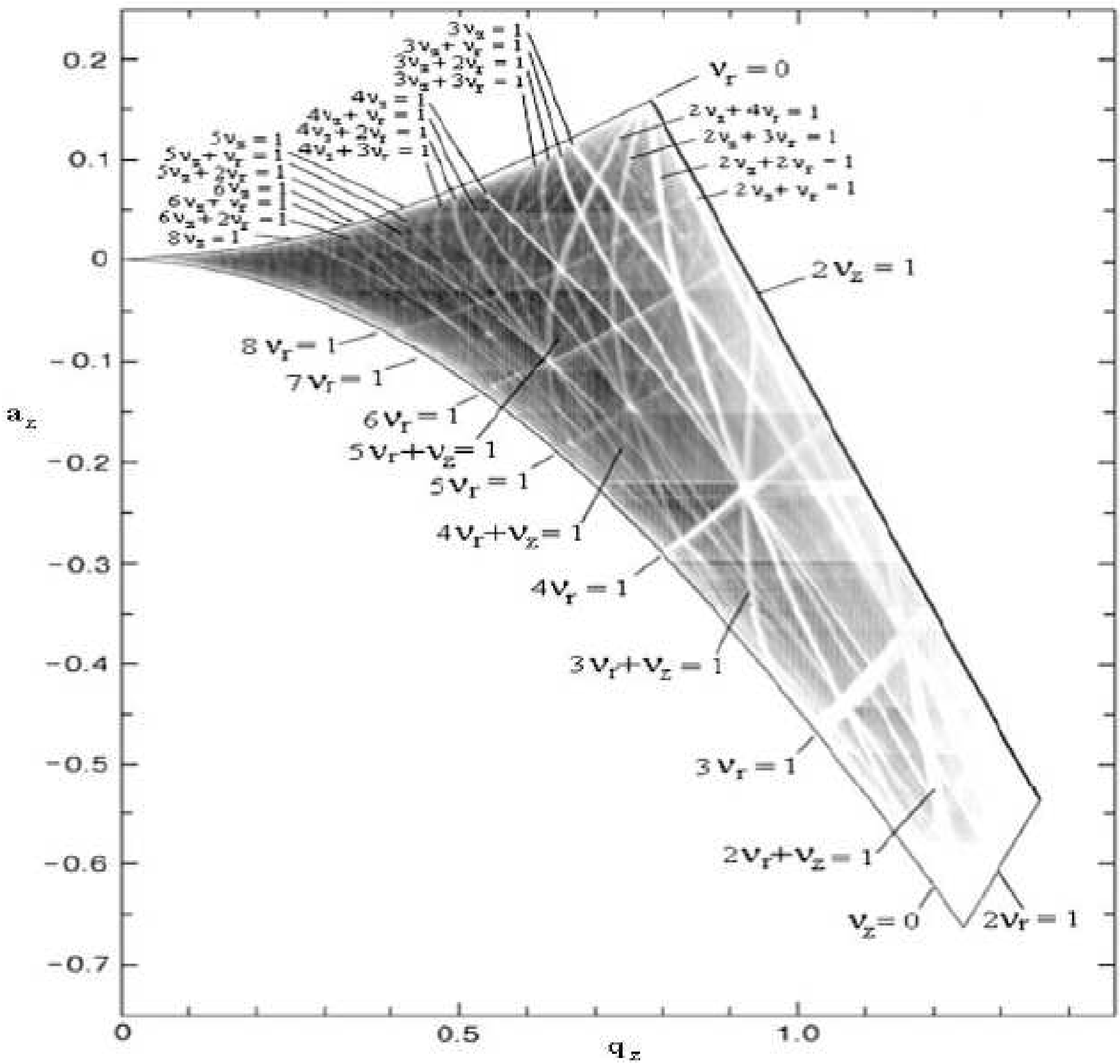

# Influence of buffer gas collisions

- $m_{gas} > m_{ion}$: ion loss
- $m_{gas} < m_{ion}$: cooling

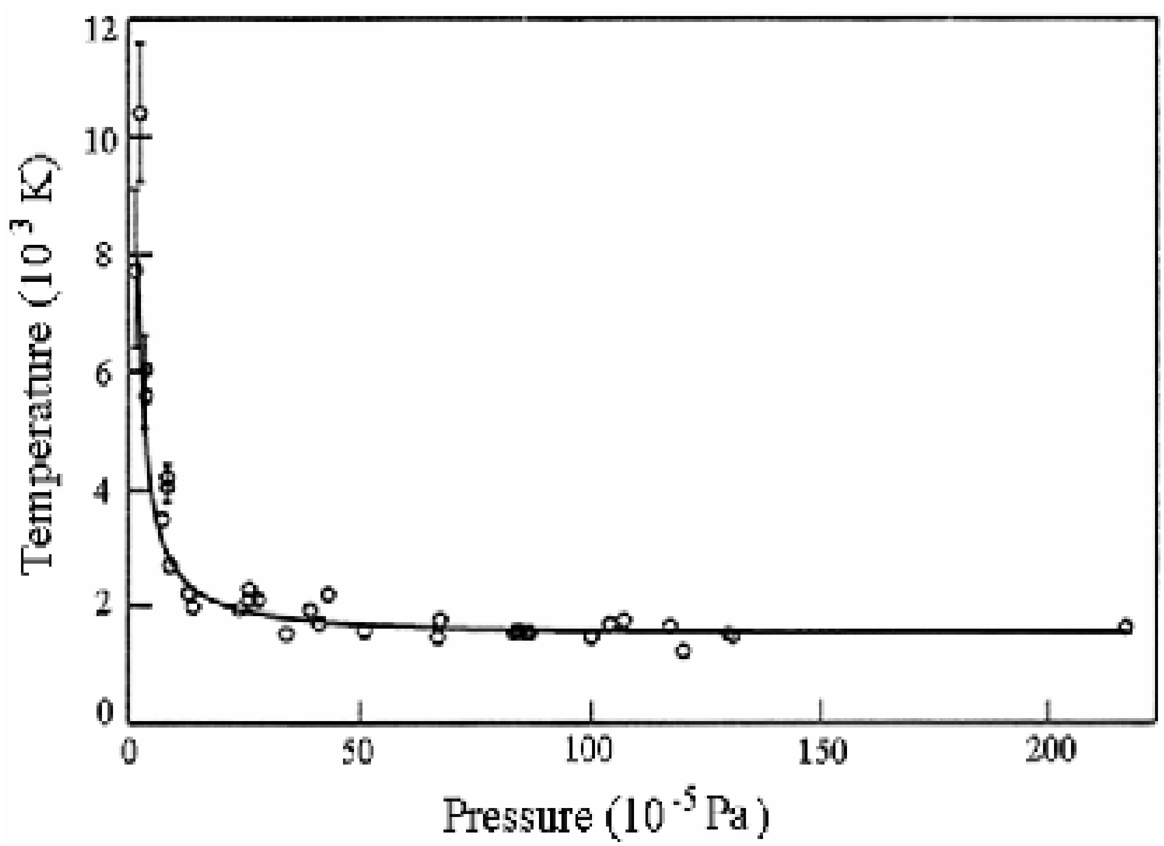


Temperature of $Ca^+$ ion cloud with He buffer gas

# Trap loading

Creation of ions inside trap by

- Electron bombardement of atoms
- Laser ionisation (element and isotope selectice)

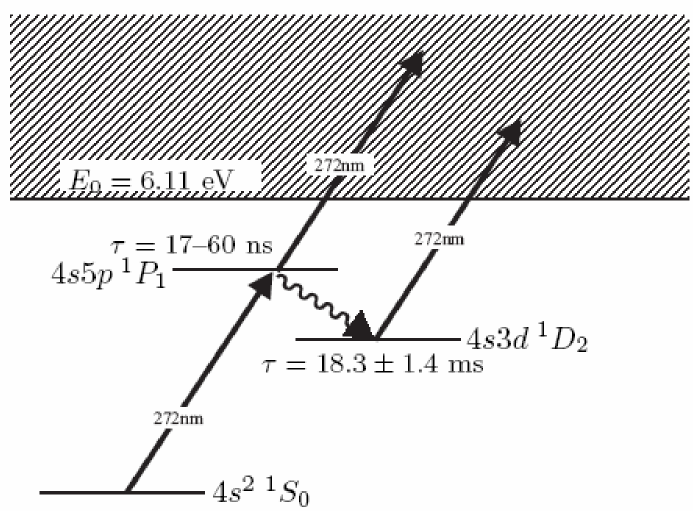


*Fig. 4.1:* Level scheme showing levels in calcium relevant for the photo-ionization of neutral calcium. The ionization threshold is 6.11 eV above the ground state in calcium [50]. The lifetimes of the excited levels are also indicated.

# Injection from outside
requires friction

(mean free path between ion-neutral collision ≈trap size)

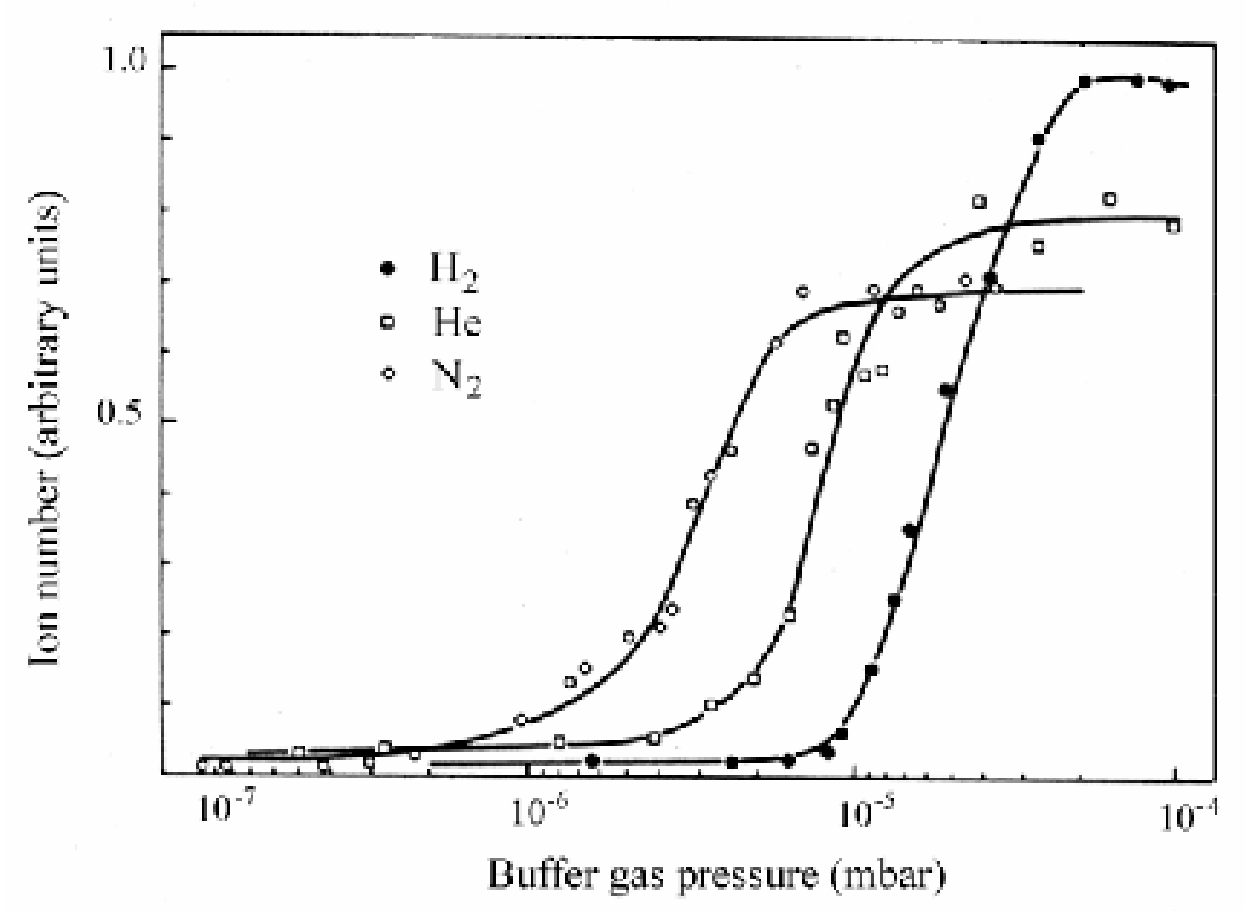


Ba $^+$ ions injected at 4 keV into 2 cm radius trap

# Ion Detection

**Destructive detection:**

**Ejection from trap by high voltage puls**

**Sensitivity: single ion**

**Non-destructive detection:**

**Absorbtion of energy from tank circuit**

**Sensitivity: $10^3$ ions (at room temperature**

**single ion (cryogenic)**

**optical detection:**

**Sensitivity: single ion**

# Destructive ion detection

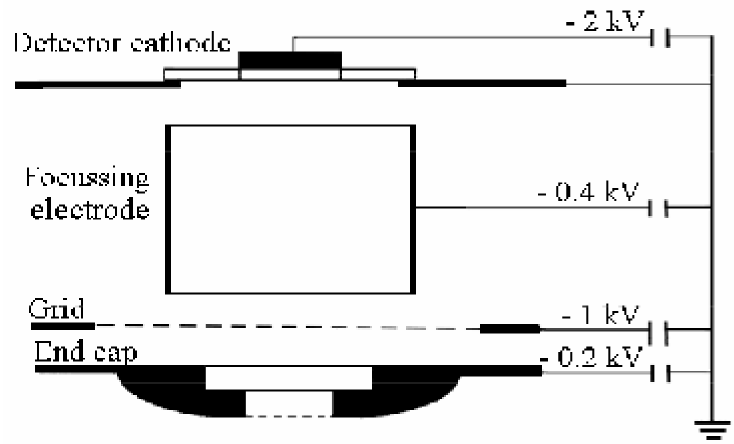


Separation of different mass ions
by different time-of-flight

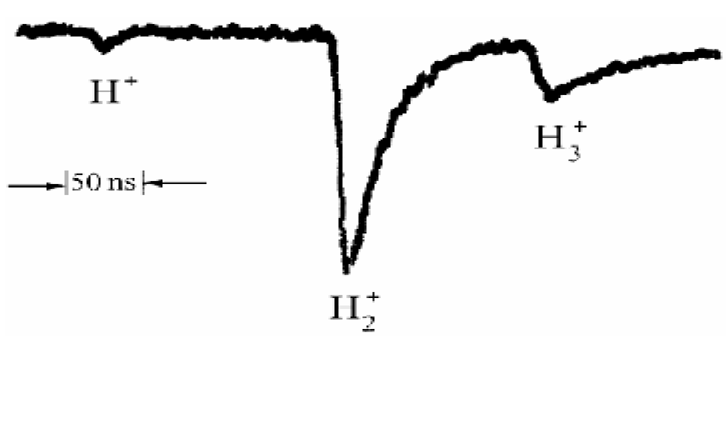

# Nondestructive detection of ion clouds

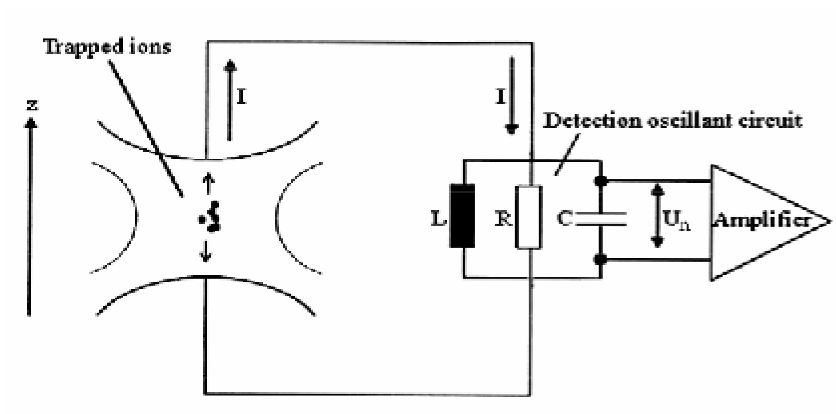


**Ramping of d.c. trap voltage.**
**$\omega_z \sim V^{1/2}$ . When $\omega_z = \omega_{Res}$, ions absorb energy from circuit $\Rightarrow$ damping of circuit**

**Damping signal from ca. $10^4$ ions**

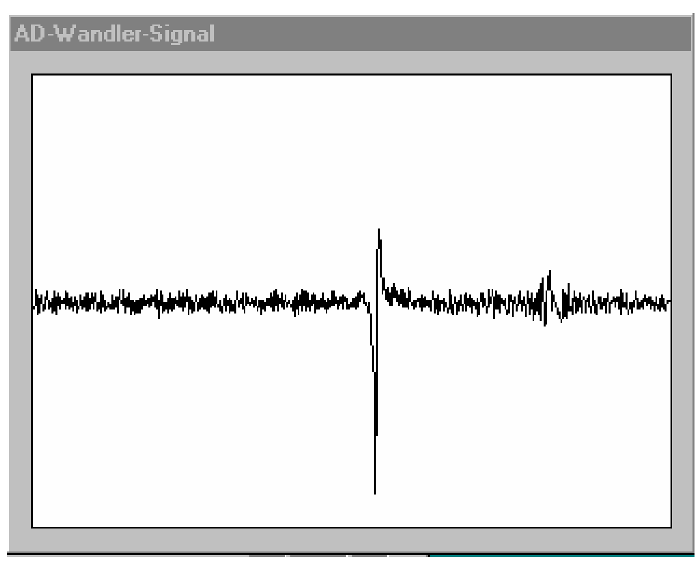

# Optical detection

Fluorescence strength from a single trapped ion continuously excited at saturation intensity on an allowed electric dipole transition: ca.$10^8$ Photons/s

Detection efficiency (solid angle, transmission losses, detector quantum efficiency): ca. $10^{-5}$

$\rightarrow$ $10^3$ detected Photons from a single ion

# Laser induced fluorescence from individual ions

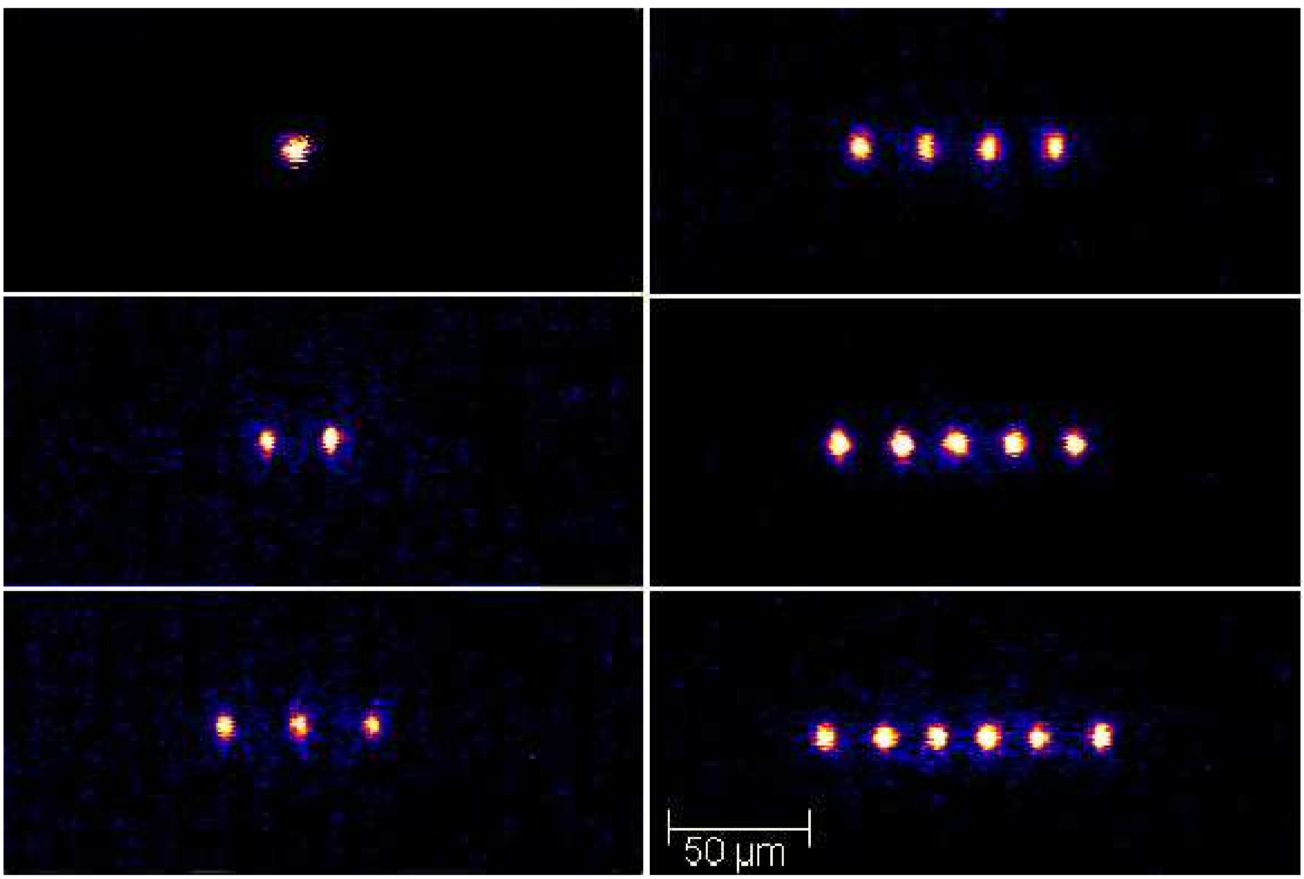

# Alternative trap geometries

**Paul-Straubel trap:**

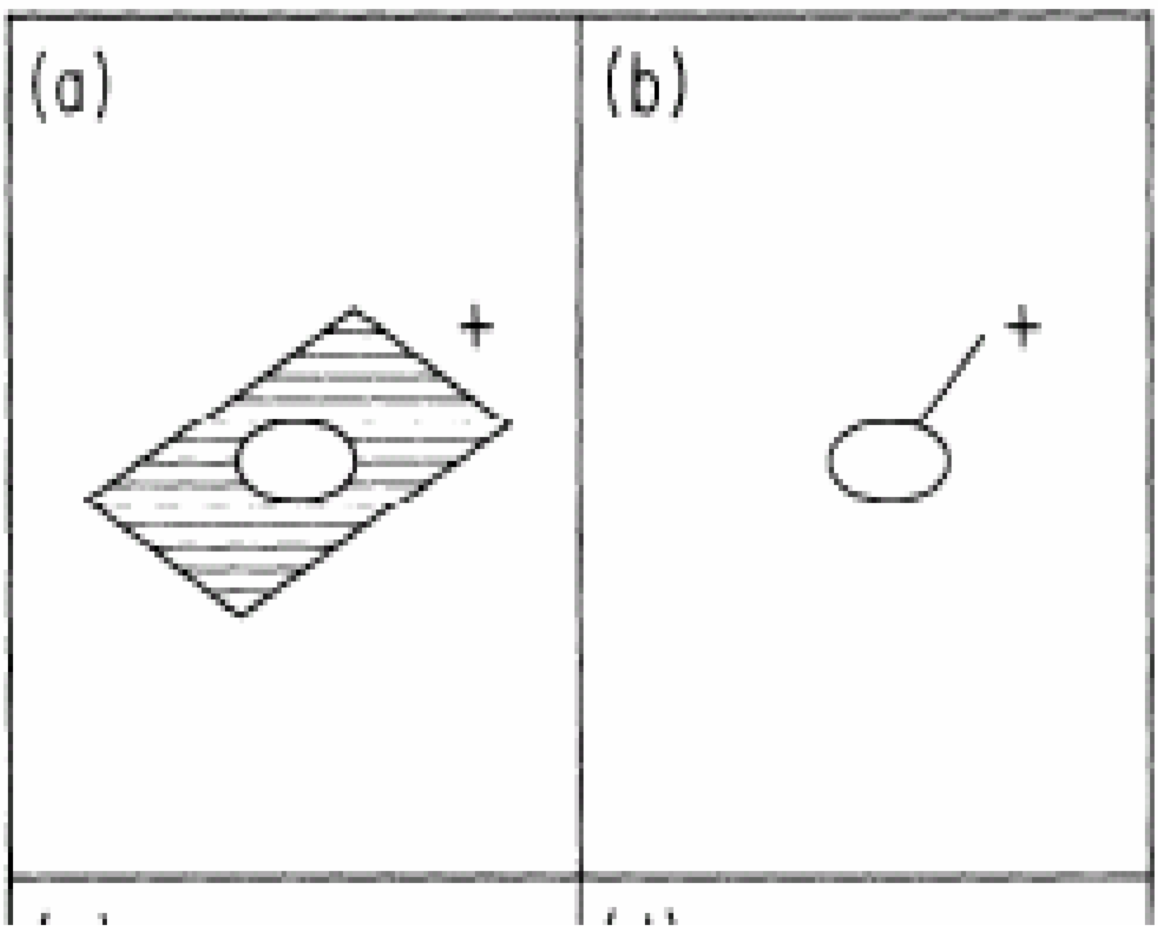

# Linear Traps

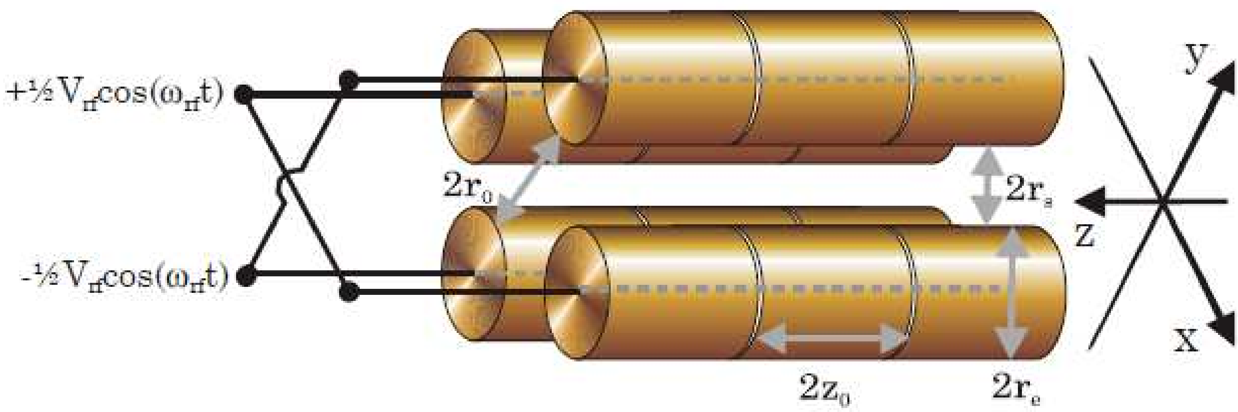


$$m\frac{d^2}{dt^2}\begin{bmatrix} X_x \\ X_y \\ X_z \end{bmatrix} = -Q\begin{bmatrix} \left(-\frac{\kappa V_{ec}}{z_0^2} + \frac{V_{rf}}{r_0^2}\cos(\omega_{rf}t)\right)x \\ \left(-\frac{\kappa V_{ec}}{z_0^2} - \frac{V_{rf}}{r_0^2}\cos(\omega_{rf}t)\right)y \\ \left(2\frac{\kappa V_{ec}}{z_0^2}\right)z \end{bmatrix}$$

Stability diagram for radial motion

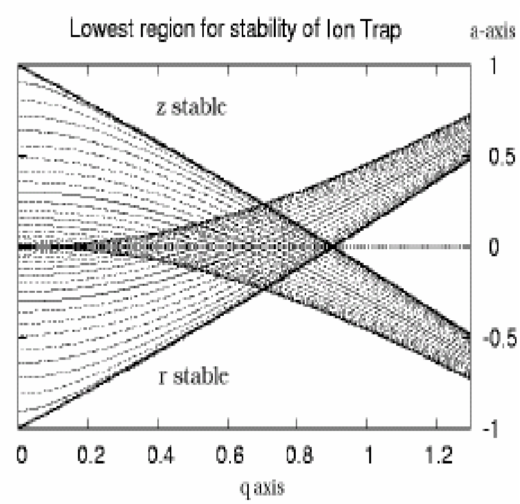

# Radial potential of a linear quadrupole trap

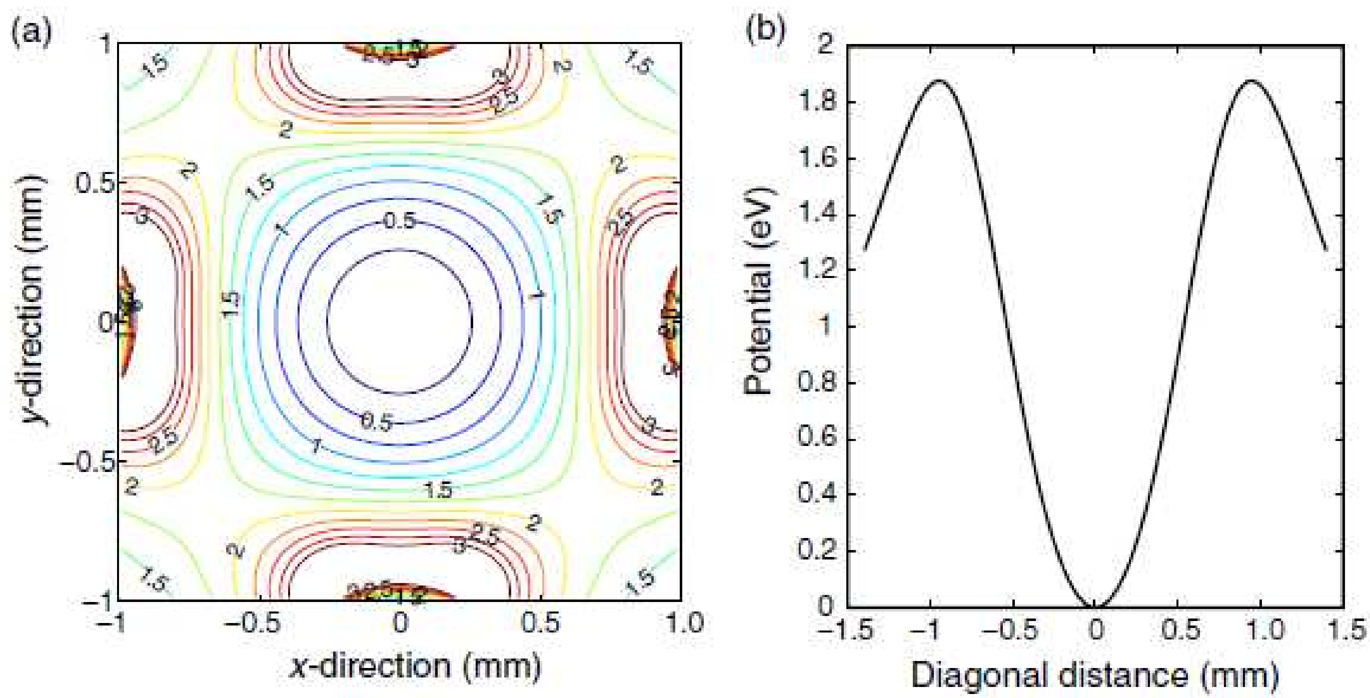

# Multipole traps

Potential of an n-pole trap: $\Phi \propto \left( \frac{r}{r_0} \right)^{n-2}$

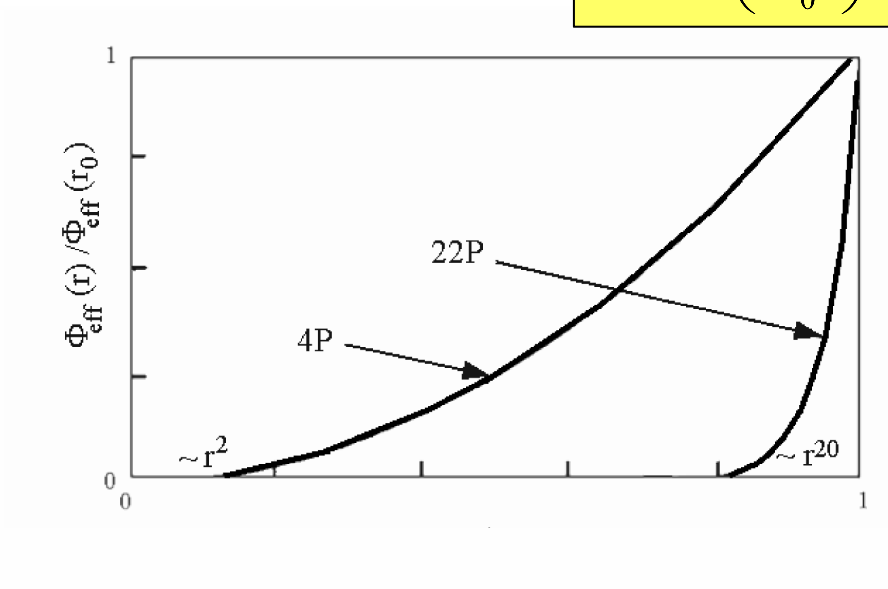


## Ion trajectories in a 32-pole trap

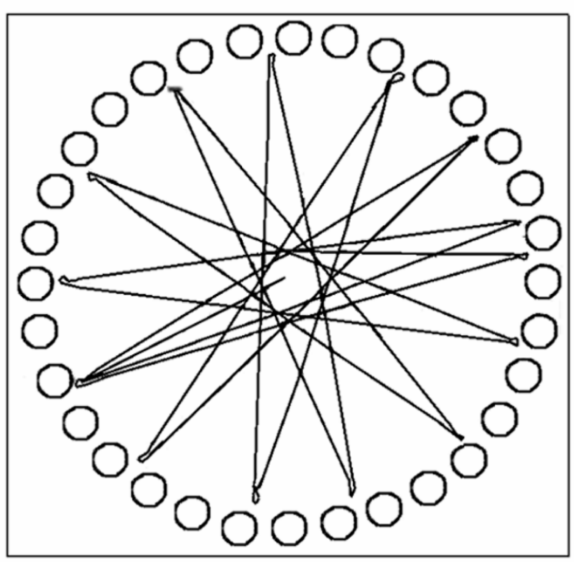

# Linear trap constructions

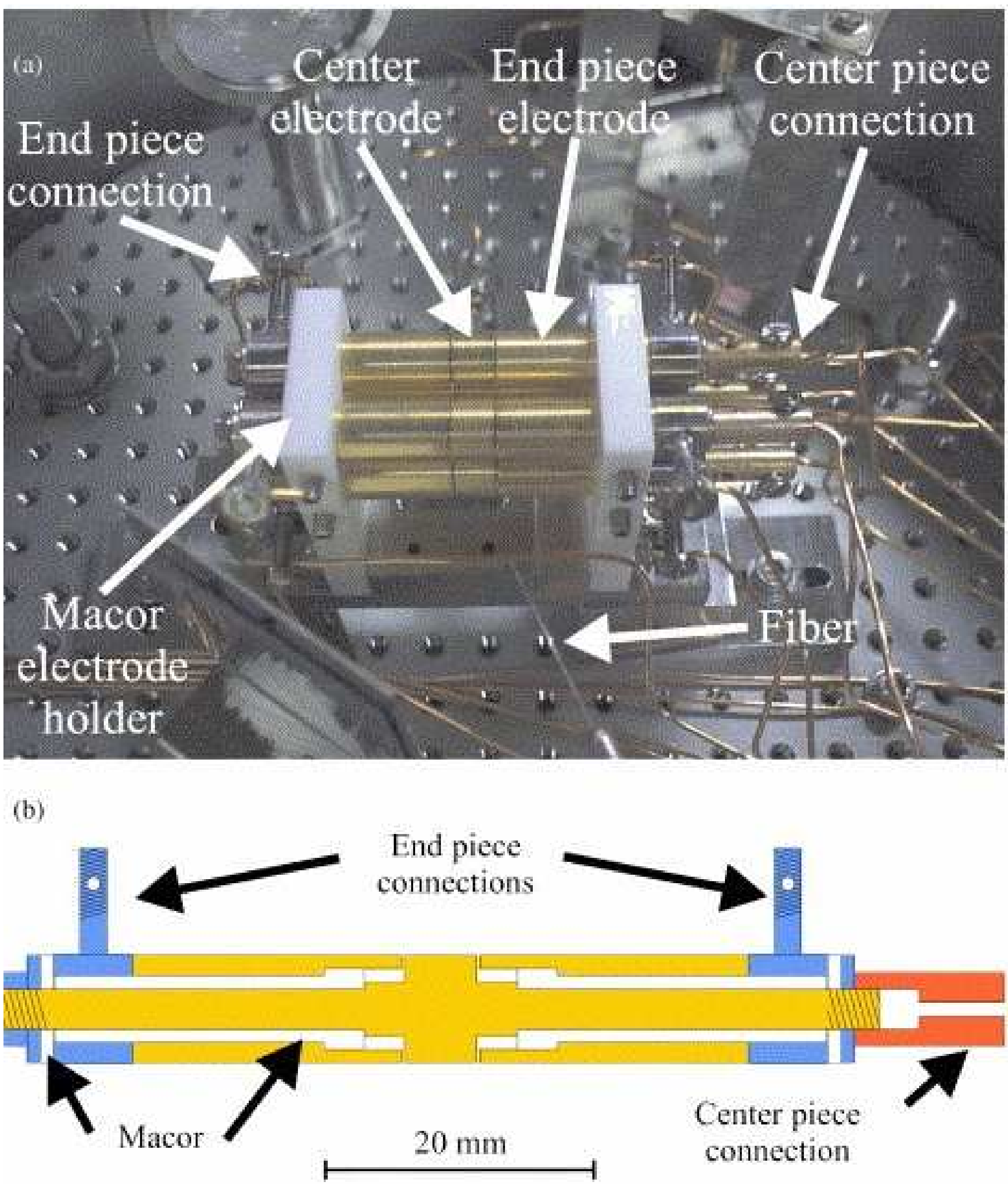


NIST, Boulder

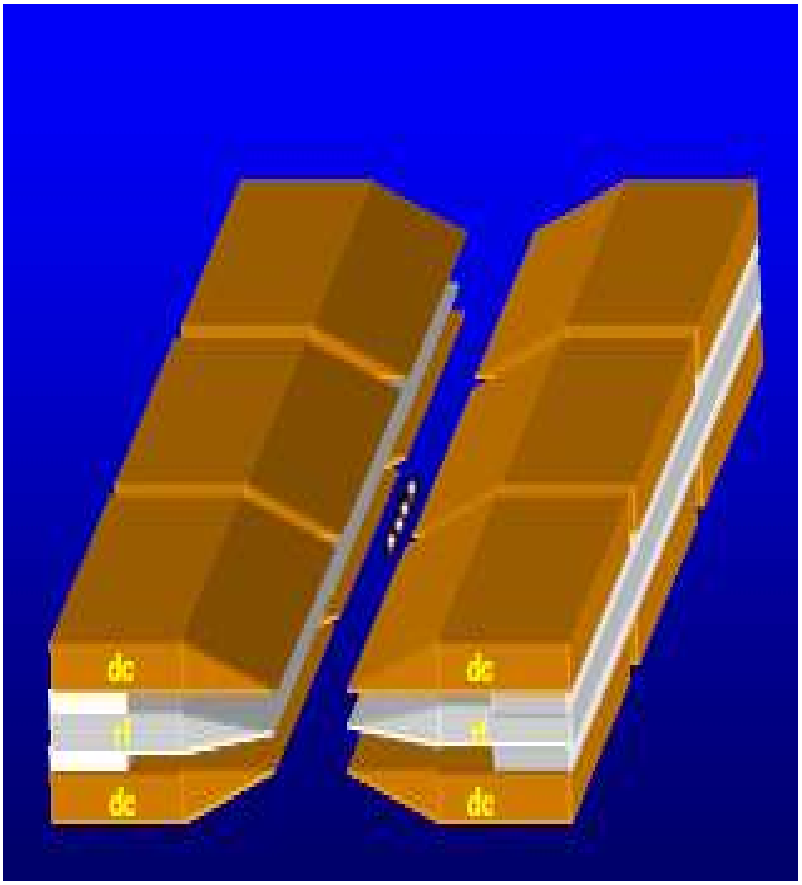


Univ. of Michigan

# Blade trap with segmented electrodes (Univ. Ulm, Innsbruck)

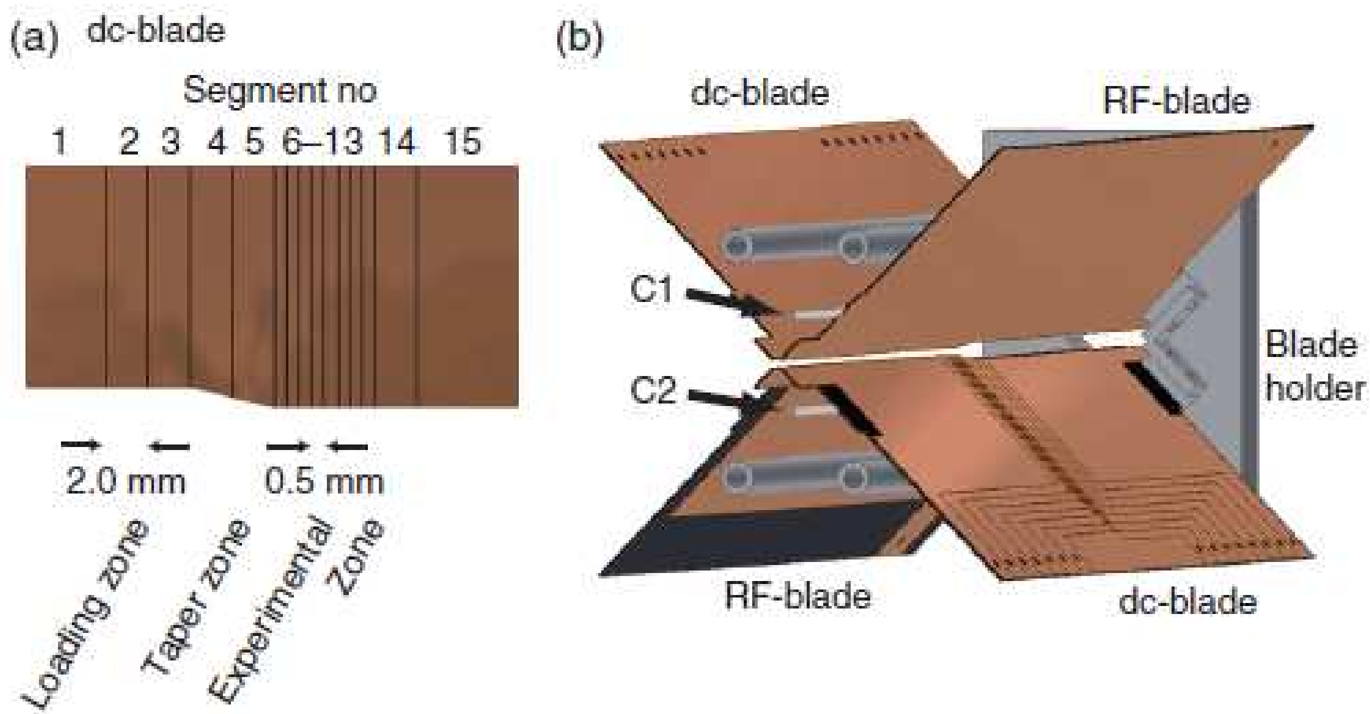

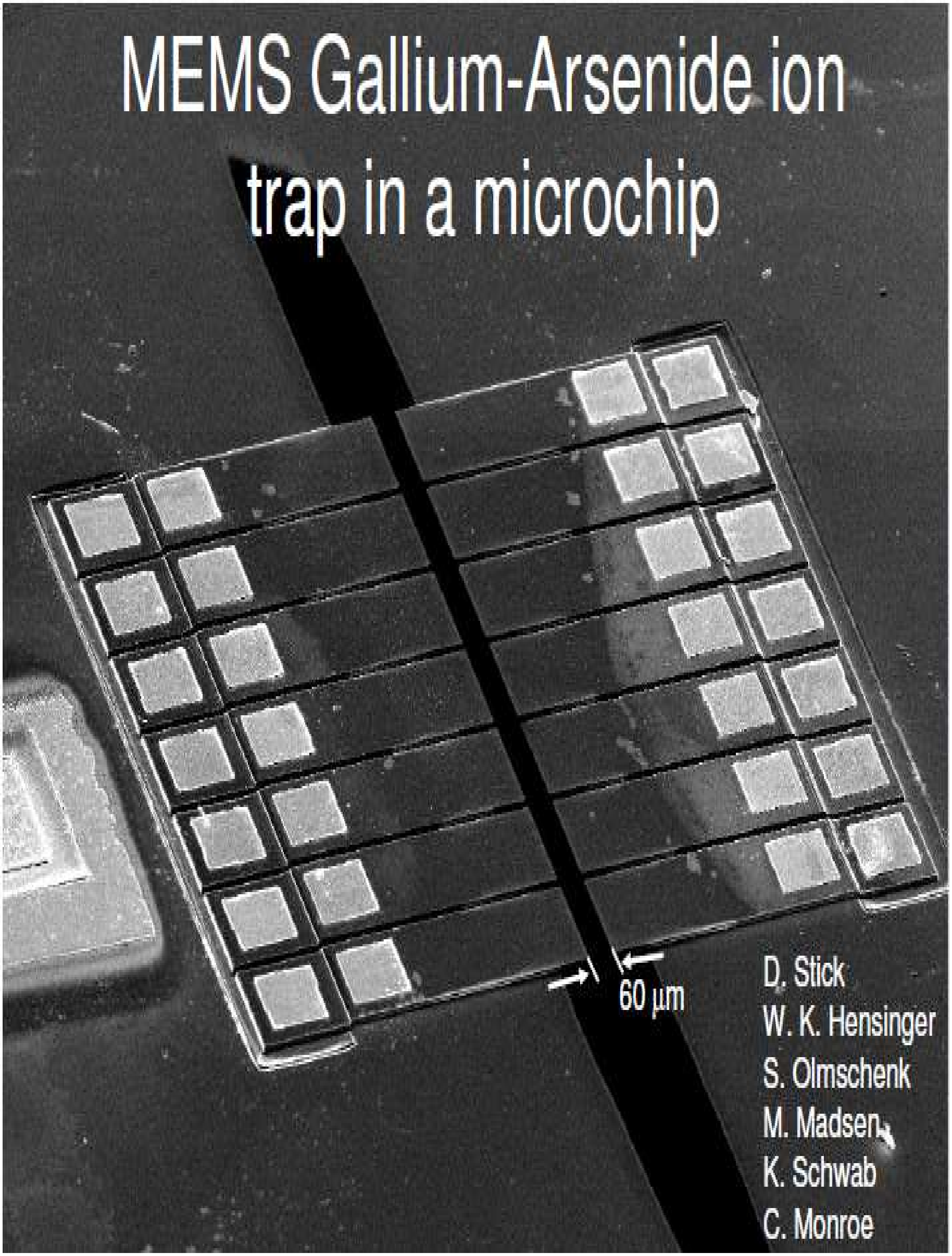
MEMS Gallium-Arsenide ion
trap in a microchip
60 μm
D. Stick
W. K. Hensinger
S. Olmschenk
M. Madsen
K. Schwab
C. Monroe

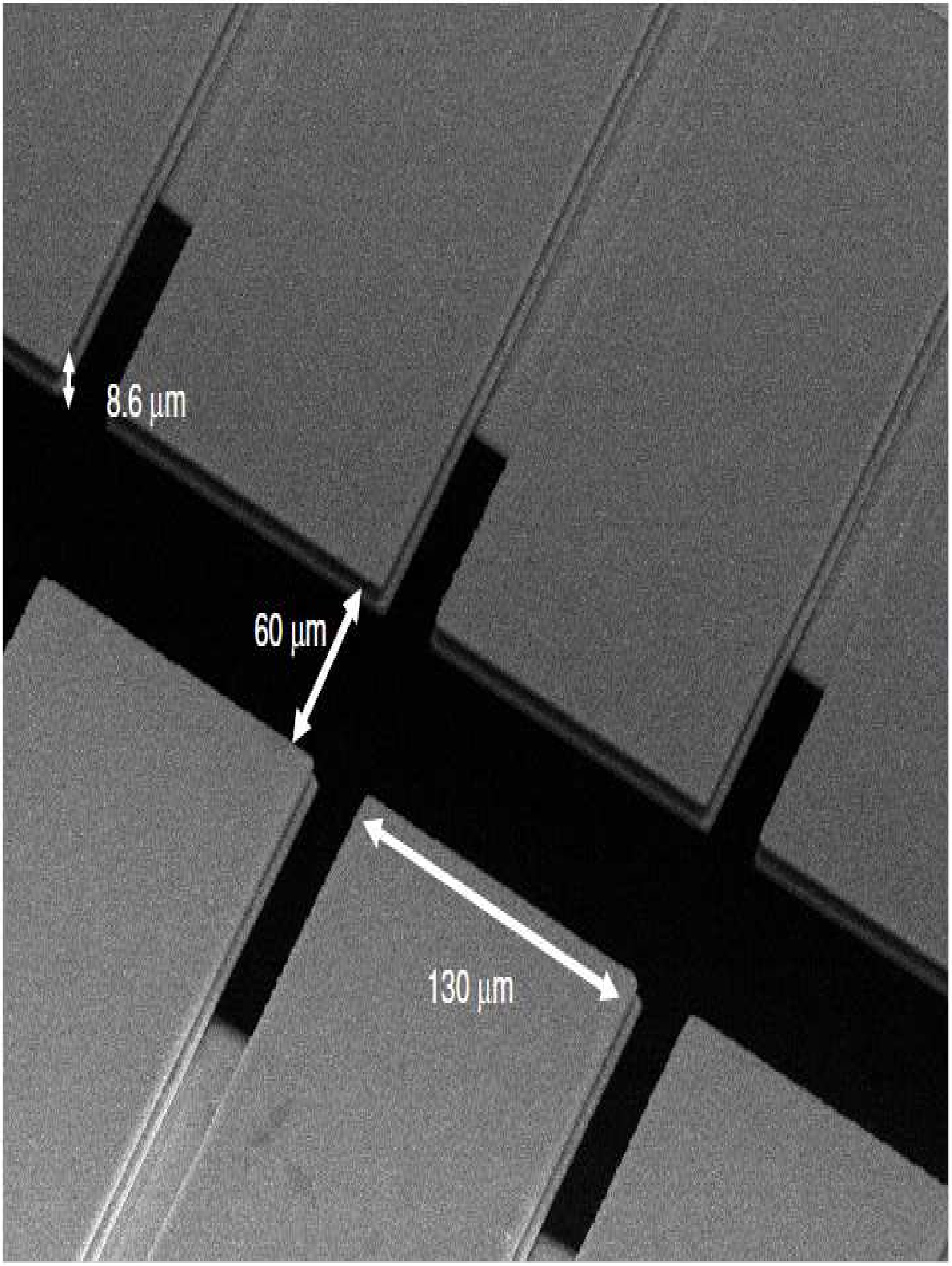
8.6 µm
60 µm
130 µm

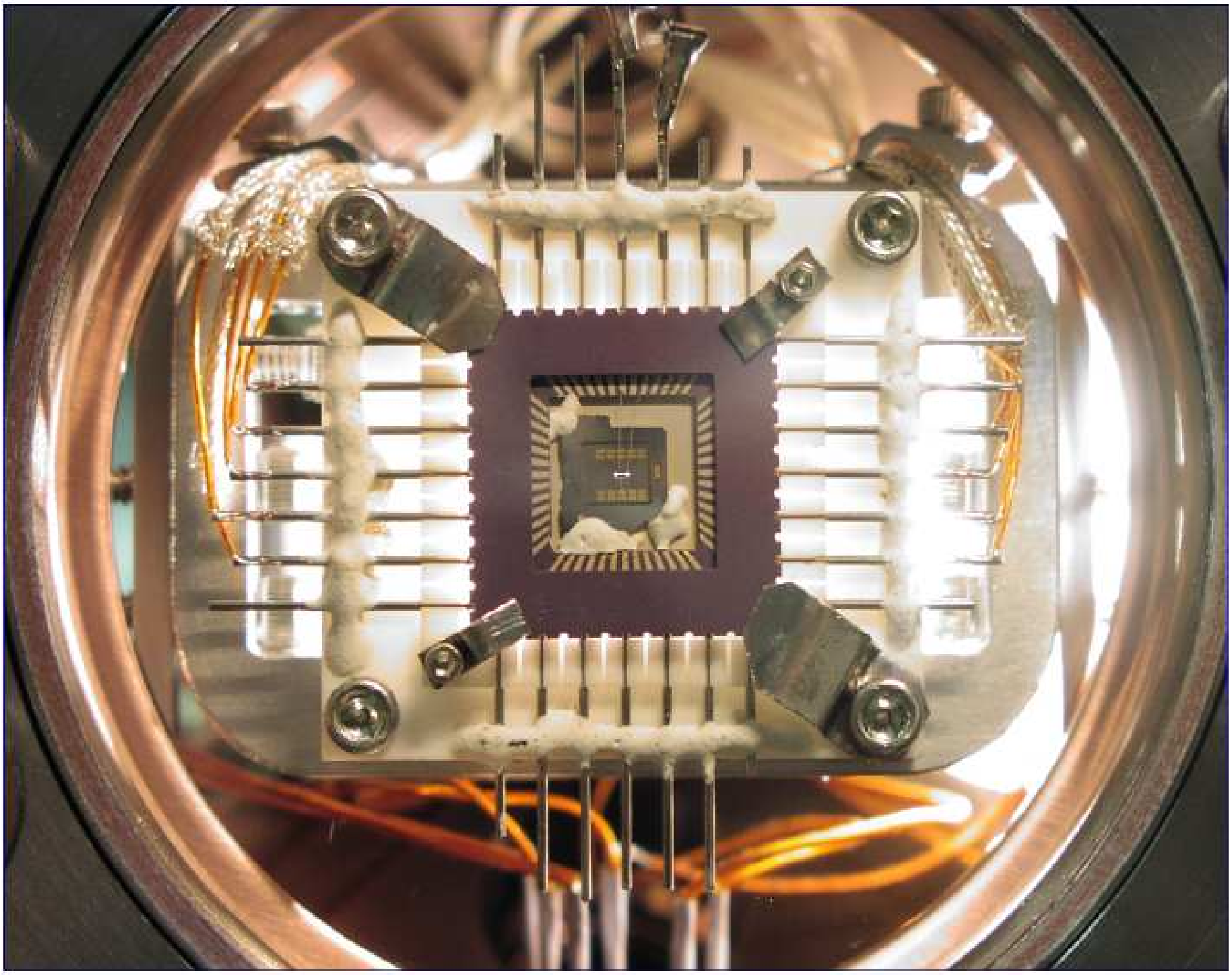

# MEMS Silicon ion traps

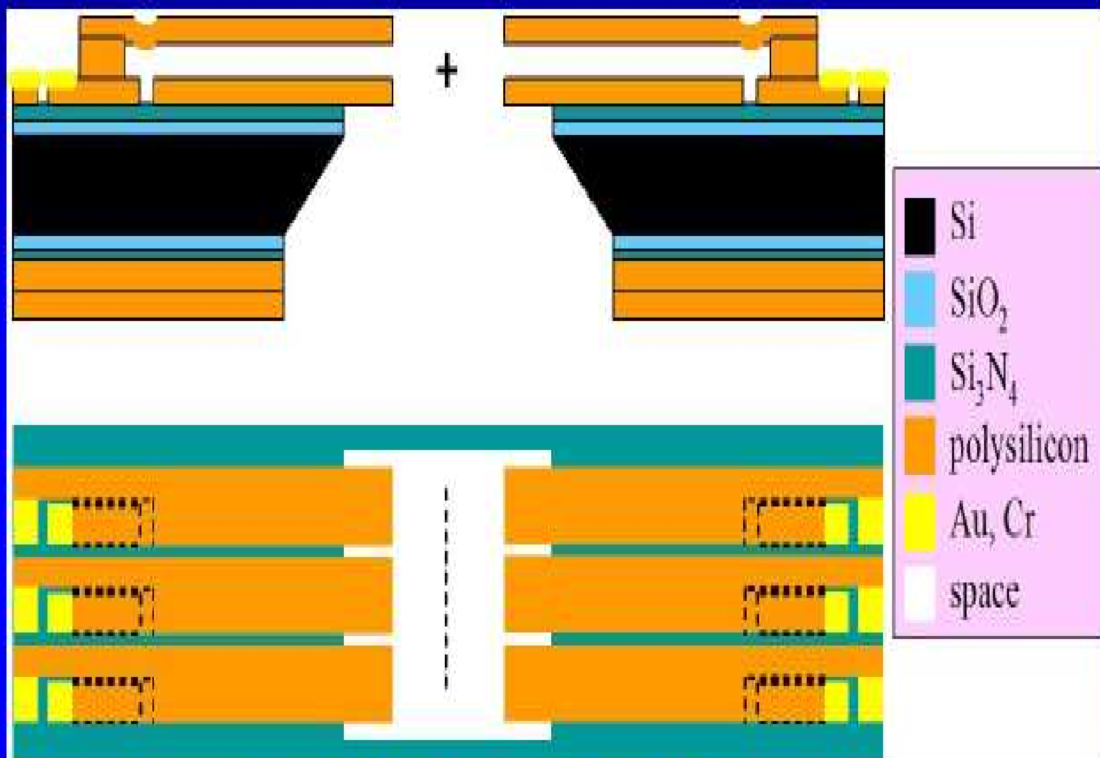


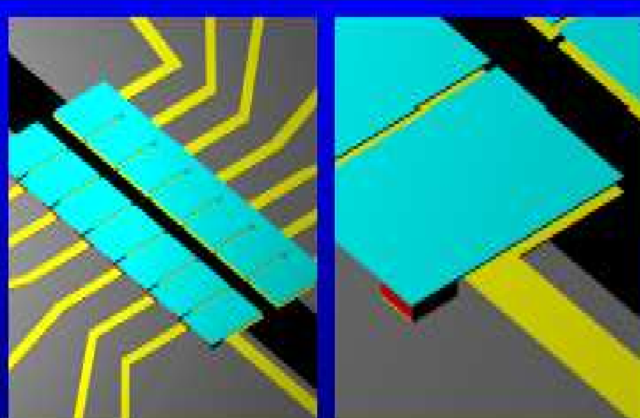

53 step process!

In collaboration with:

Dan Stick, Jon Sterk, Martin Madsen, Winfried Hensinger, Chris Monroe, Bill Noonan, Michael Pedersen, Steve Gross, and Michael Huff

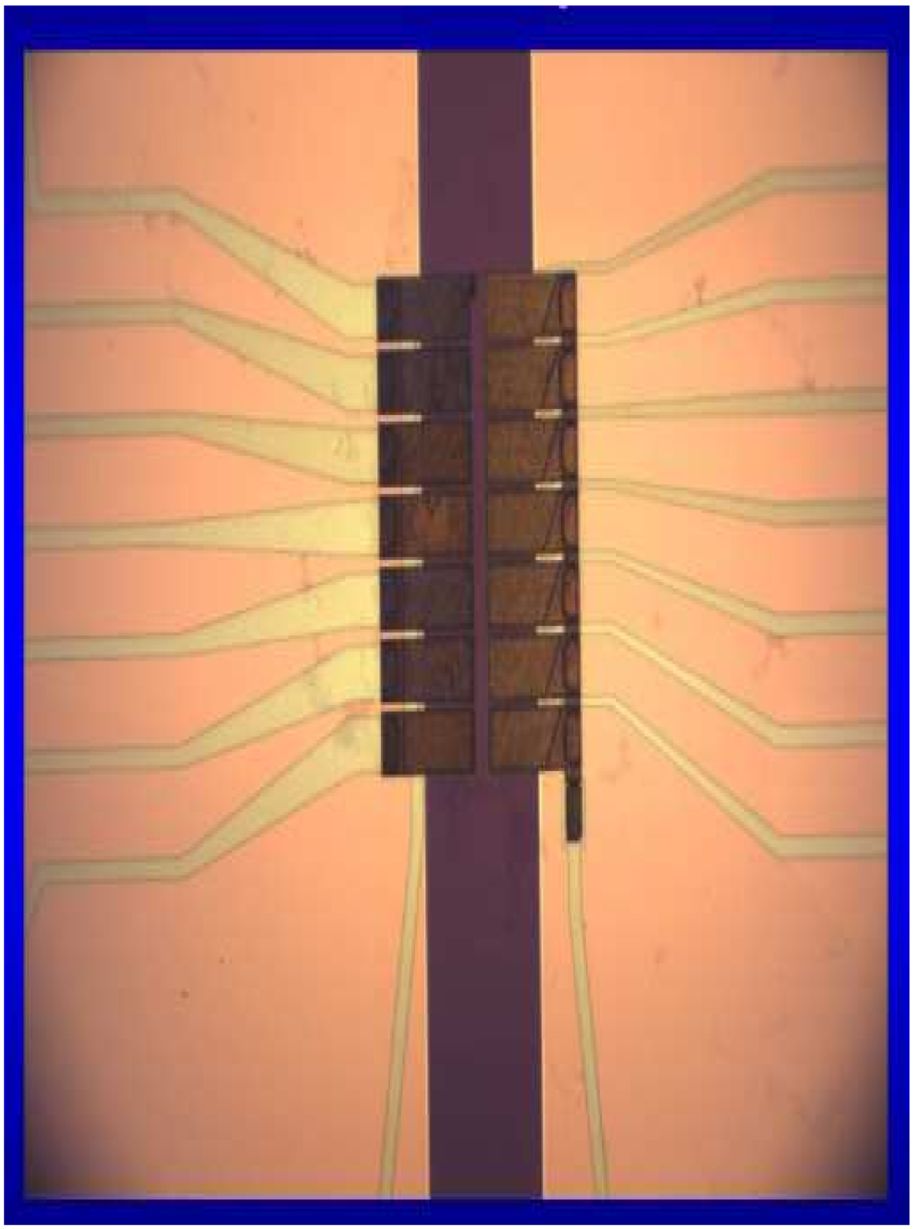

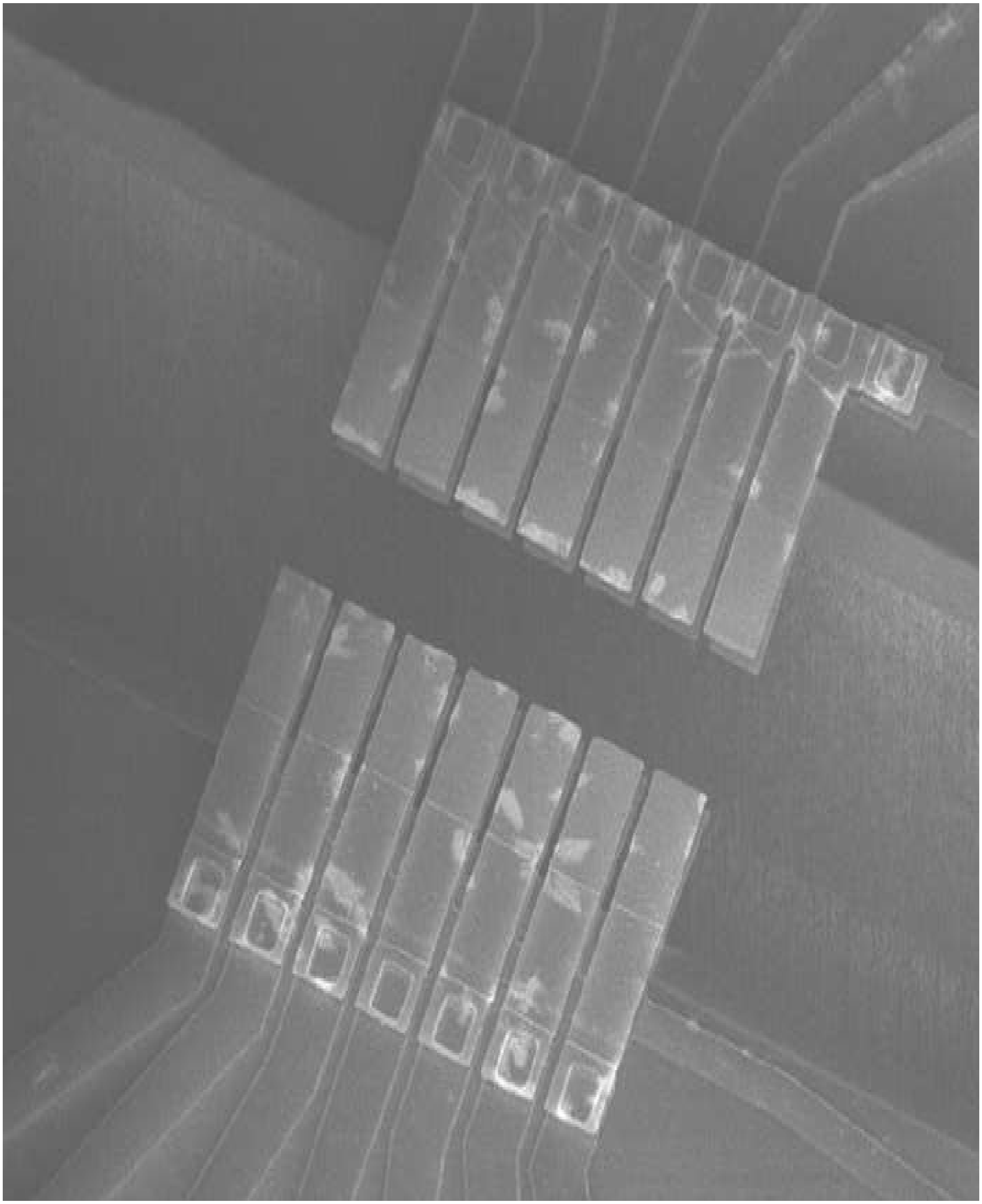

# NIST Planar Trap Chip

Gold on fused silica

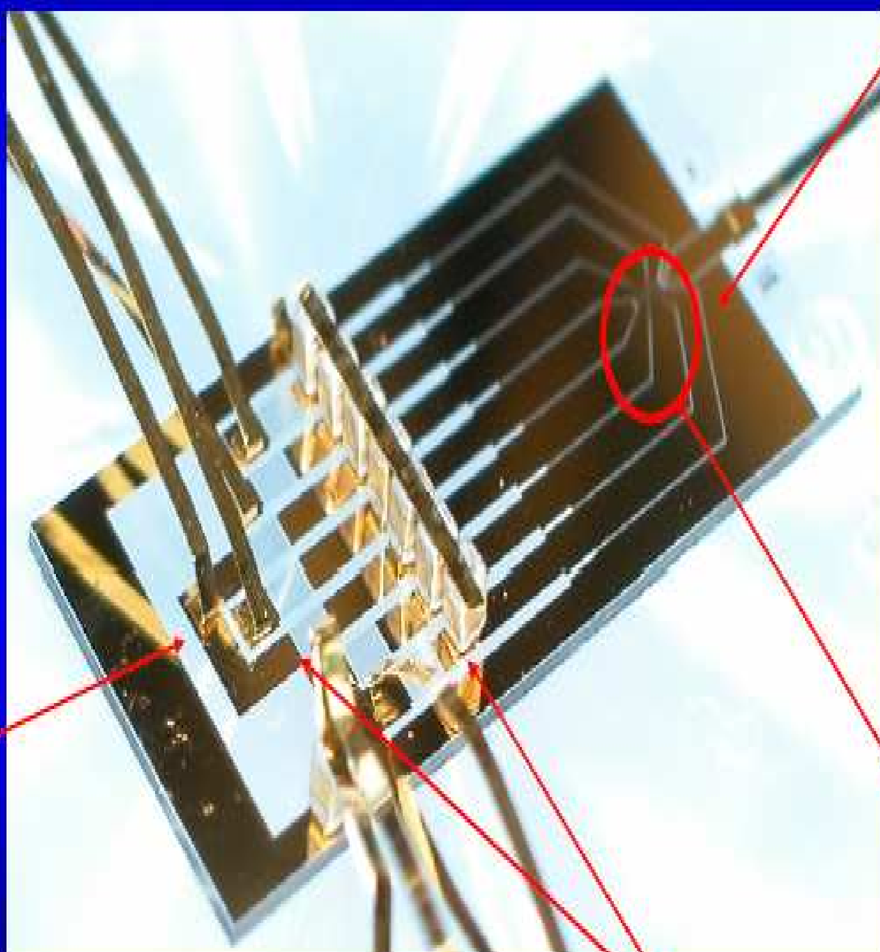

RF

DC
Contact
pads

trapping
region

low pass filters

John Chiaverini, Signe Seidelin, Didi Leibfried, David Wineland (NIST)

# NIST Planar Trap Chip

Magnified trap electrodes

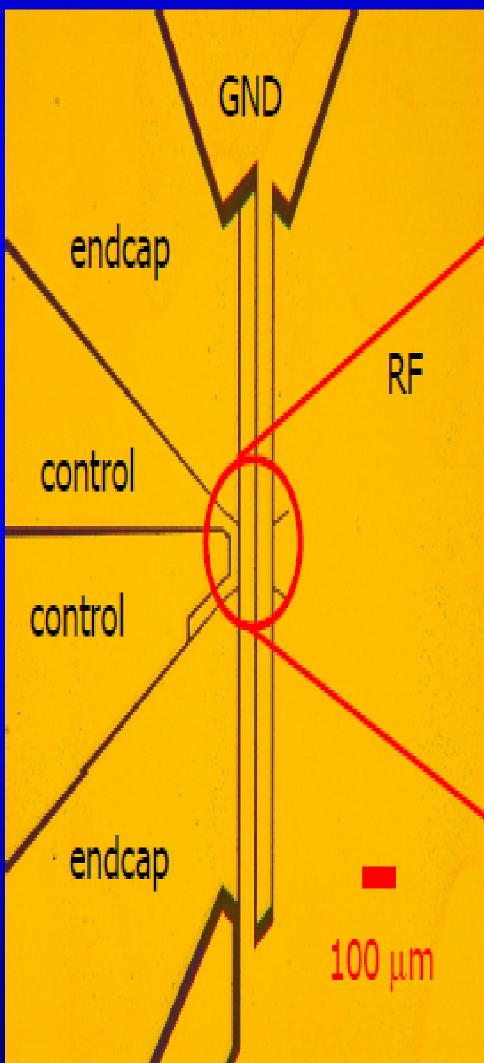


CCD pictures of strings of Mg+ ions (trapped 40 mm above surface)

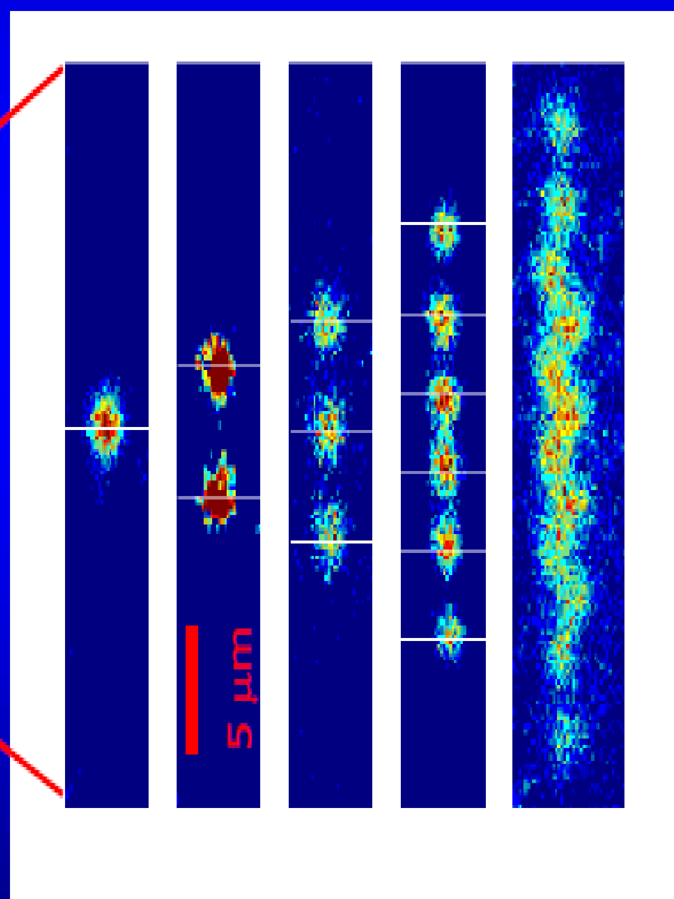


Seidelin *et al.*, PRL **96**, 253003 (2006).

John Chiaverini, Signe Seidelin, Didi Leibfried, David Wineland

# NPL design

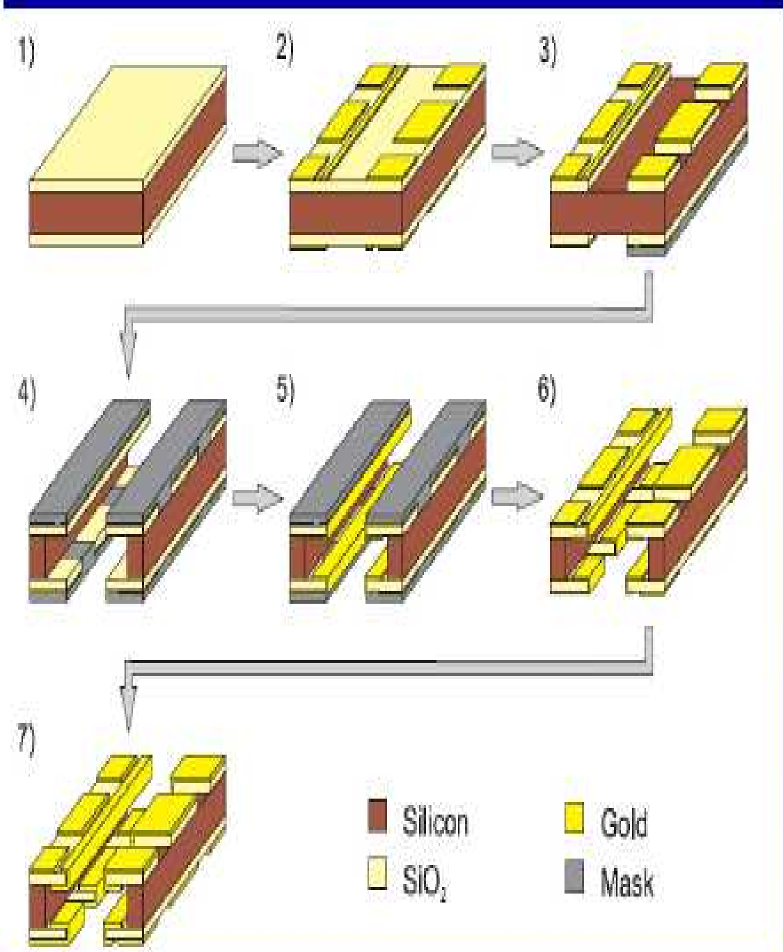


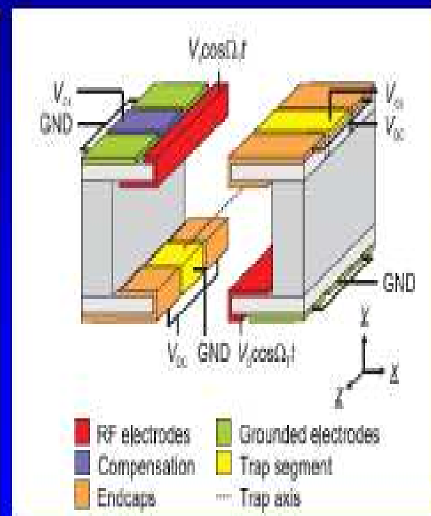


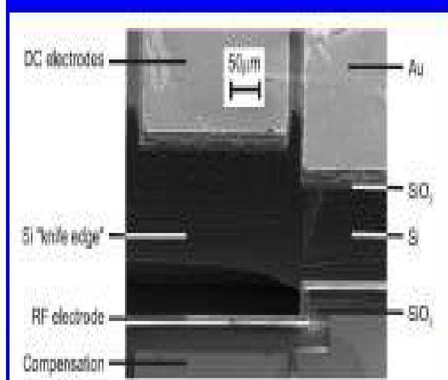


*Monolithic microfabricated ion trap chip design for scaleable quantum processors*
M. Brownnutt, G. Wilpers, P. Gill, R.C. Thompson, A.G. Sinclair, New J. Phys. 8, 232(2006).

# NIST two layer cross trap

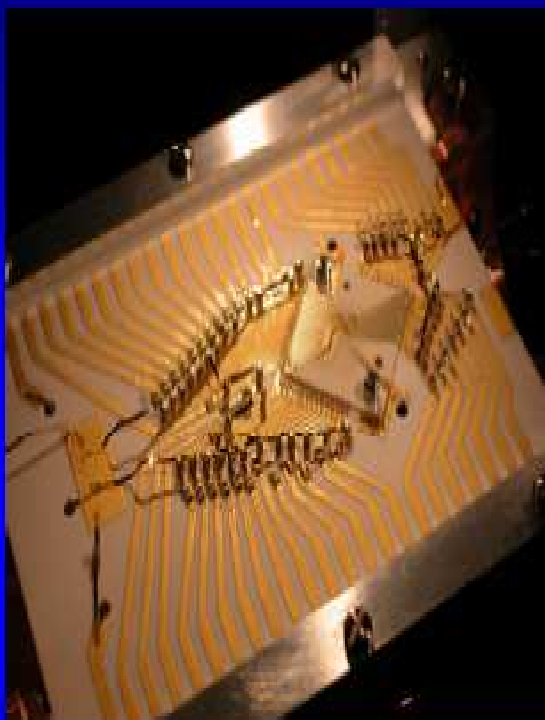

2 wafers of alumina (0.2 mm thick)
gold conducting surfaces (2 μm)


18 zones, 1 cross

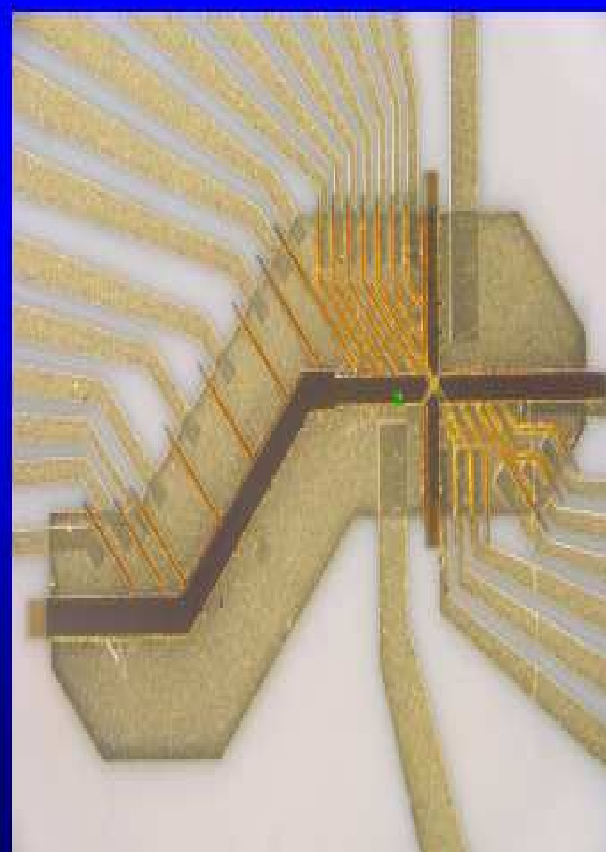

$Mg^+$ and $Be^+$ moved through junction > $10^4$ times without ion loss

Characterization of heating during shuttling in progress

Brad Blakestad, Didi Leibfried and David Wineland

# Ulm linear multizone trap

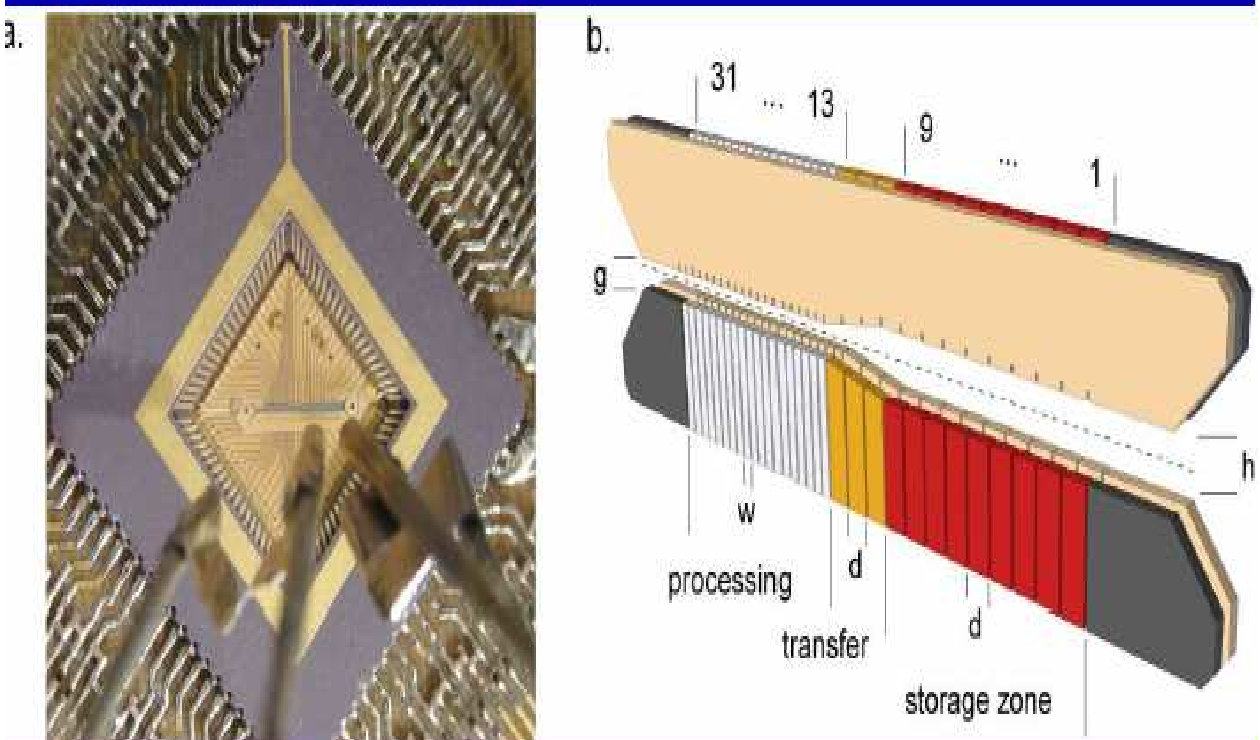


Stefan Schulz, Ulrich Poschinger, Frank Ziesel and Ferdinand Schmidt-Kaler

# 3-dim. stack of single ion traps

**K. Ravi, S. Rangwala et al, 2009**

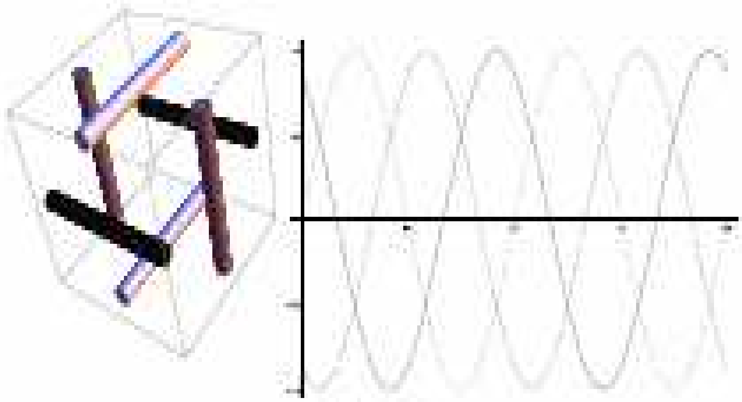

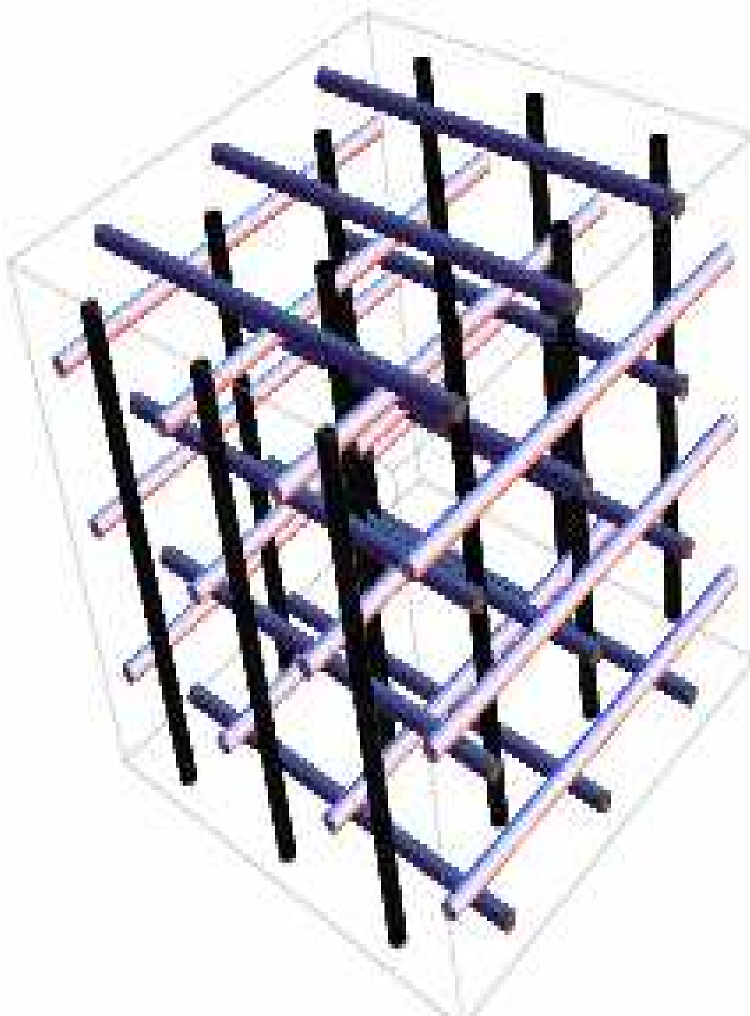

# **Trap applications**
# without ion cooling:
# Hyperfine spectroscopy

- No limitation of linewidth fromHeisenberg uncertainty because of „infinite“ long coherence time
- Spectral resolution limited mainly by technical reasons (collisions with background gas molecules, fluctuations of residual magnetic field, finite spectral purity of exciting radio-frequency field)
- No first order Doppler effect even for uncooled ions because of Dicke effect (wavelength of radiation large compared to ion oscillation amplitude)
- Limitation in accuracy by second order Doppler effect $\Delta\omega/\omega = (v^2/2c^2)$

  ($\approx 5\ 10^{-10}$ at T = 10 000 K)

  ($\approx 5\ 10^{-14}$ at T = 1 K)

# Experimental method: Laser-microwave double resonance

- Selective excitation of one hyperfine level by laser excitation leads to population difference between hyperfine levels (optical pumping)
- Inducing transitions beween hyperfine levels by microwave field

  (selection rule: $\Delta F = 0,1$; $\Delta m_F = 0,1$)
- Detection of resonant excitation by observation of change in fluorescence intensity

# Example: Hyperfine separation in the $S_{1/2}$ ground state of $^{171}Yb^{+}$ (***I* = ½**)

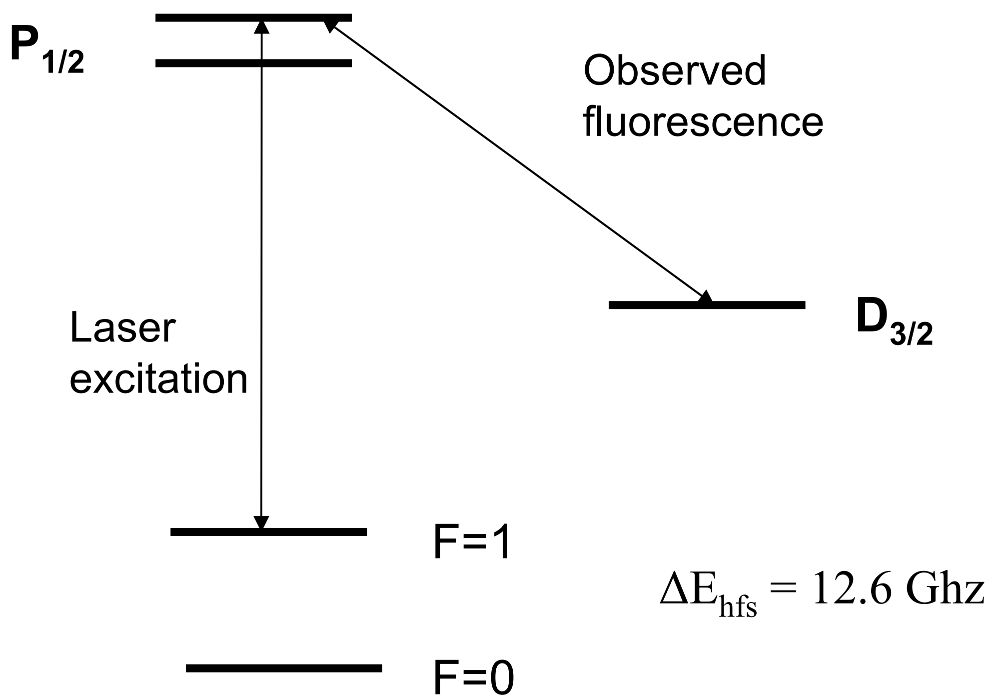


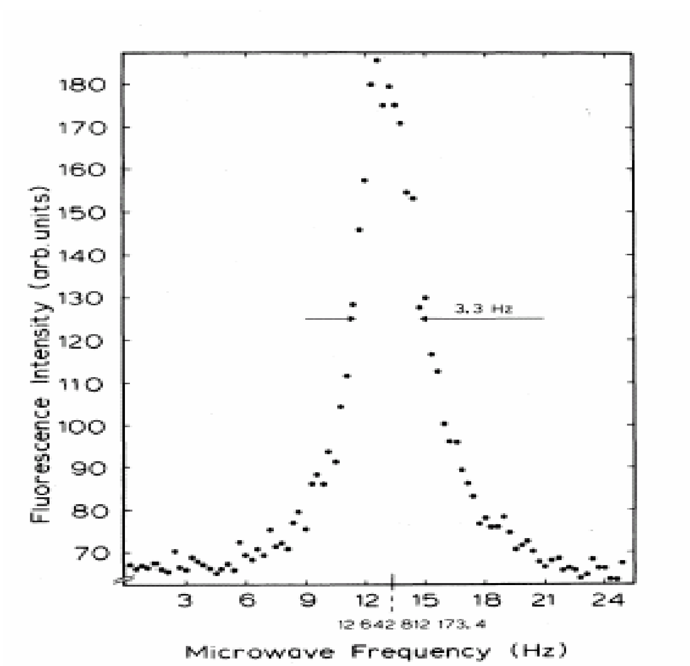


Microwave induced F=0→F=1 transition

$\delta\nu/\nu = 10^{-10}$

# More complex ion: $Eu^+$

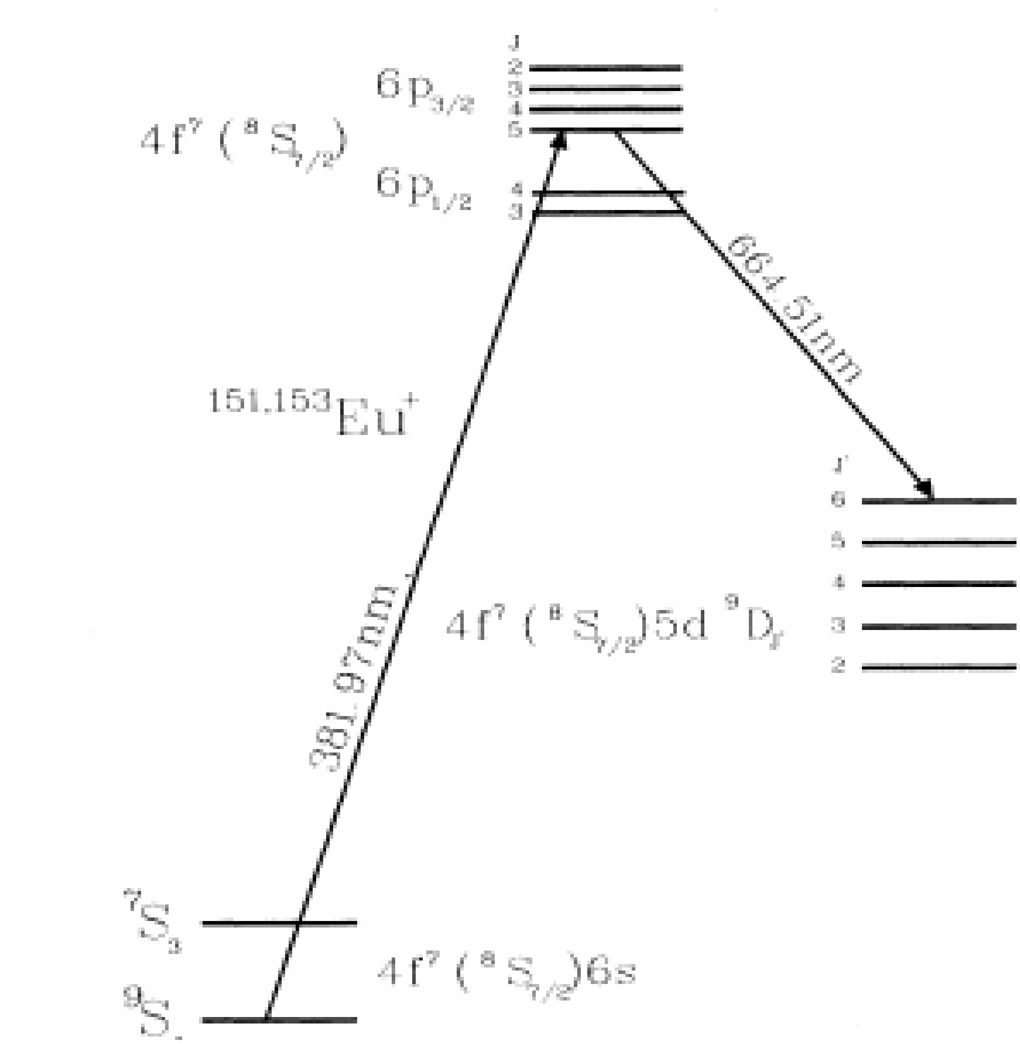

# Optical excitation spectrum in a mixture of natural isotopes

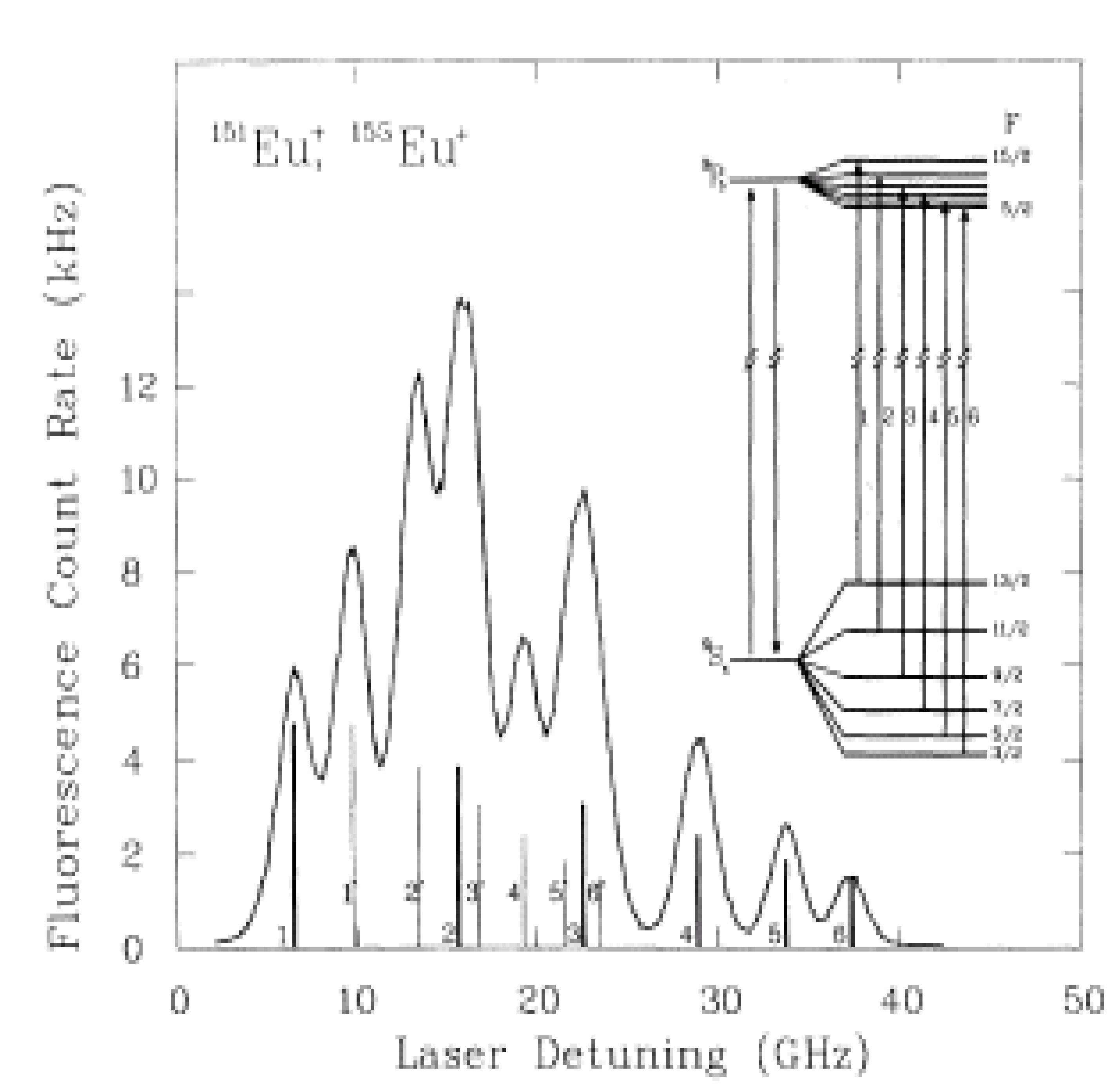

# Micowave induced $\Delta m_F=0$ hyperfine transitions between the F=11/2 and F=13/2 hyperfine levels in the $^9S_4$ ground state of $^{151}Eu^+$

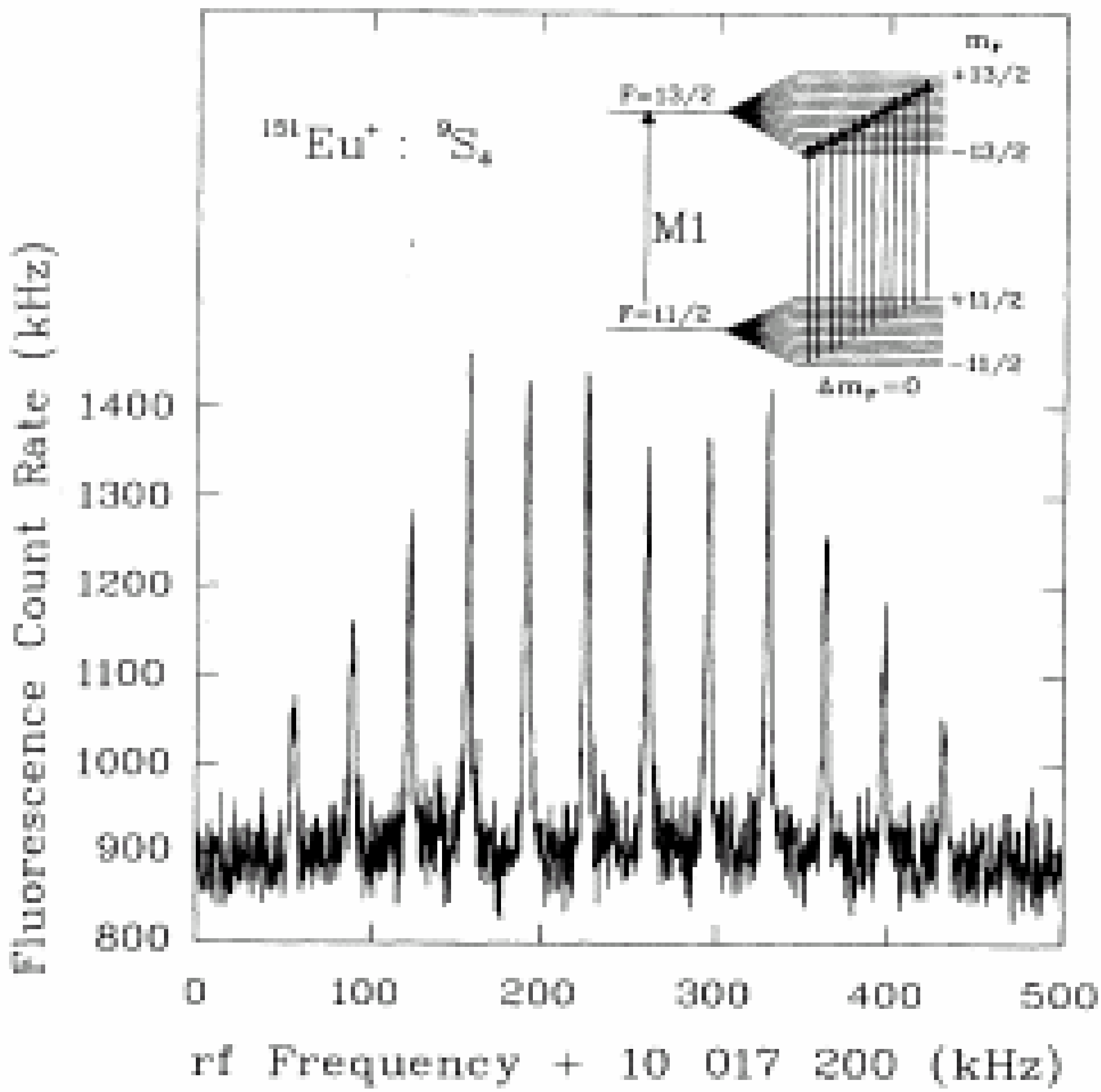

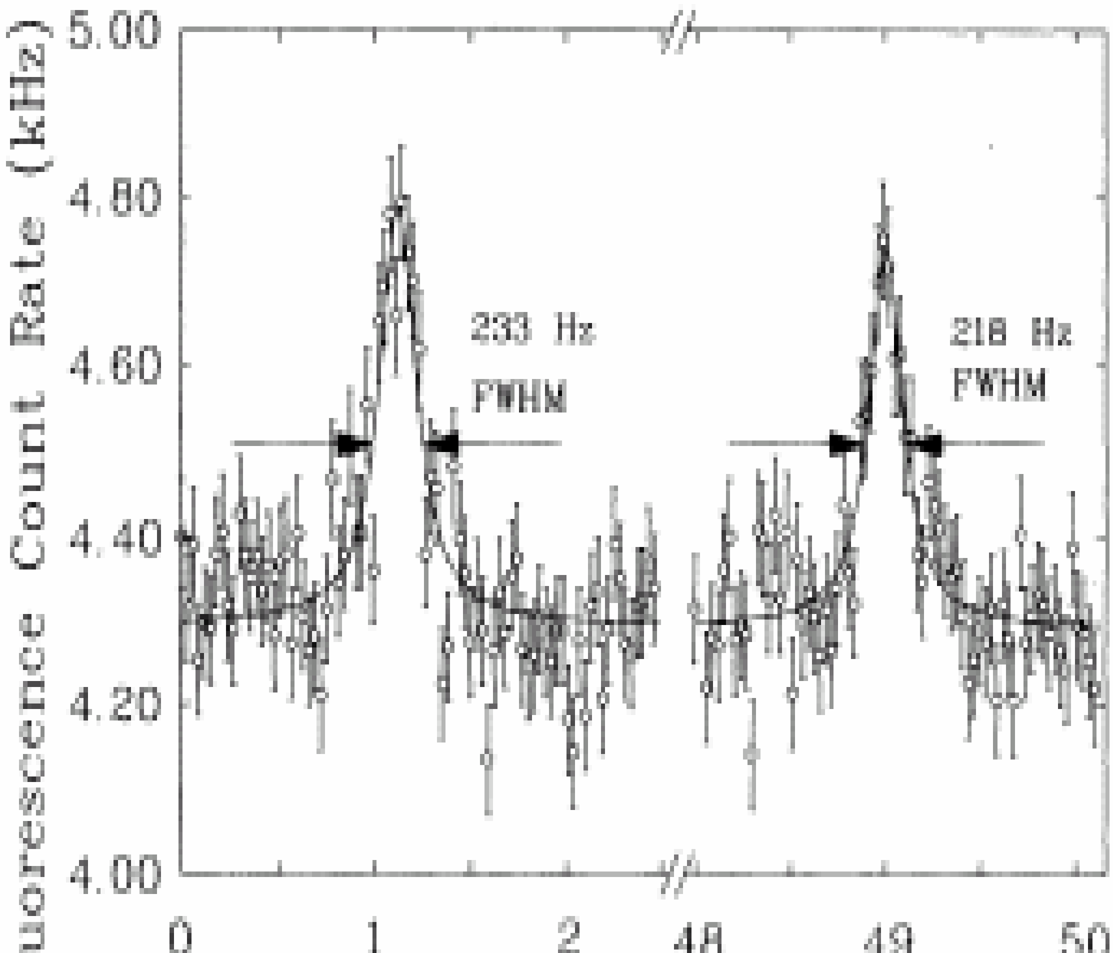

Fluorescence Count Rate (kHz)
5.00
4.80
4.60
4.40
4.20
4.00
233 Hz
FWHM
218 Hz
FWHM
0
1
2
48
49
50
rf Frequency + 10 017 418 (kHz)

# Features of ion traps

- Storage time:

  minutes - days

  **(depending on background gas conditions)**

- Detection sensitivity:

  Single ion

- Storage Capacity:

  $\sim 10^6$ ions/cm$^3$

  **(limited by space charge)**

- Ion oscillation amplitude:

  mm - μm

  **(depending on ion temperature)**

- Ion temperature:

  $10^4$K - 0.1 mK

  **(depending on cooling method)**

# Principle of the Penning trap

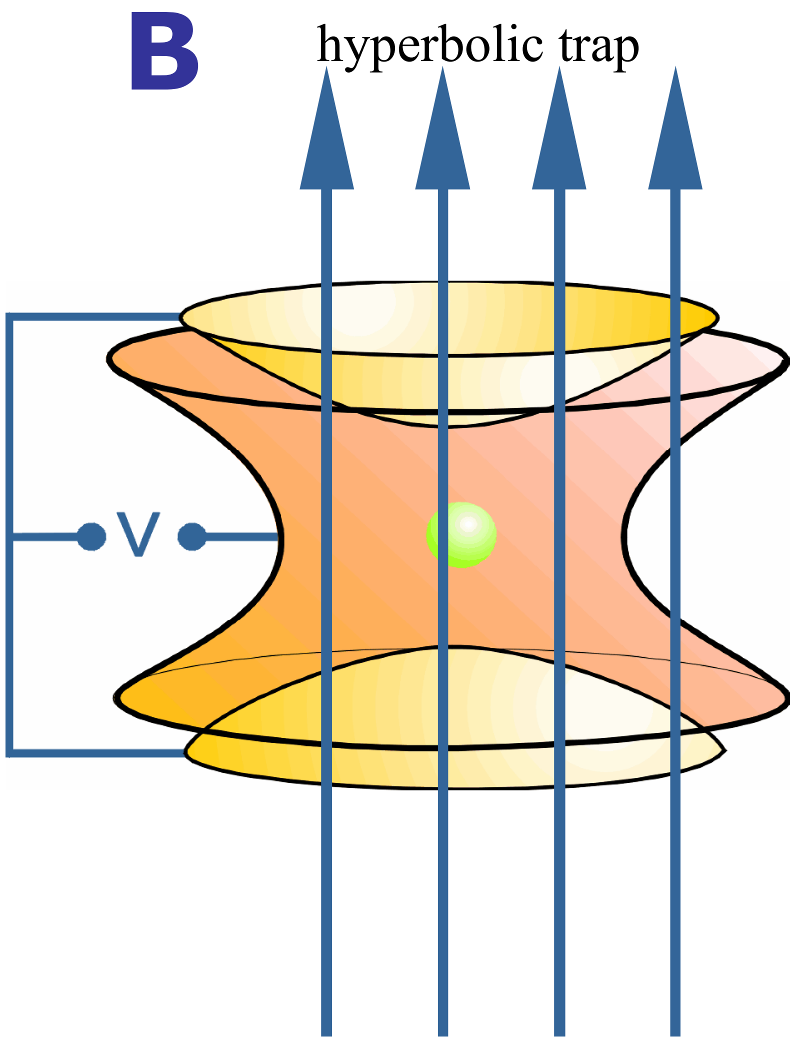


$$\Phi = \frac{U}{r_0^{\ 2}}(x^2 + y^2 - 2z^2)$$

**confinement in axial direction by electrostatic field**

**confinement in radial direction by strong homogeneous magnetic field**

# Trap geometries

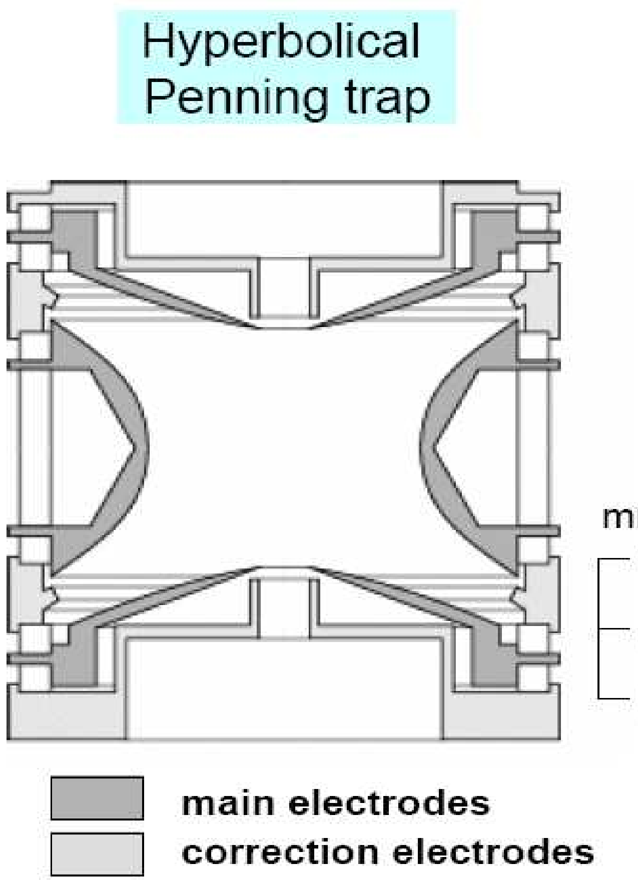


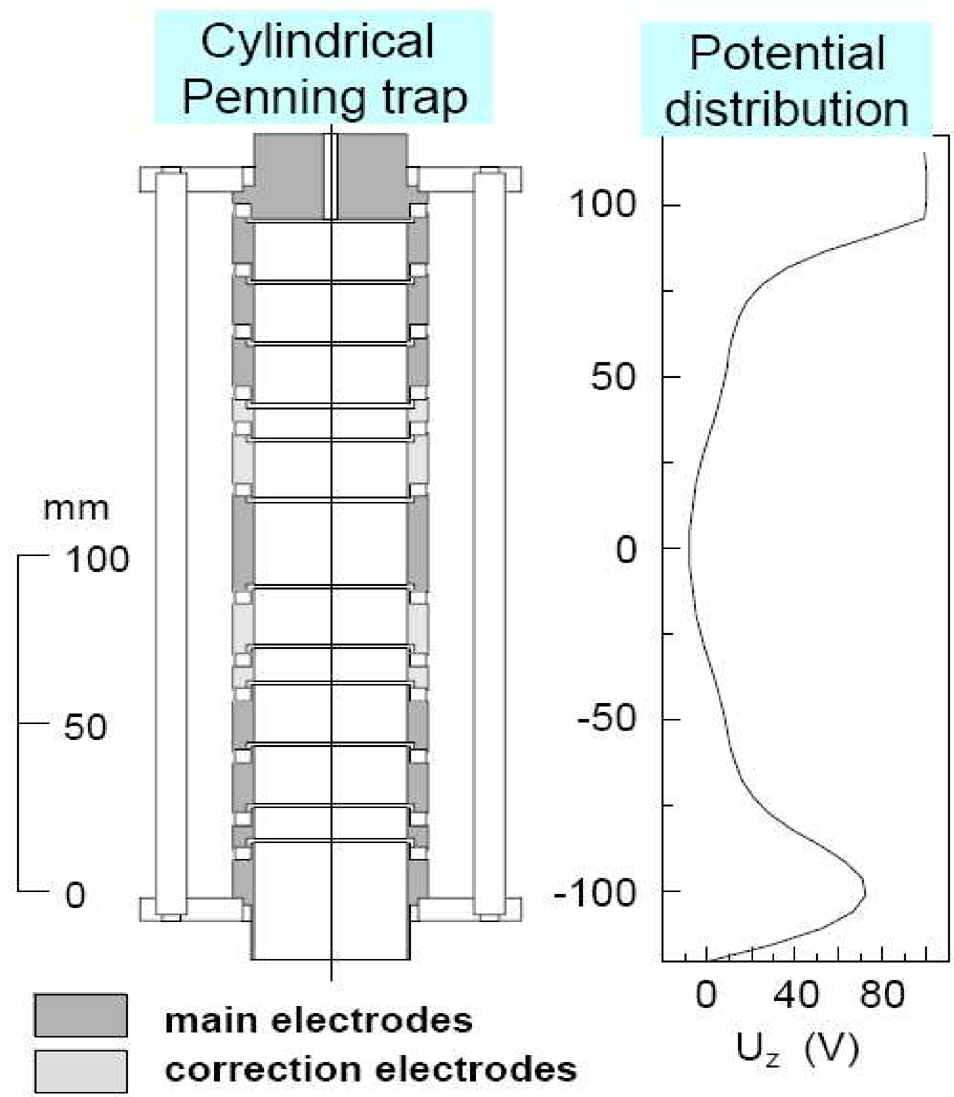

**Electric quadrupole field and homogeneous magnetic field in axial direction**

## Force acting on charged particle in 3D:

$$\vec{F} = -e \nabla \Phi + e(\vec{v} \times \vec{B})$$

$$\Phi = \frac{U_0}{2d^2}(2z^2 - x^2 - y^2)$$

**Equations of motion:**

$$\frac{d^2x}{dt^2} - \omega_c \frac{dy}{dt} - \frac{1}{2}\omega_z^2 x = 0 \quad (1)$$

$$\frac{d^2y}{dt^2} + \omega_c \frac{dx}{dt} - \frac{1}{2}\omega_z^2 y = 0 \quad (2)$$

$$\frac{d^2z}{dt^2} + \omega_z^2 z = 0 \quad (3)$$

$$\omega_c = \frac{e}{m} B$$

Axial direction: Harmonic oscillation: $z(t) = Z(0)e^{-i\omega_z t}$

$$\omega_z = \sqrt{\frac{eU}{md_0^2}}$$

Radial direction: decouple (1) and (2) via: $u(t) = R_+ e^{-i\omega_+ t} + R_- e^{-i\omega_- t}$

$u = x + iy$

Eigenfrequencies:

$$\omega_+ = \frac{\omega_c}{2} + \sqrt{\frac{\omega_c^2}{4} - \frac{\omega_z^2}{2}}$$ modified cyclotron frequency

$$\omega_- = \frac{\omega_c}{2} - \sqrt{\frac{\omega_c^2}{4} - \frac{\omega_z^2}{2}}$$ magnetron frequency

$$\omega_c = \frac{e}{m} B$$

Hierachy of frequencies: $\omega_+ >> \omega_z >> \omega_-$

# Stability limit in a Penning trap

$$\omega_c{}^2 \geq 2\omega_z{}^2$$

$$\frac{e}{M}B^2 \geq \frac{8U}{r_0{}^2}$$

**Numerical examples:**
**B=1T, $r_0$=1 cm the maximum trap voltage for stable confinement for m=100 a.u. : 20 V**
**for electrons at B=100 G, $r_0$=1 cm: $U_{max}$= 400 V**

# Single particle motion in a Penning trap

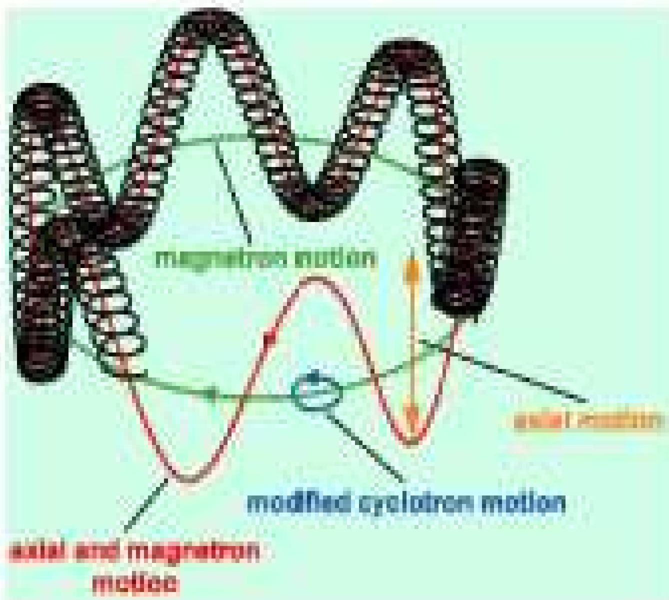


F is ∞ to charge e (or q)

Typical frequencies
$q$ = e, $m$ = 100 u,
$B$ = 6 T

$\Rightarrow$ $f_- \approx 1$ kHz
$f_+ \approx 1$ MHz

**Stability limit:**

$$\omega_c^2 \geq 2\omega_z^2$$

$$\frac{e}{m}B^2 \geq \frac{8U}{d^2}$$

## important relations

$$\omega_c = \omega_+ + \omega_-$$

$$\omega_c^2 = \omega_+^2 + \omega_z^2 + \omega_-^2$$

L.S. Brown, G. Gabrielse, Rev. Mod. Phys. 58, 233 (1986).

# Quantum mechanical eigenstates of particle motion

$$E = (n_+ + 1/2)\hbar\omega_+ - (n_- + 1/2)\hbar\omega_- + (n_z + 1/2)\hbar\omega_z$$

All three motions are independent of each other and can be described as harmonic oscillators.

Negative sign of the magnetron energy indicates the metastability of motion:
larger magnetron radius (higer quantum number) corresponds to smaller potential energy (important for cooling!)

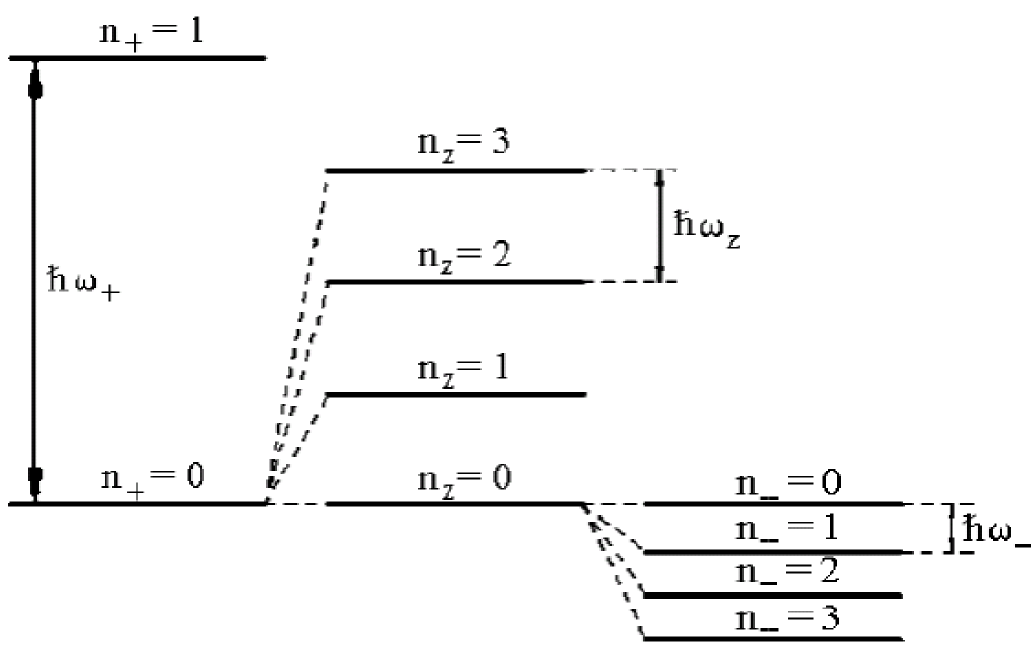

# Experimental motional frequencies in a Penning trap

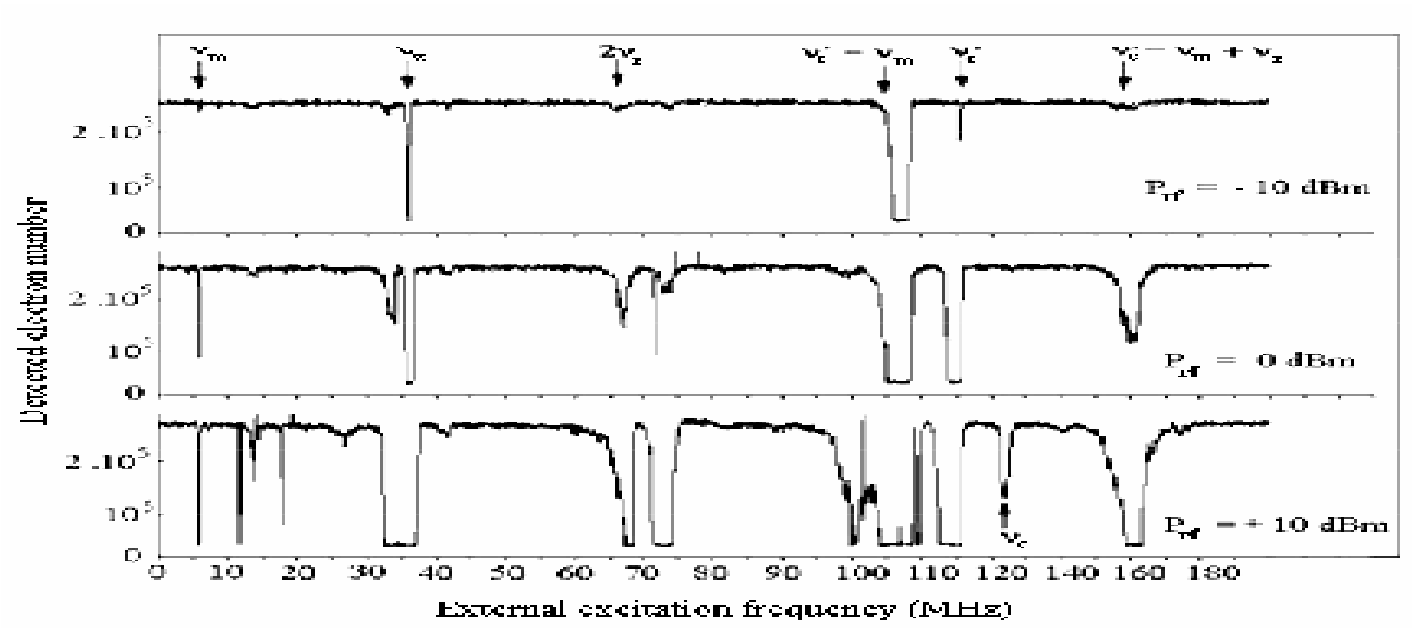


**Excitation of ion oscillations**
**Leads to particle loss at resonance**

# Rotating wall compression of ion clouds
## (Univ. of Calif., San Diego)

**Application of a rotating electric field to segments of the ring electrode:**
**Change of density due to additional centrifugal force**

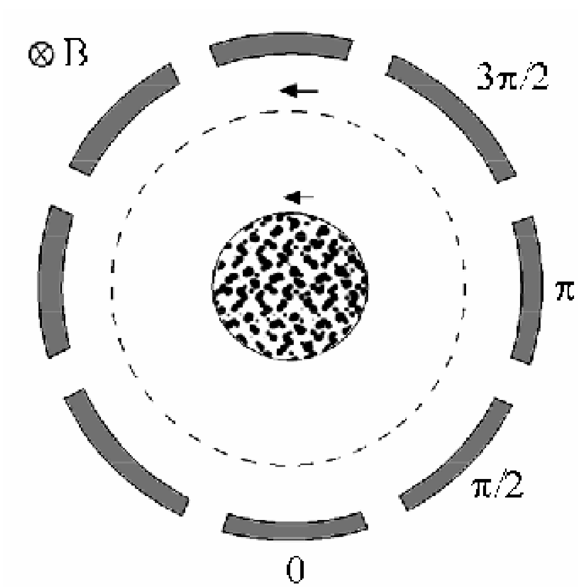


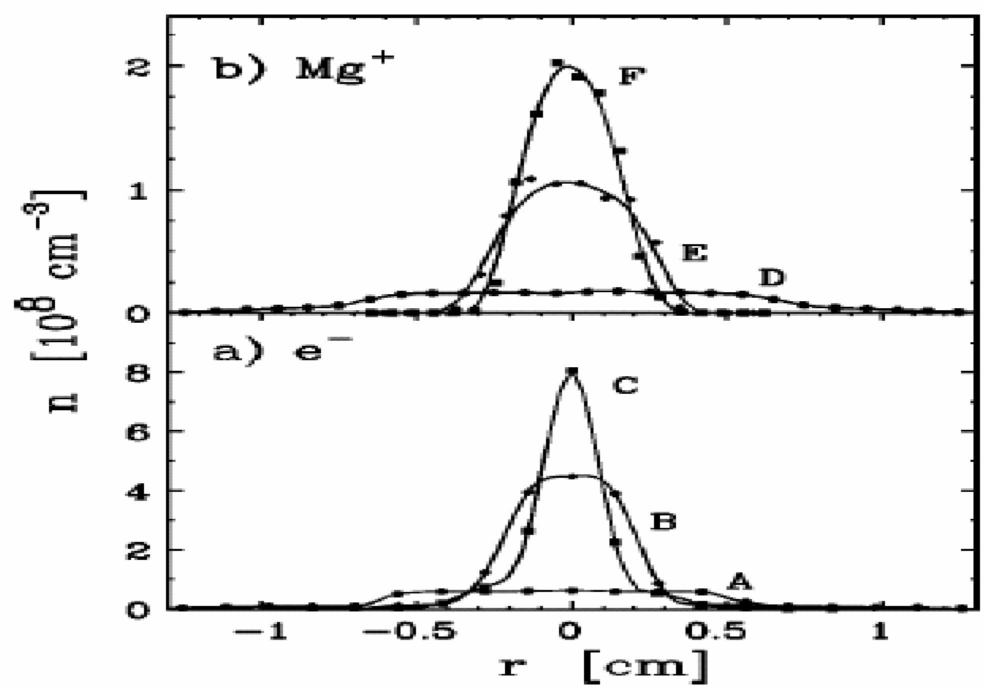

# Effect of background gas collisions

Cyclotron orbit is reduced by damping force
Magnetron orbit is increased due to metastability of magnetron motion
→ ion loss from trap

Coupling of magnetron and cyclotron motion by quadrupole field leads to aggregation of ions near trap center

# Effect of mode coupling on ion trajectory

r.f.field at sum frequency of both oscillations applied between adjacent segments of ring electrode

$$\omega_+ + \omega_- = \omega_c$$

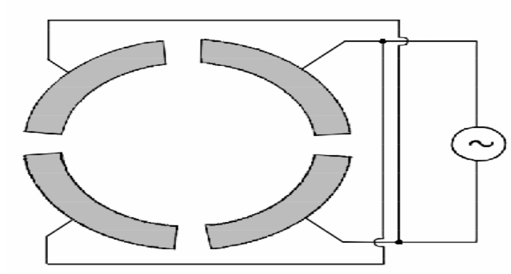

**Ion trajectories with buffer gas collisions:**

Without mode coupling

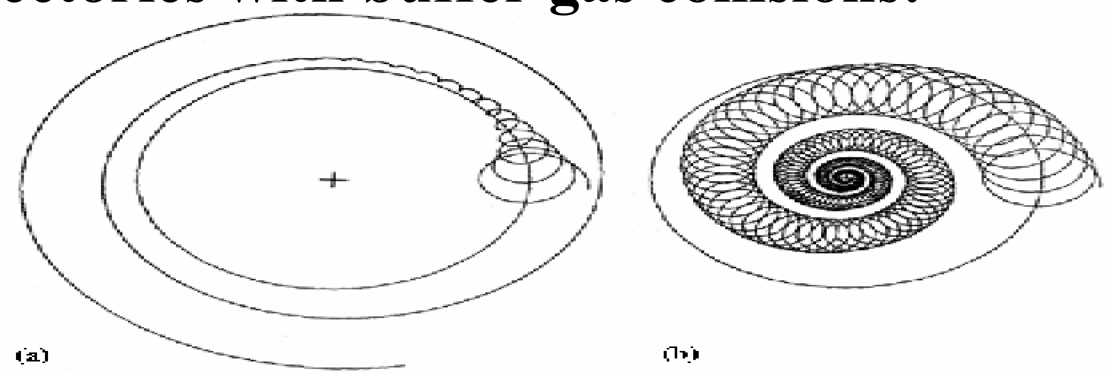


With mode coupling

# Imperfect Penning trap

**Similar as in Paul traps:**

**(a) Shift of eigenfrequencies proportional to**

- **higher order parts in trap potential**
- **magnetic field inhomogeneity**
- **ion energy**
- **Space charge density**

**(b) Instabilitiy of ion motion when**

$$n\omega_z + m\omega_- = k\omega_+$$

**n,m,k integer**

# Space charge shift of motional frequencies

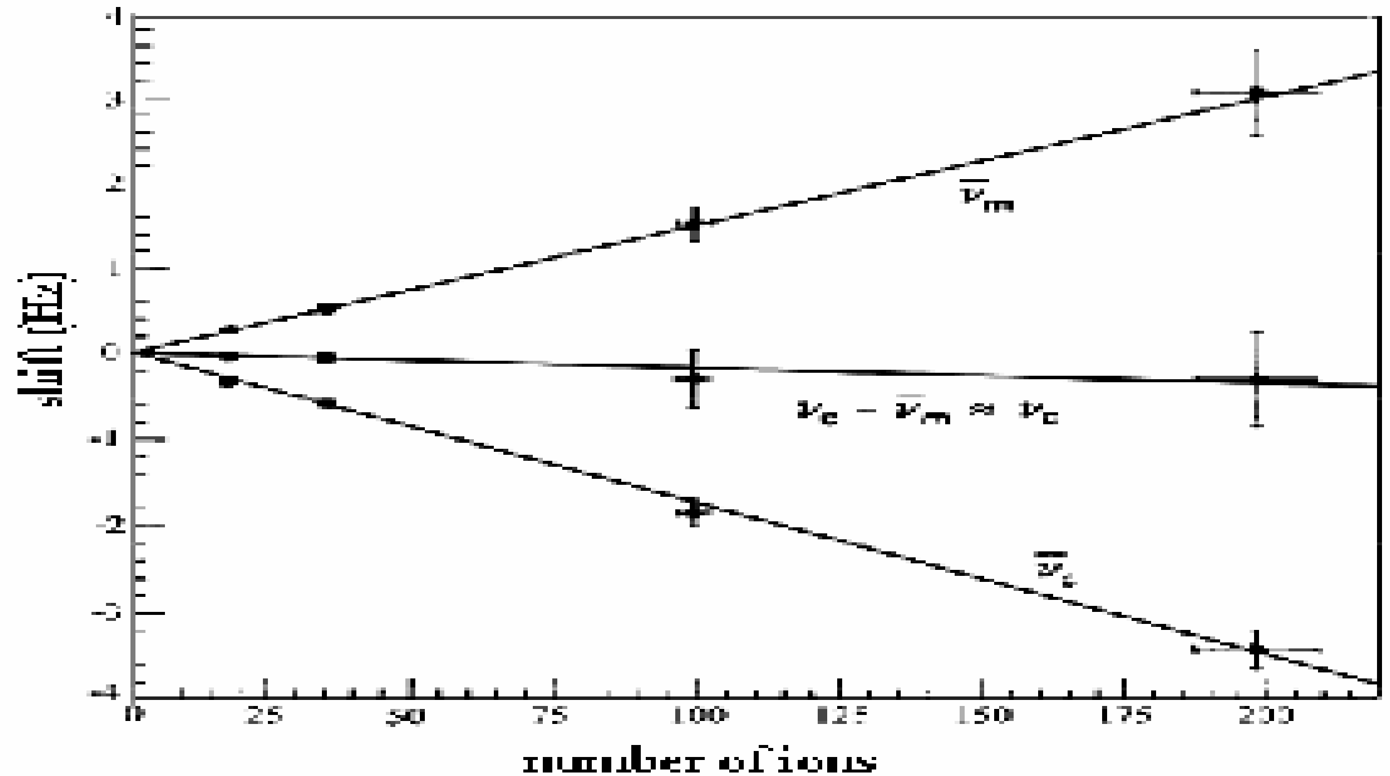


$$\nu_+ + \nu_- = \nu_c$$

# Observed Instabilities for electron confinemet

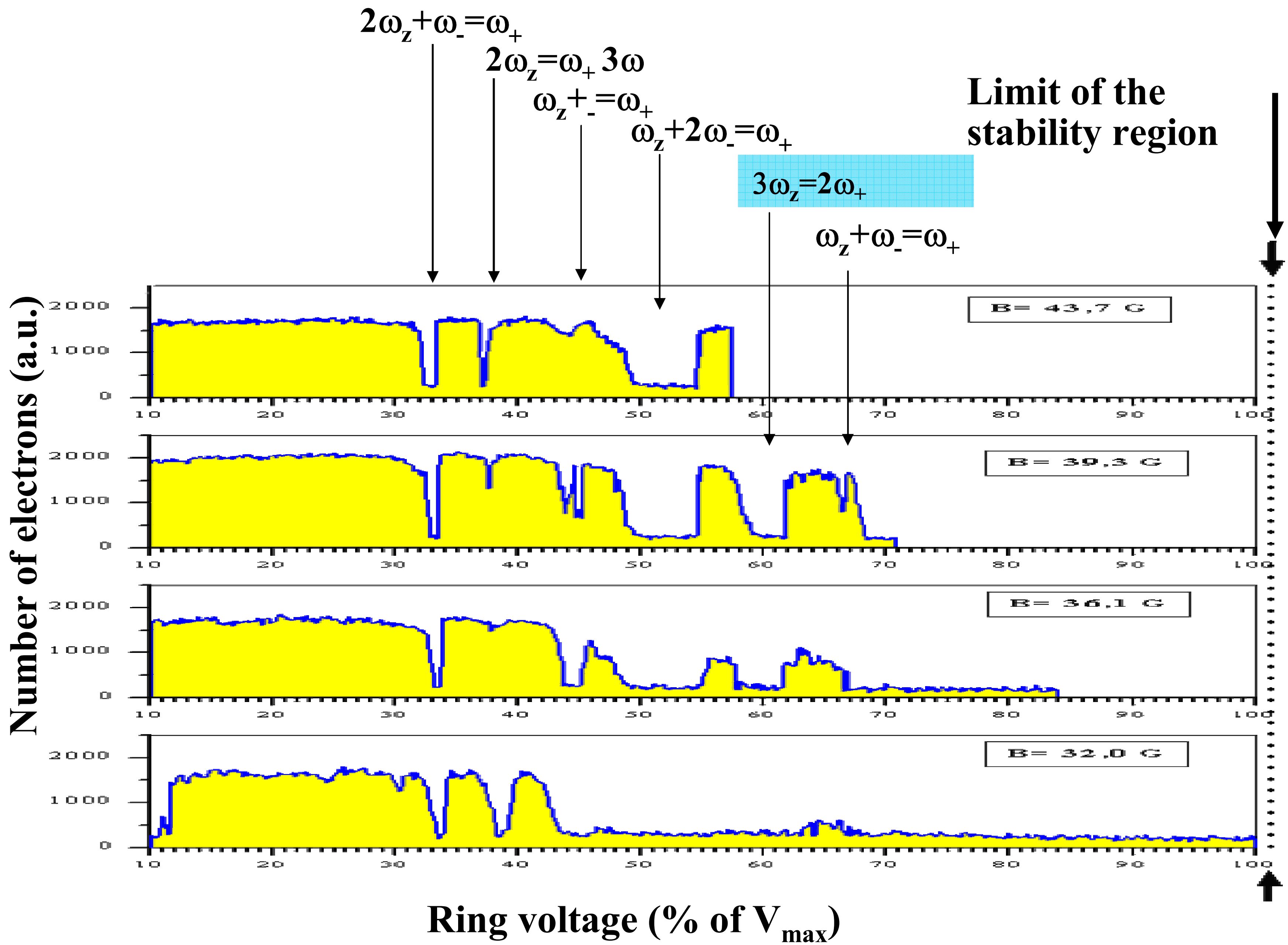

# Instabilities in a Penning trap for different storage times

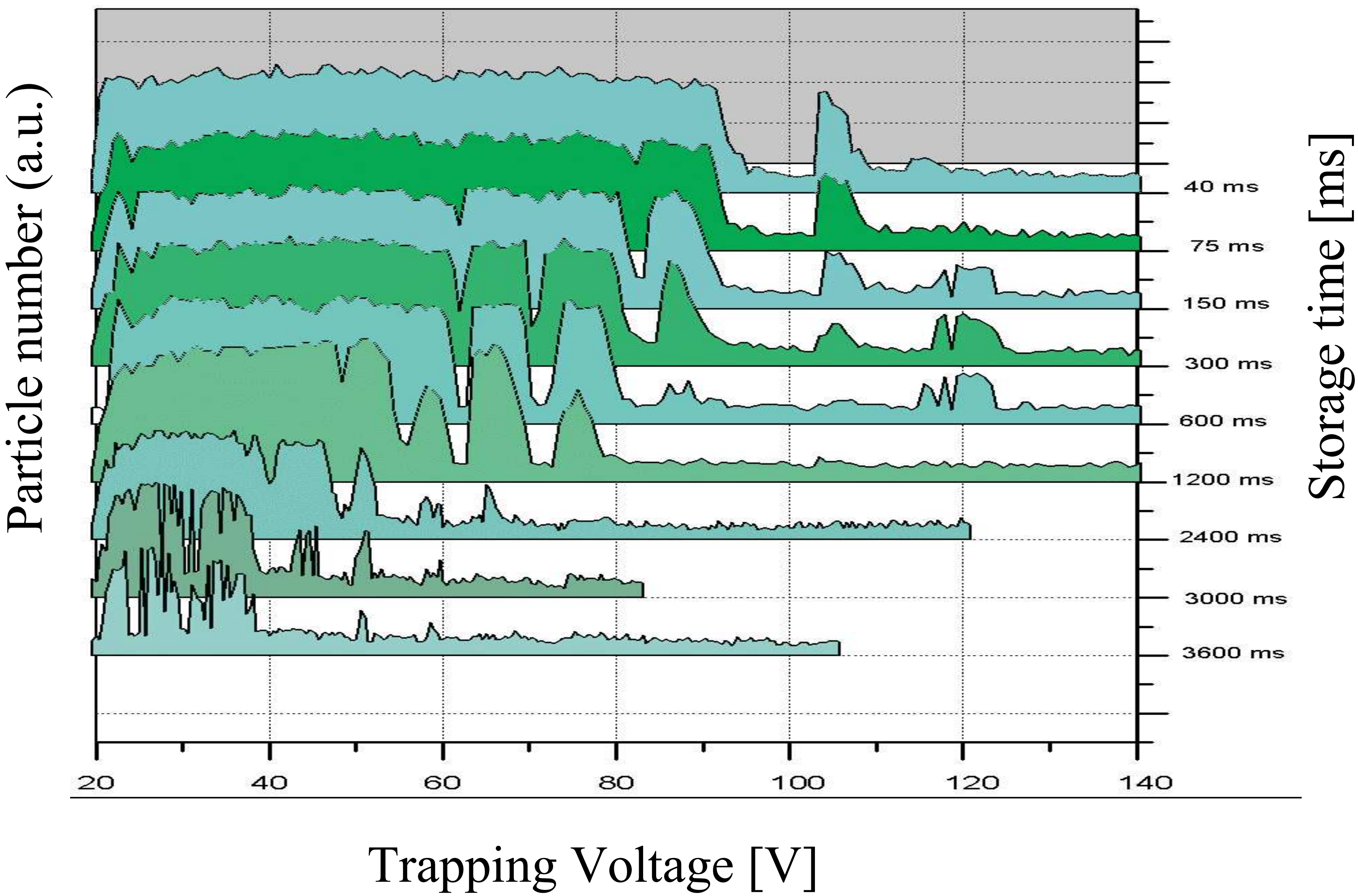

# Ion Detection

## Destructive detection:

**Ejection from trap by high voltage puls**

**Sensitivity: single ion**

## Non-destructive detection:

**(a) Absorbtion of energy from tank circuit at room temperature**

**Sensitivity: $10^3$ ions**

**(b) Induced noise in tank circuit**

**Sensitivity: single ion (at 4 K)**

**(c) optical detection**

**Sensitivity: single ion**

# Cylindrical Trap with detection circuit attached to endcap electrode

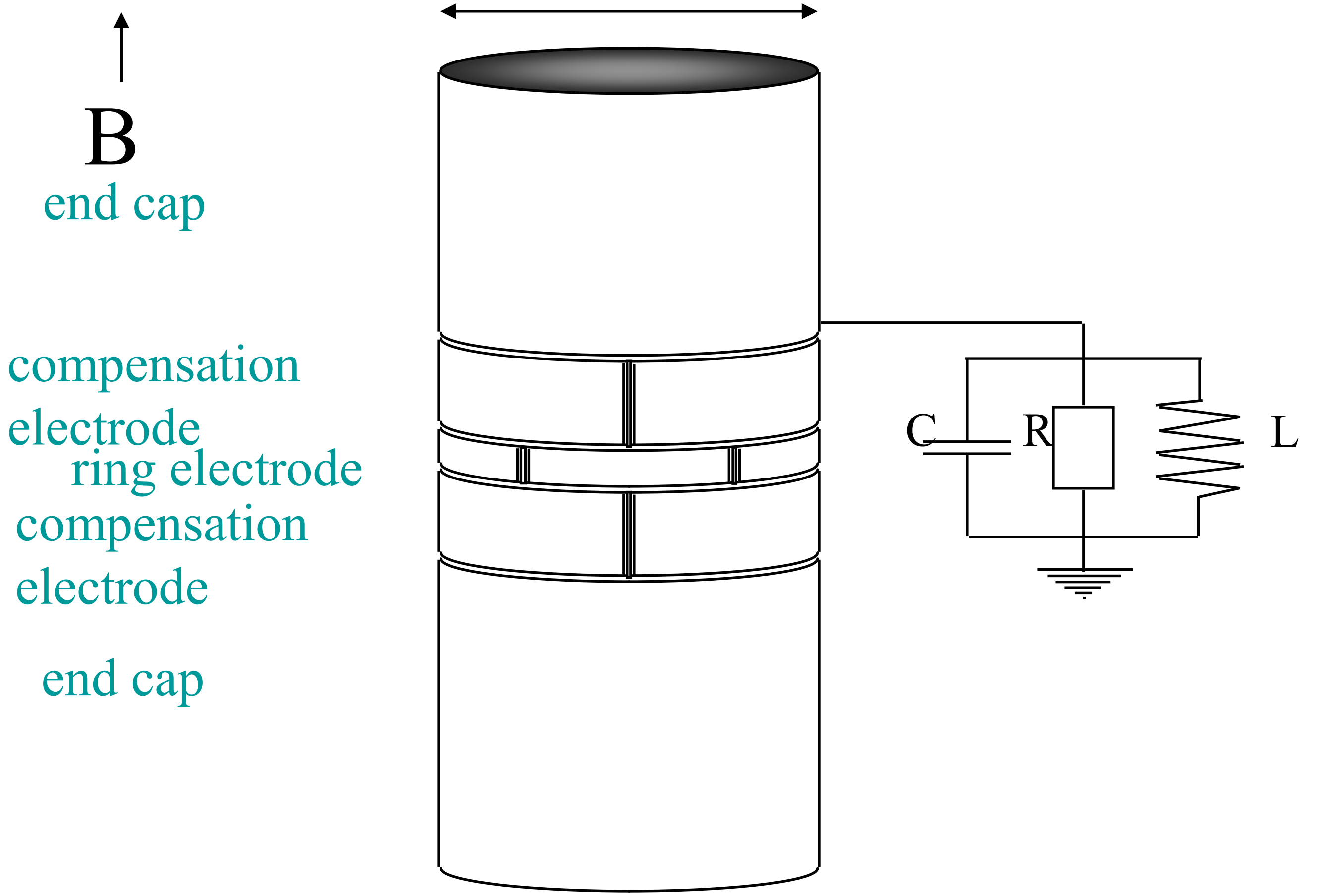

# Detection of stored ions by induced voltage in endcap electrode

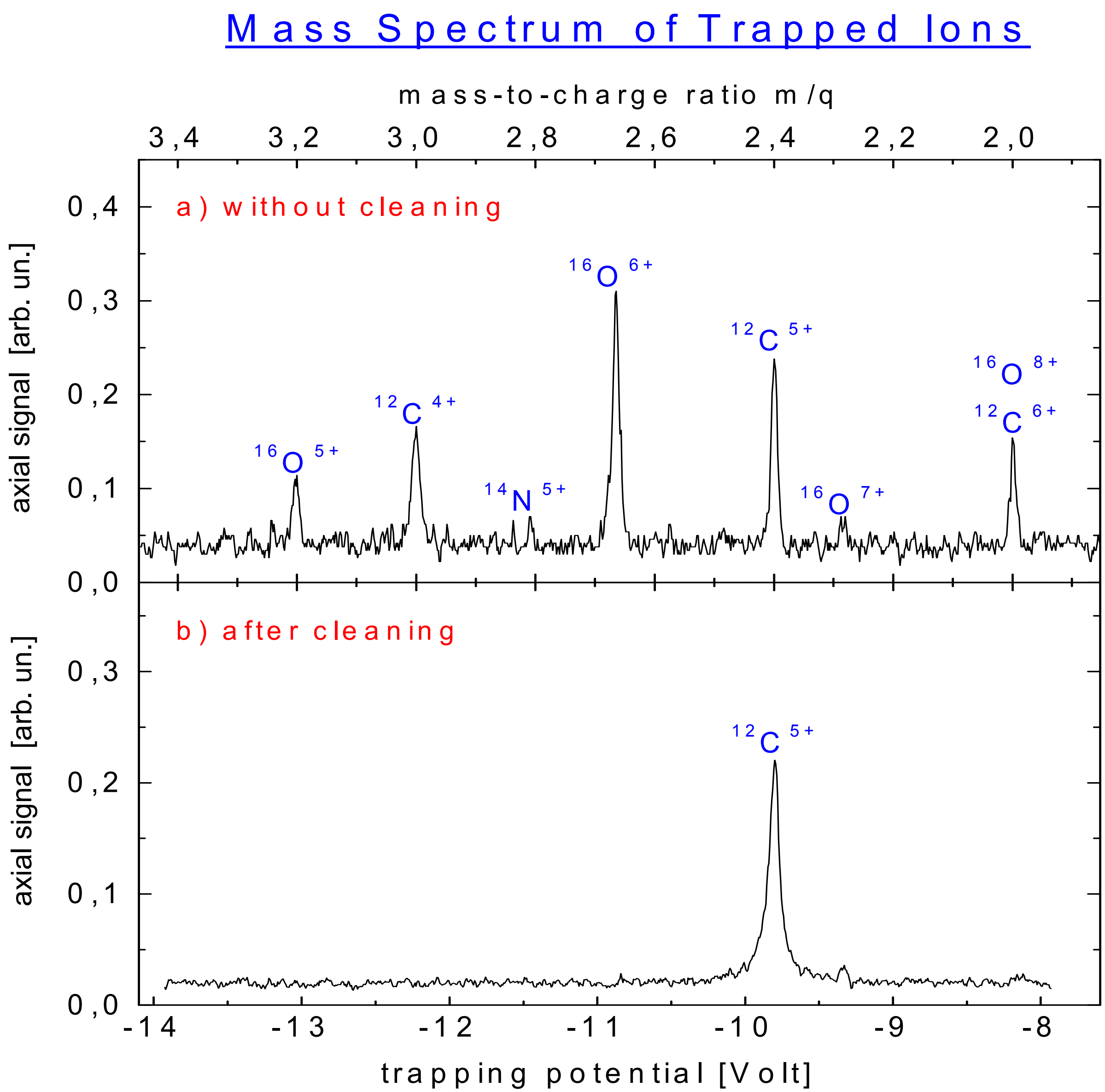

# Induced noise from individual electrons

Dehmelt 1987

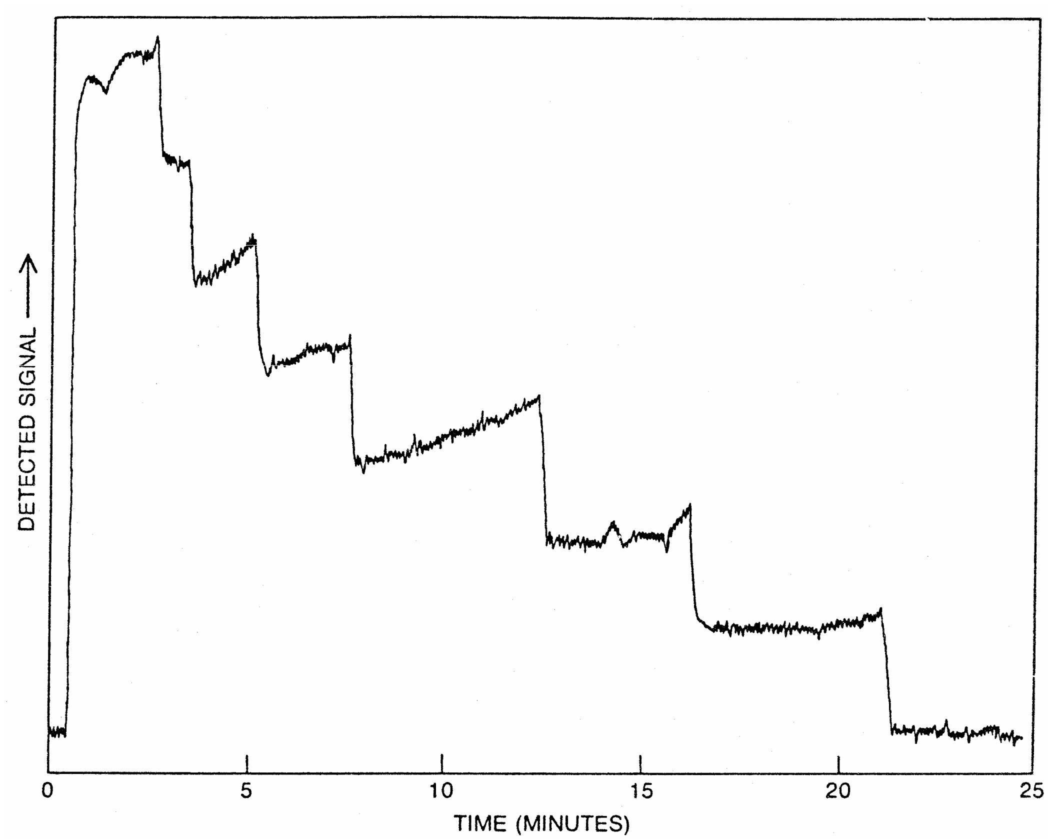

# Fourier transform of induced noise in ring electrode at the cyclotron frequency in an inhomogeneous magnetic field

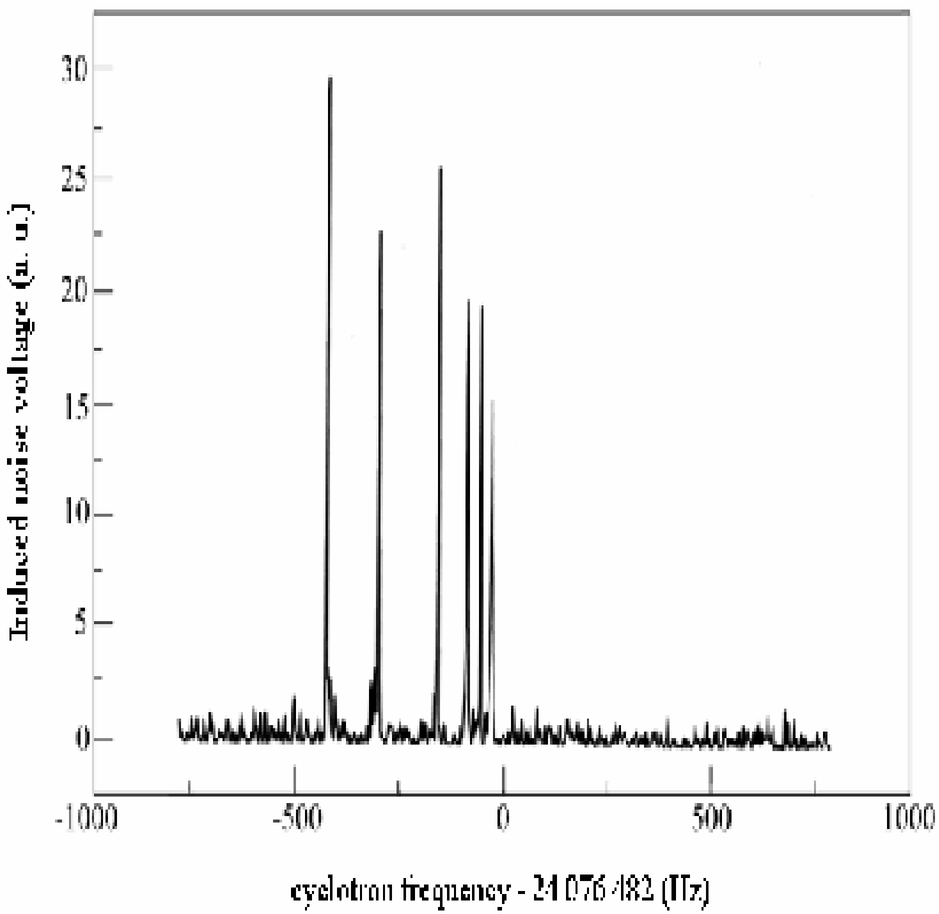


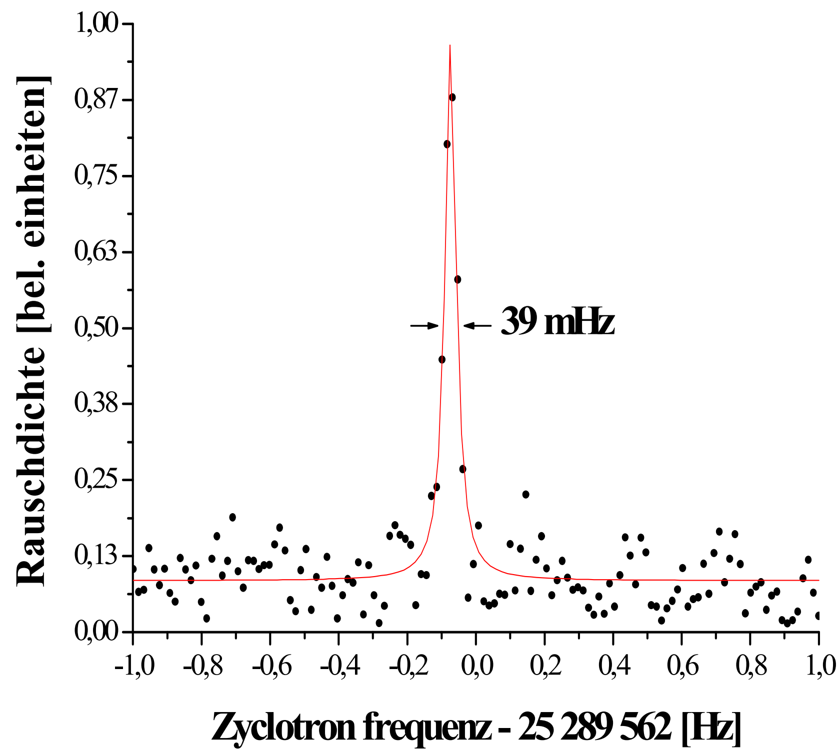

# Resistive cooling of a single ion ($C^{5+}$)

**Exponential energy dissipation through resistor**

**Time constant: $\tau=(2z_0/q)^2\,(m/R)$**

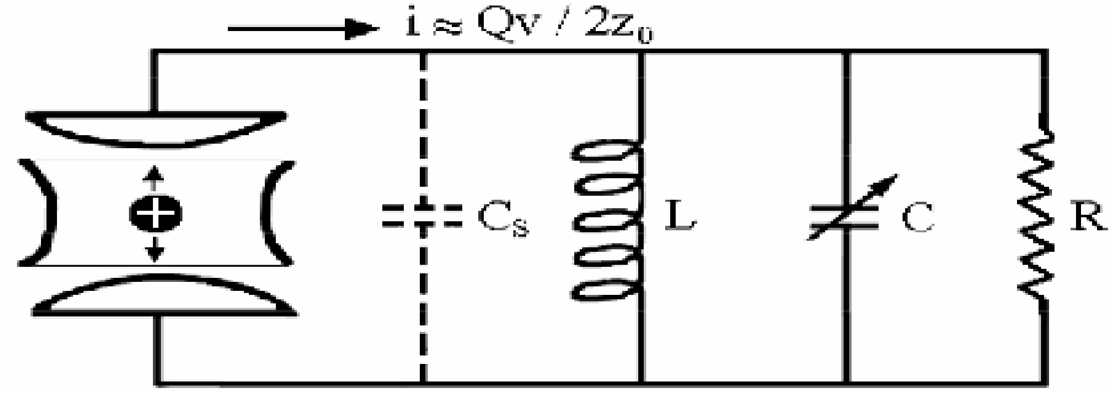


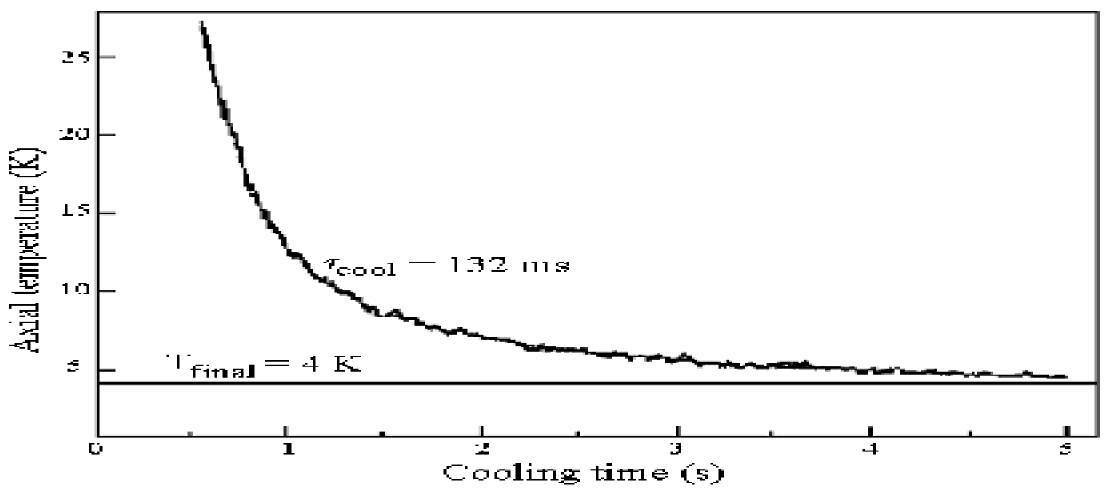

## Cooling of an ion cloud:

Resistive cooling applies only to center-of-mass motion.

Individual ion oscillation is coupled to center-of-mass through Coulomb interaction.

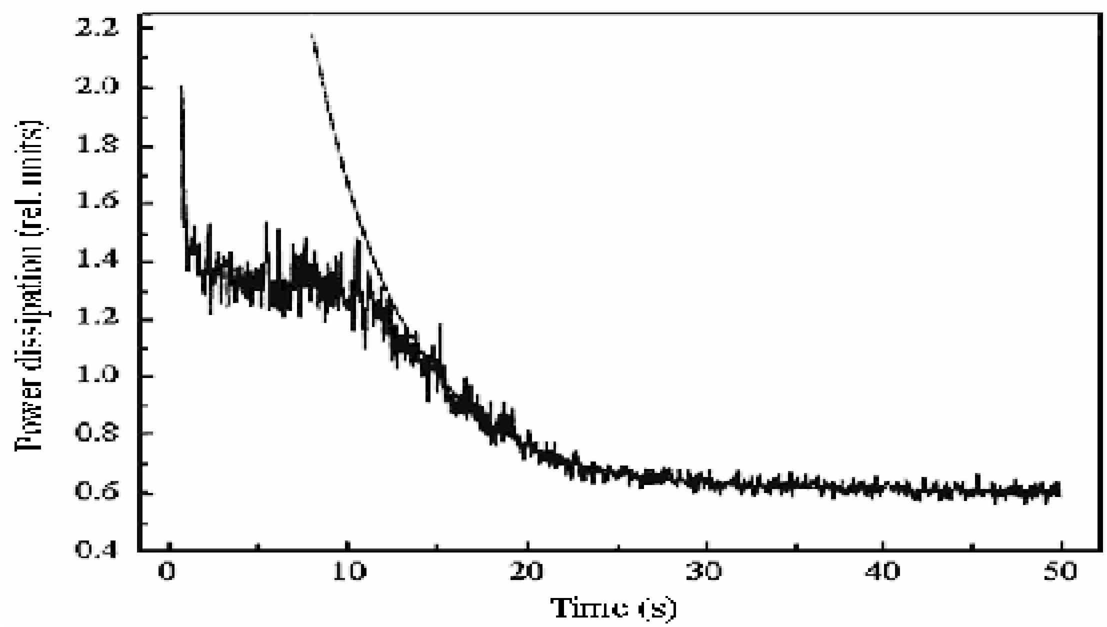


**Cooling of an ion cloud: 2 time constants**

# Detection od a single ion in thermal equilibrium
# Fourier Transform of noise in axial circuit

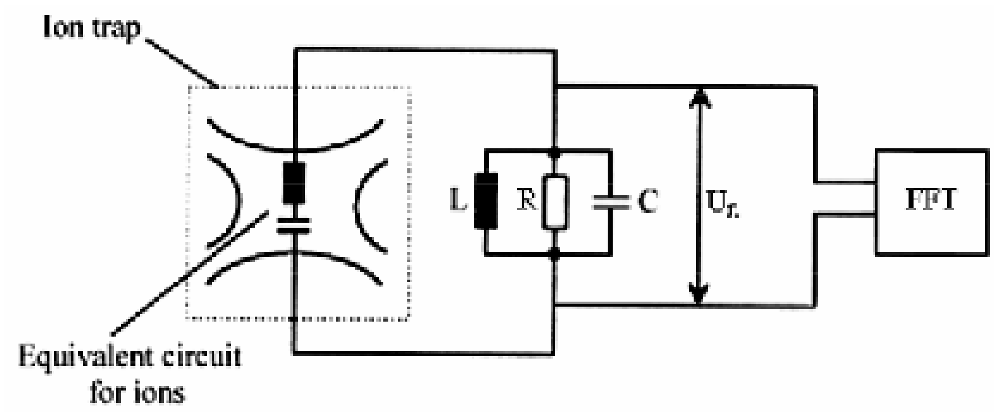


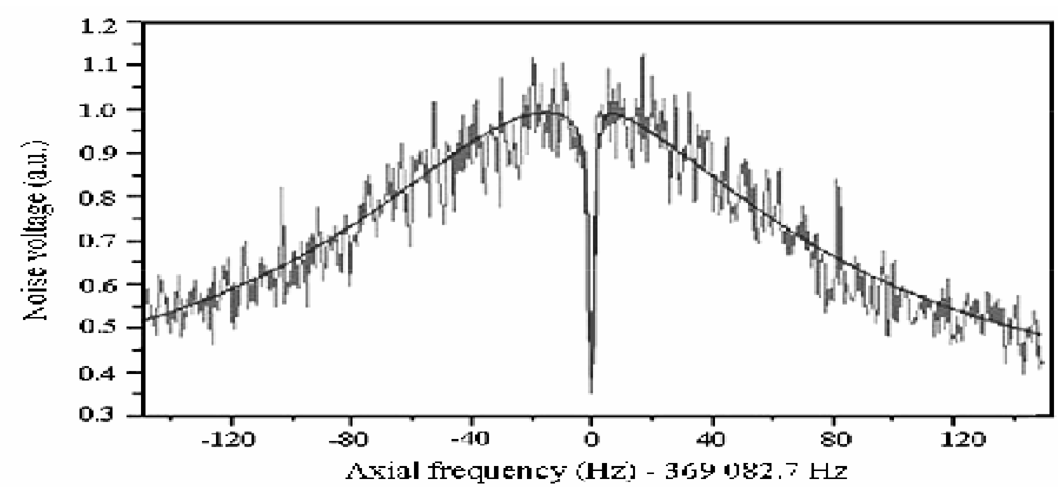

# Optical detection of ions in Penning trap

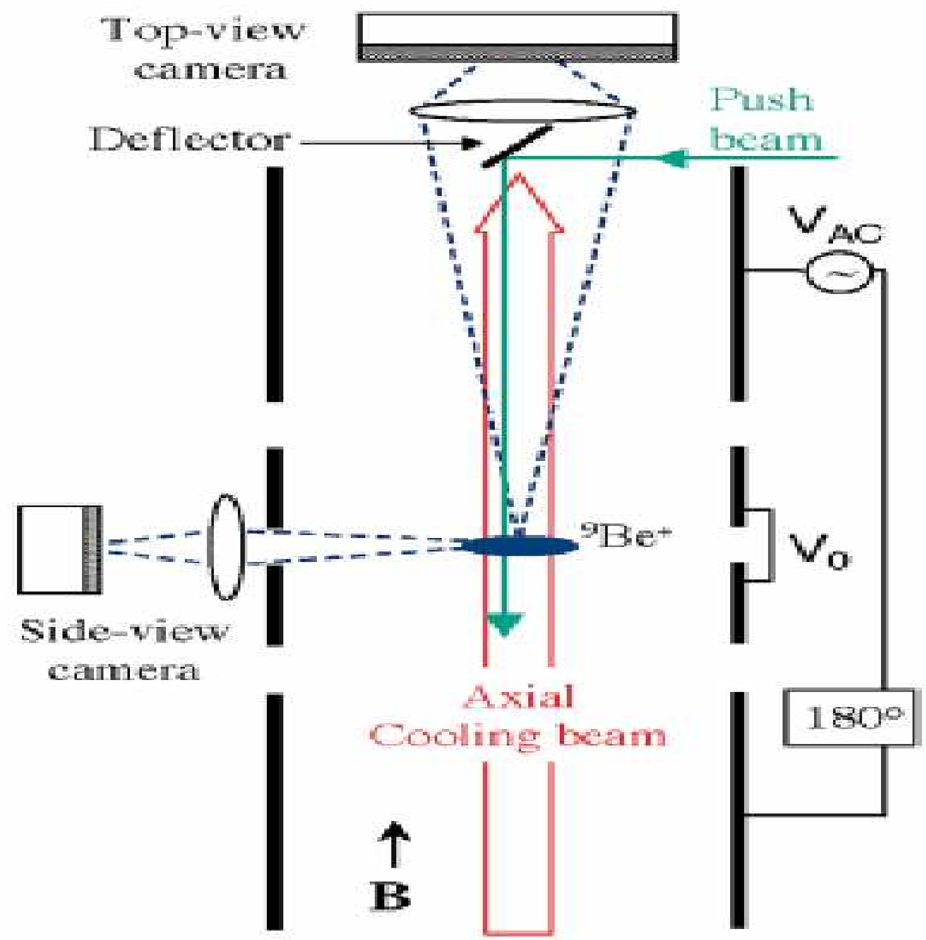


Fluorescence images taken for differents phases
and amplitudes of the excitation voltage $V_{ac}$

Bollinger et al., NIST

# Observation of plasma oscillations of an ion cloud

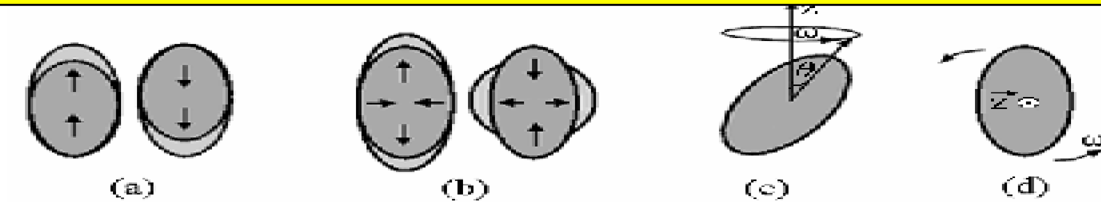


dipole quadrupole tilt asymmetry

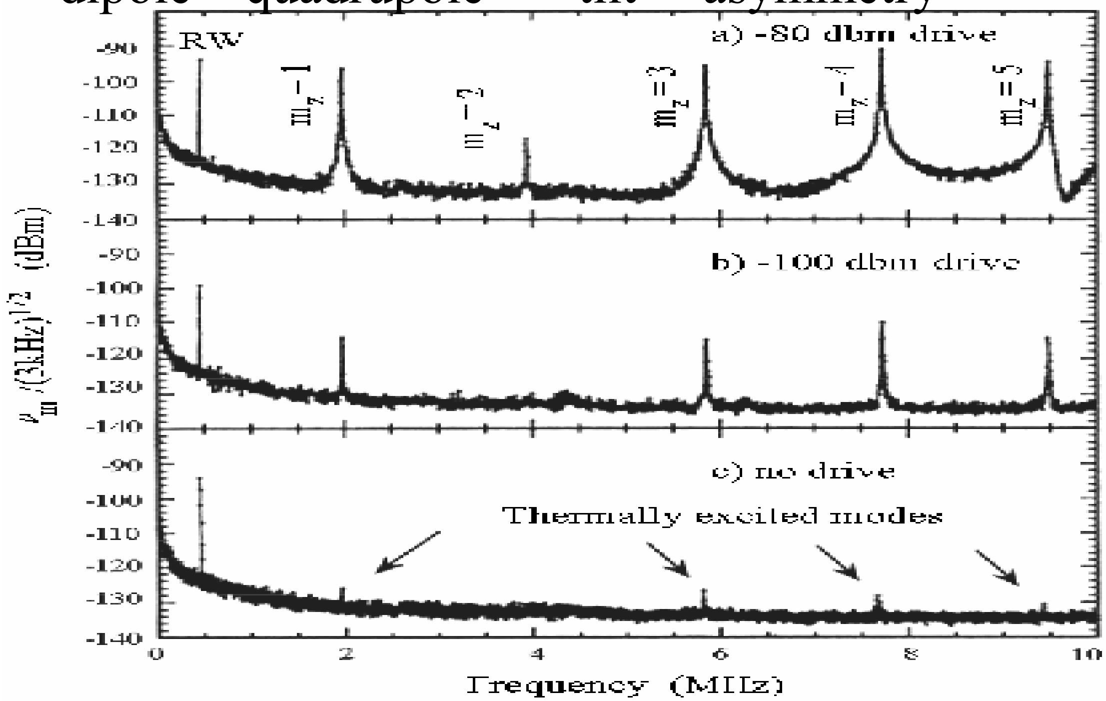


**Observation by induced noise in trap electrodes**

F. Anderegg et al., PRL 90, 115001 (2003)

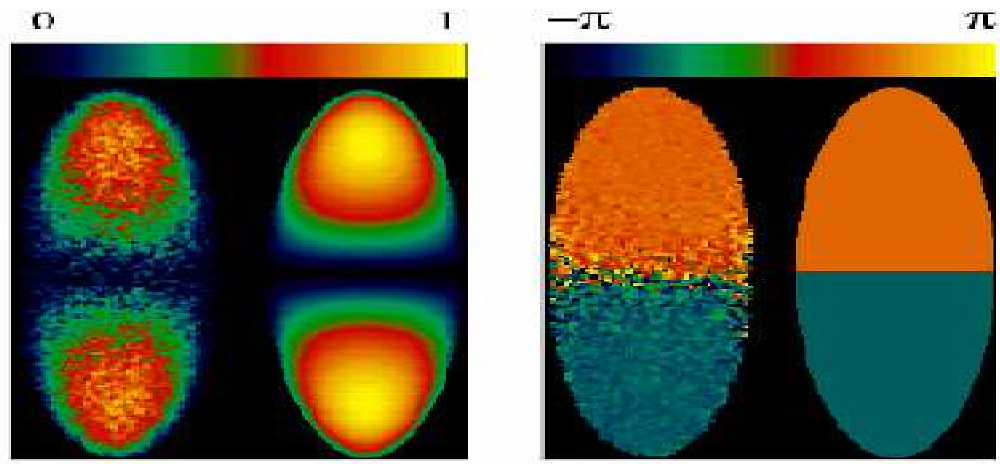


(a) (b)

Amplitude (a) and phase (b) of the (2.0)-mode
by Doppler imaging
left: experiment; right: simulation

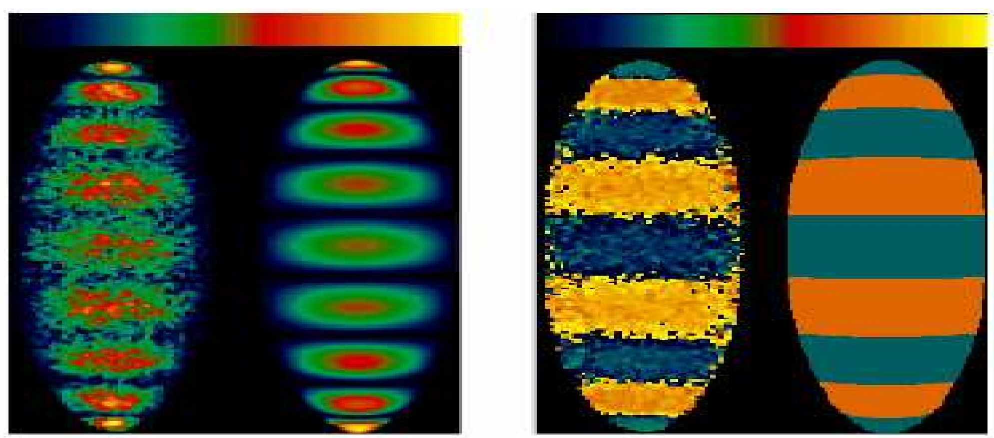

(9,0)-mode

Mitchell et al, opt. Express 2, 314 (1998)

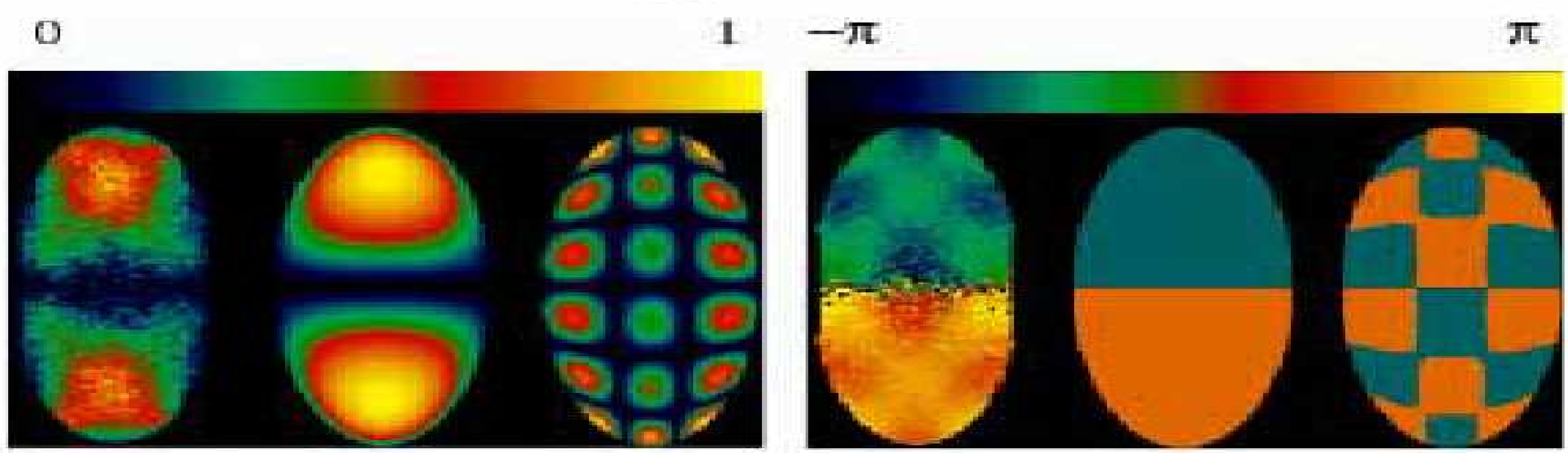


**Mitchell et al, opt. Express 2, 314 (1998)**

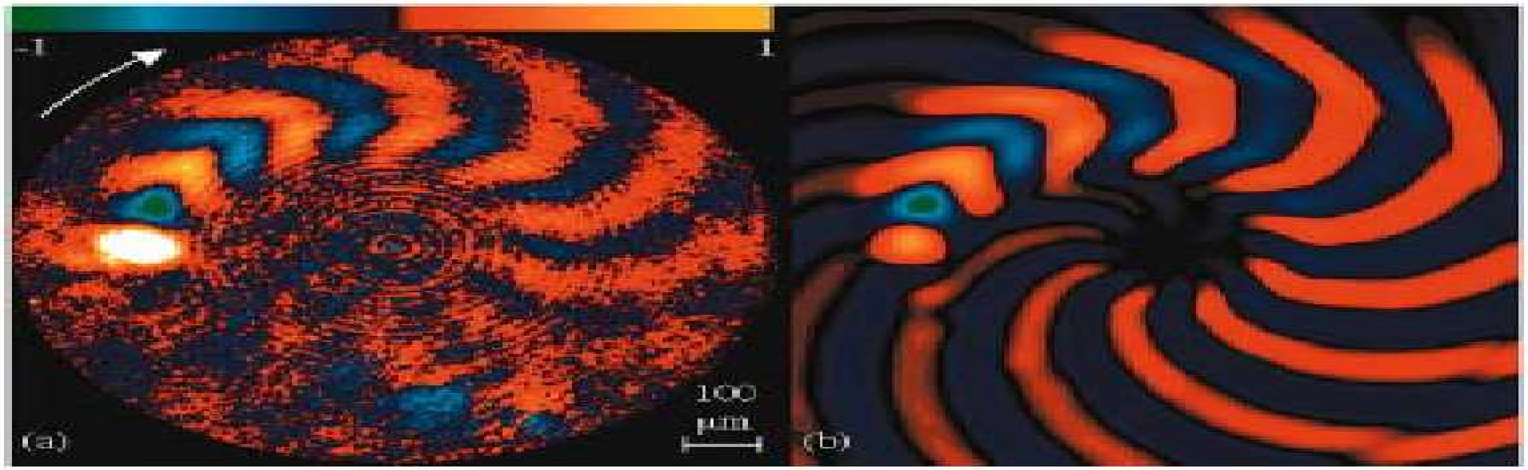


Top-view images of the differential intensities, proportional to the ion velocities, induced by a laser push beam (white spot) incident on a disk-shaped ion
plasma rotating clockwise. (a) shows experimental results while (b) shows the prediction from theory.

Mitchell et al, opt. Express 2, 314 (1998)

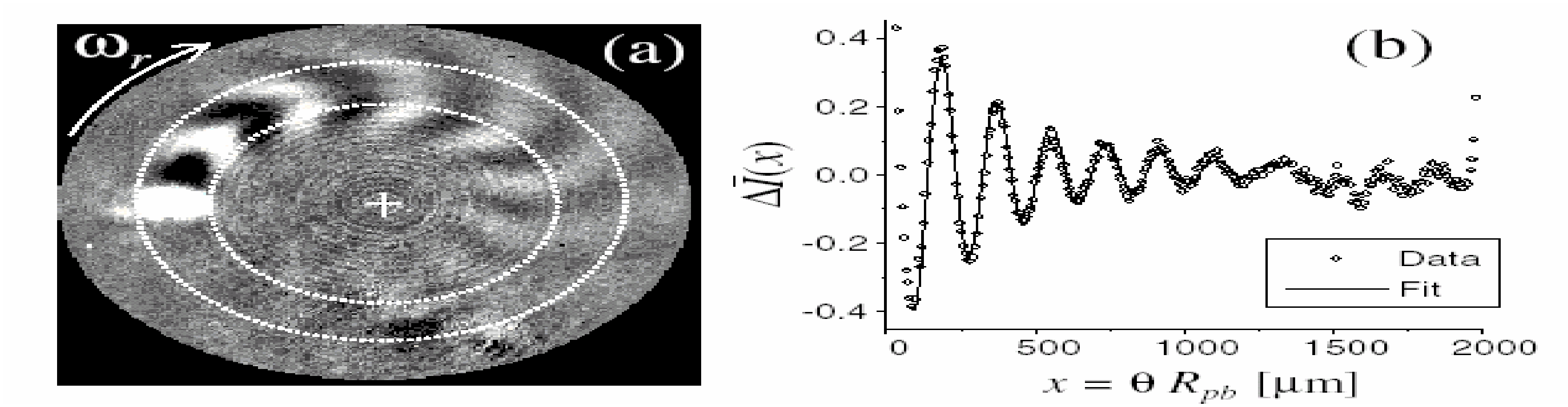


(a) Differential top-view image of a laser-induced wake in a clockwise rotating Be+ ion crystal.
(b)Average fractional change in fluorescence for the annular region between the white circles in (a). $x = 0$ is defined to be at the centre of the push beam. The solid curve is a fit to the data using a damped sinusoid

J.J. Bollinger et al.,J. Phys. B: At. Mol. Opt. Phys. **36** (2003) 499–510

# Alternative trap geometries

- Multiple traps
- Planar traps

# Pentatrap (Max-Planck Inst., Heidelberg)

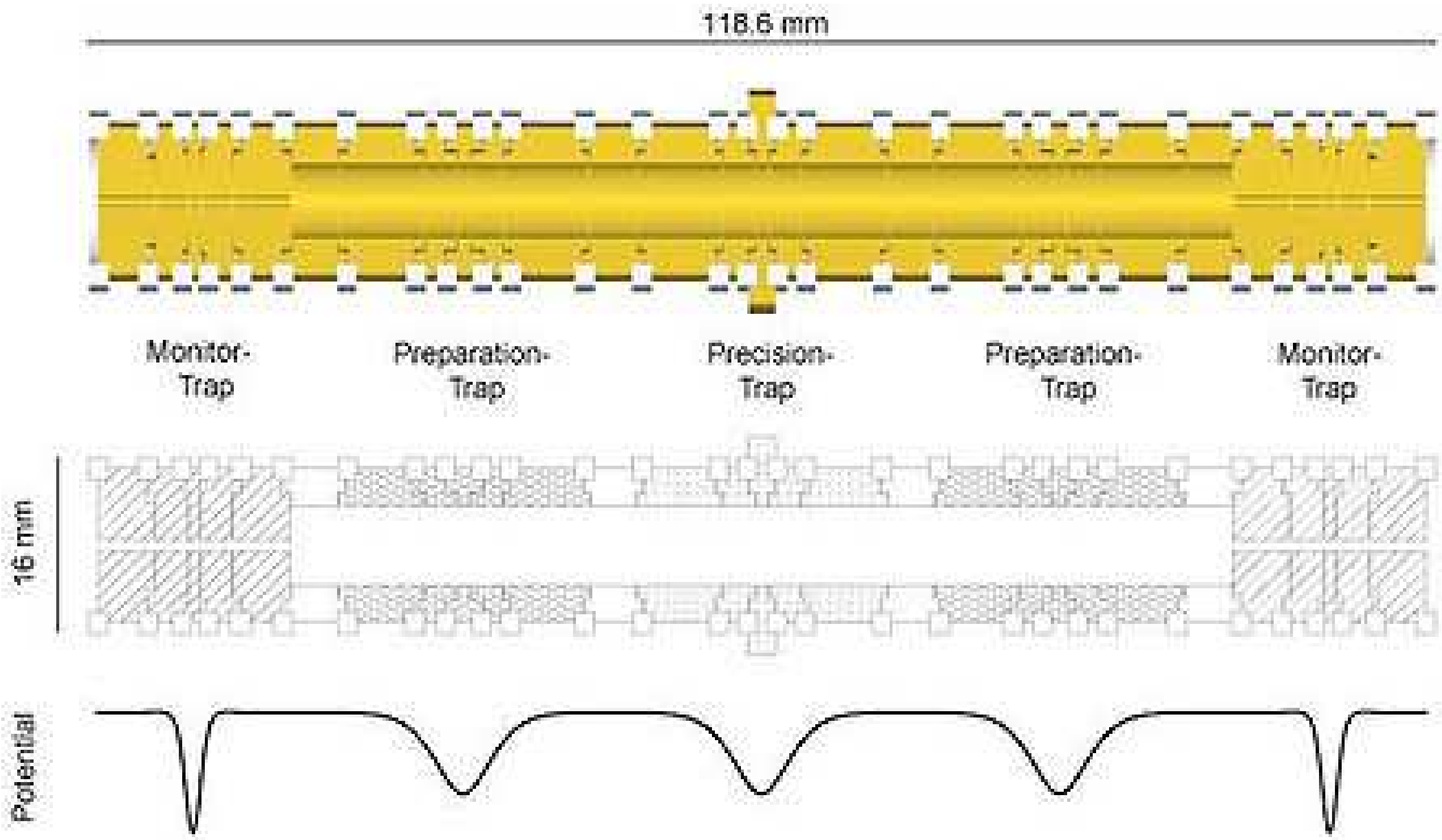

# A planar Penning trap

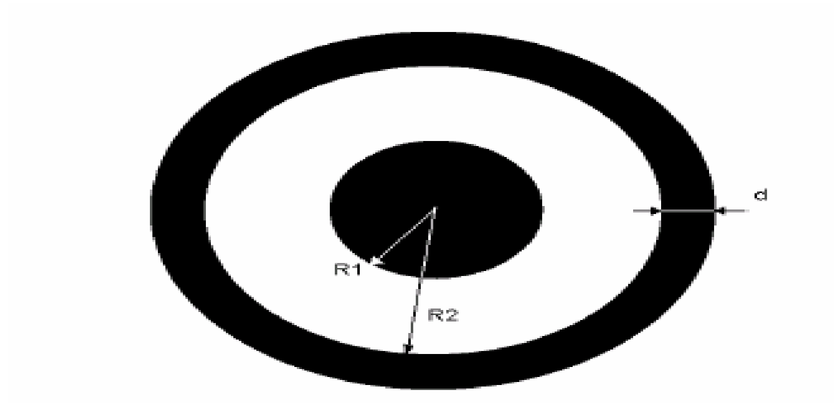


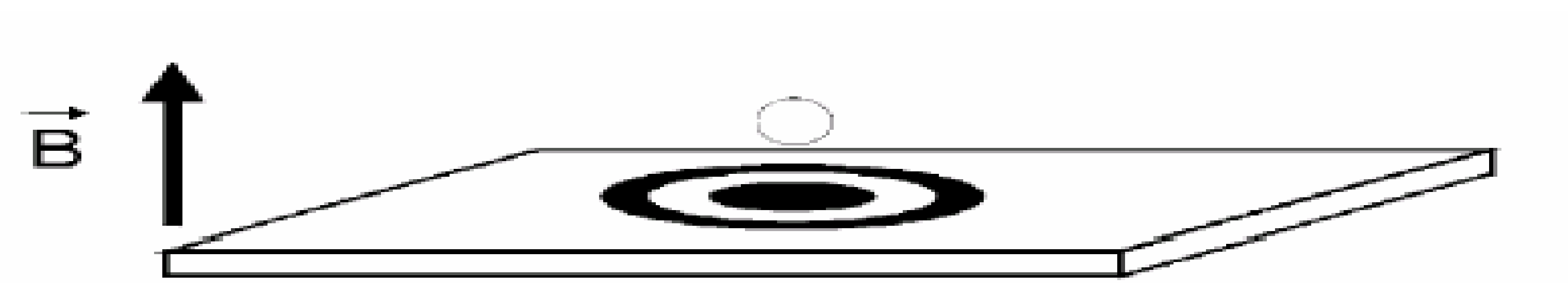

# Axial potential of the planar Penning trap
## (2 concentric ring electrodes, infinite ground)

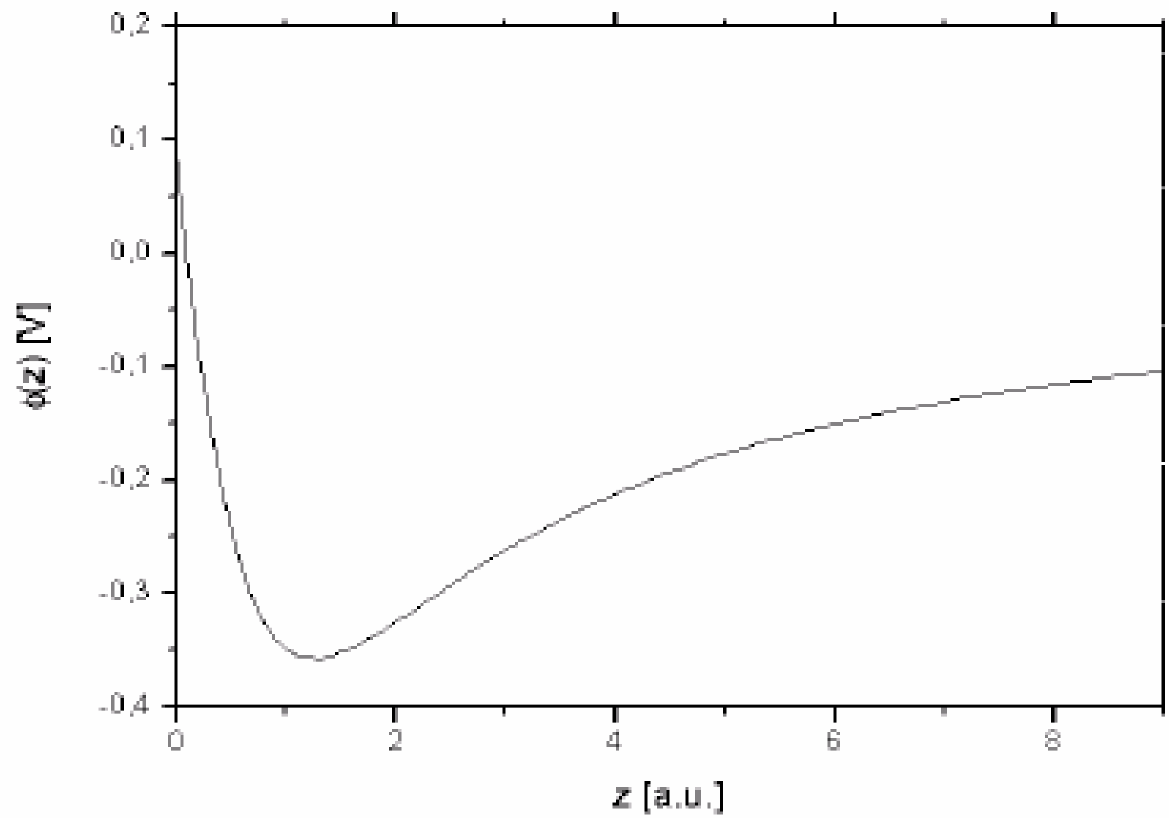

# Trap potentials for a 3 ring configuration and various voltage settings

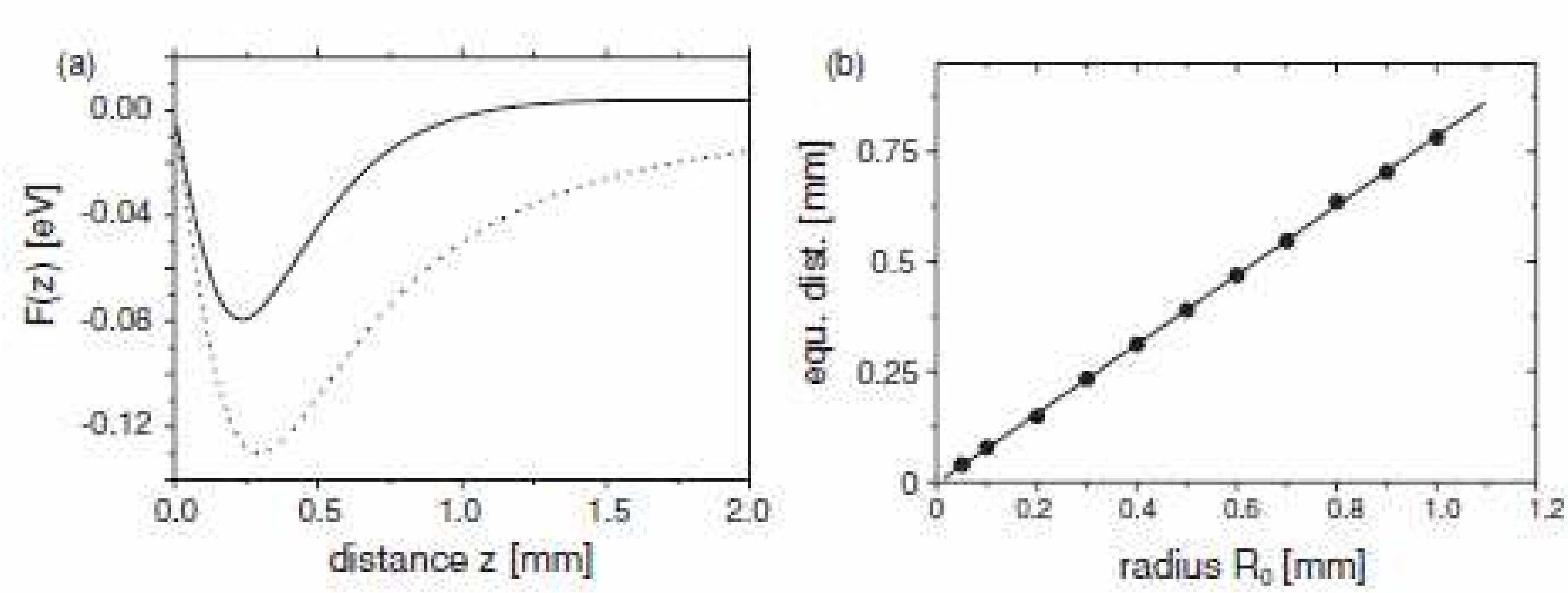


**Figure 3.** (a) Electric potential $\Phi^{el}(z)$ for a trap with $R_0 = 300\ \mu$m, $R_1 = 600\ \mu$m, $R_2 = 900\ \mu$m and $U_0 = 0$ V, $U_1 = +0.5$ V, $U_2 = 0$ V leading to a potential with a minimum near $z = 296\ \mu$m and an axial frequency of $\omega_z/(2\pi) = 89.9$ MHz (dashed). Anharmonicities are minimized by changing the compensation voltage to $U_2 = -0.417$ V. The minimum is shifted to a distance of $234\ \mu$m for the axial frequency of 99.0 MHz (solid line). (b) Location of the equilibrium position above the surface for the case of a compensated potential. Th distance scales linearly as $0.78\ R_0$.

# Prototype planar trap (Univ. Mainz)

# „Stylos Trap“

Maiwald et al., Nature Physics online (2009)

b

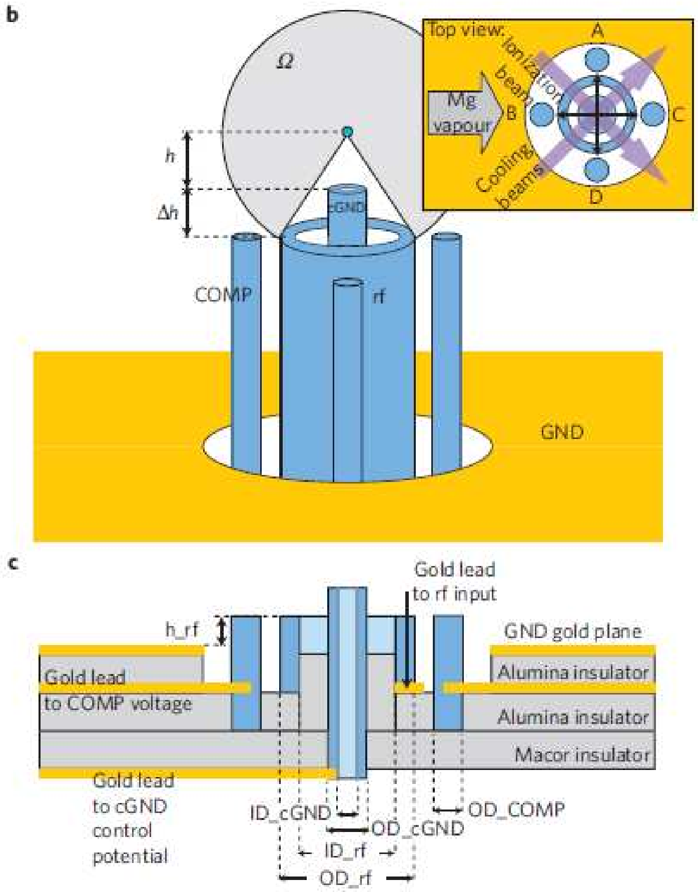


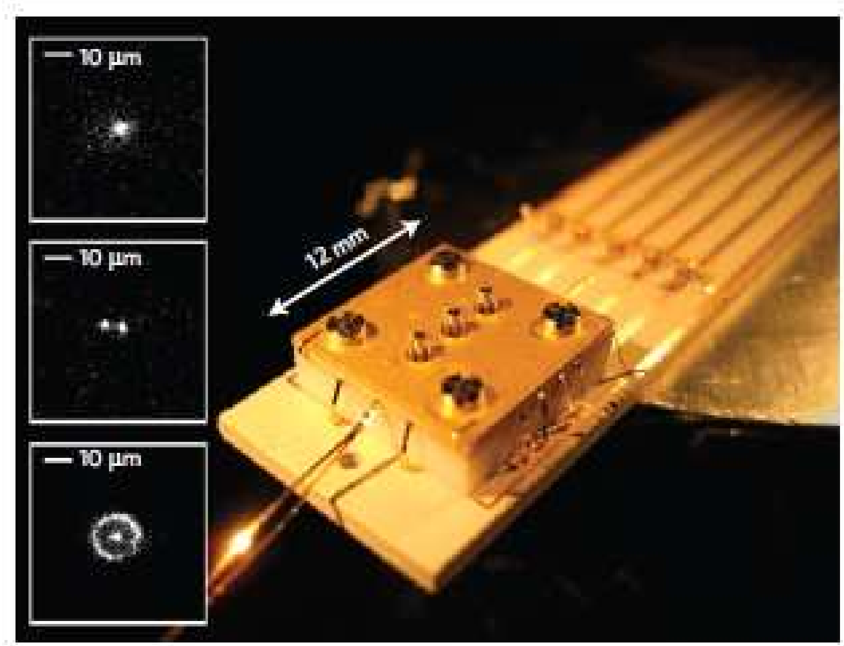

# Pixel trap (Univ. Ulm/Mainz)

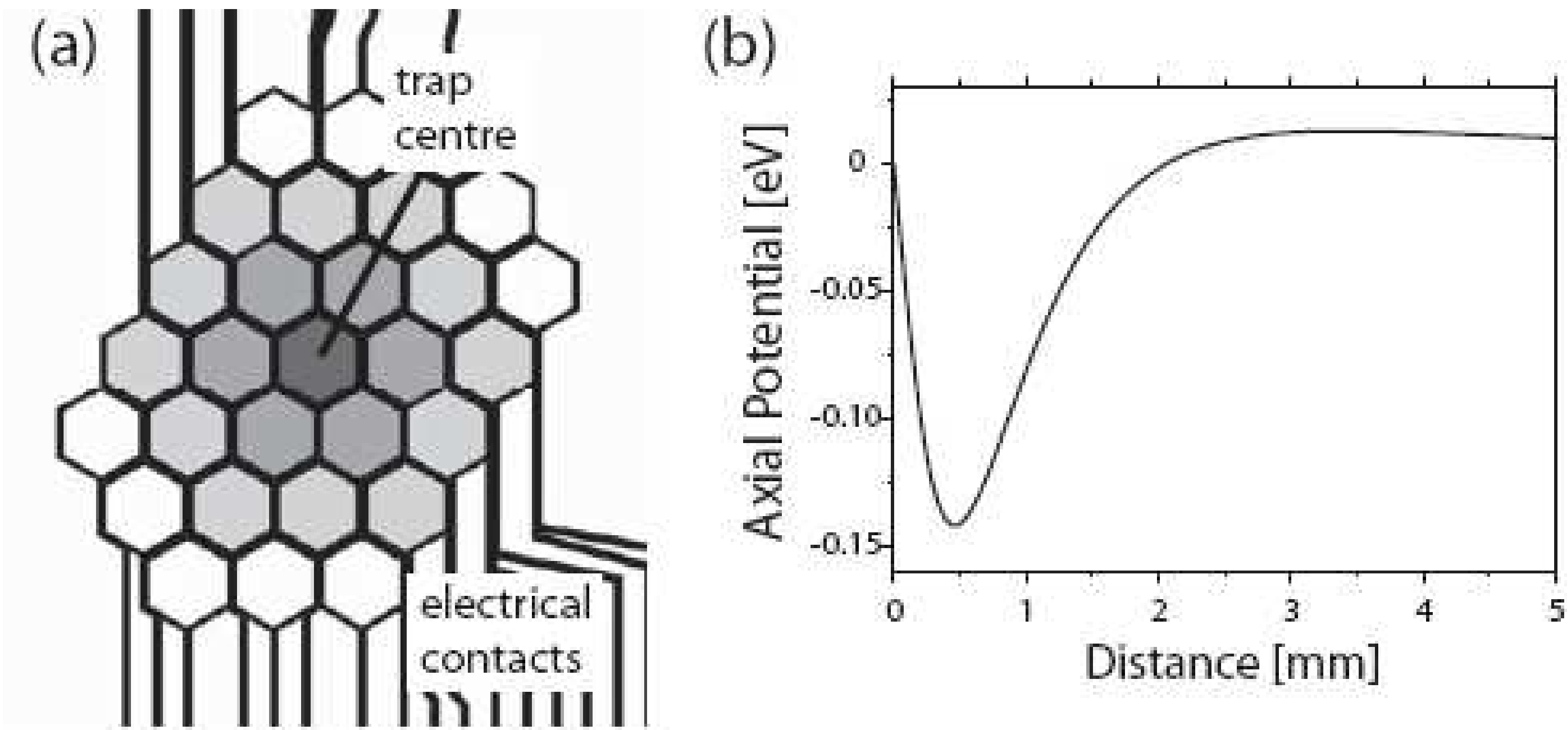

# Pixel trap

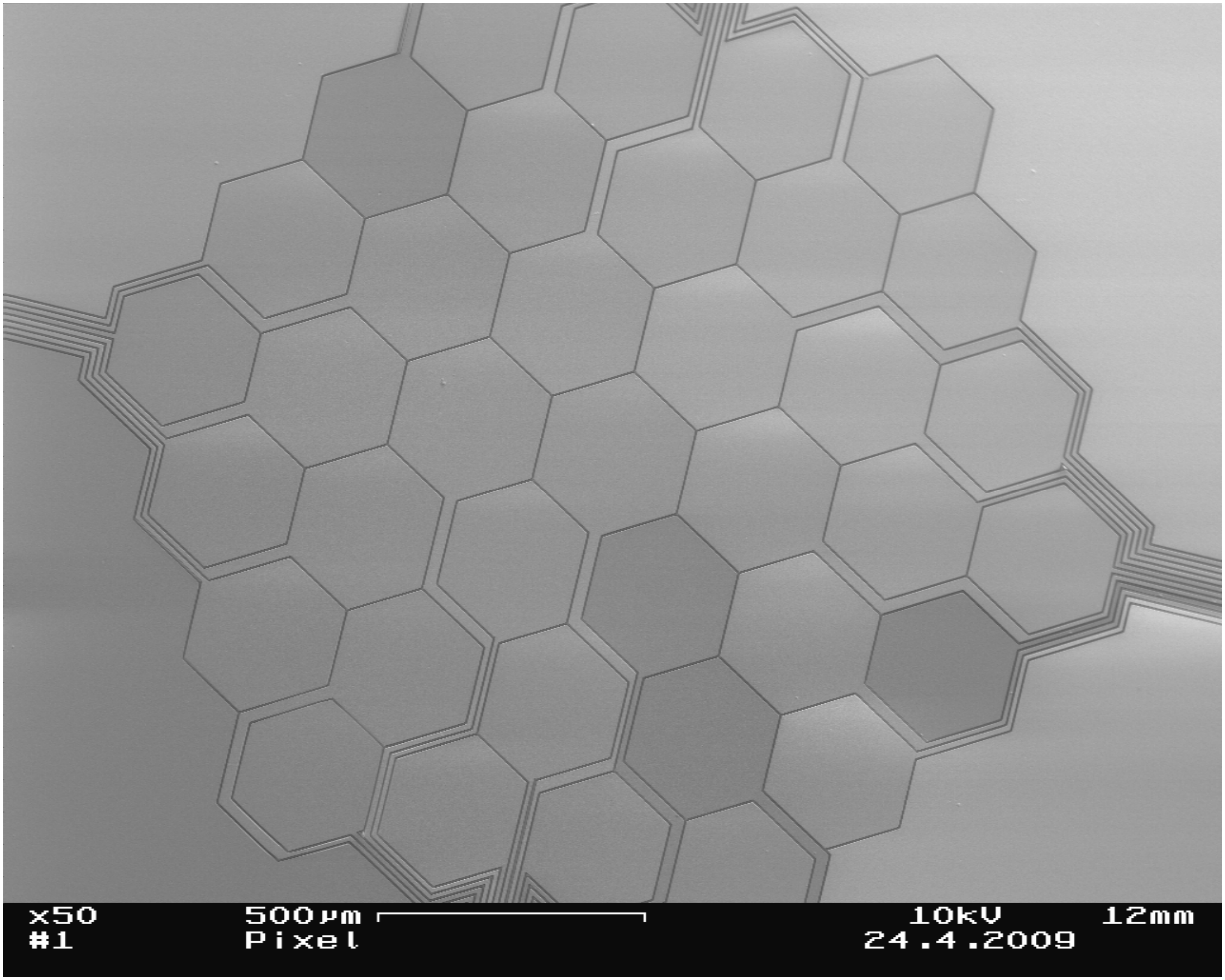

# Onion trap (Univ. Ulm/Mainz)

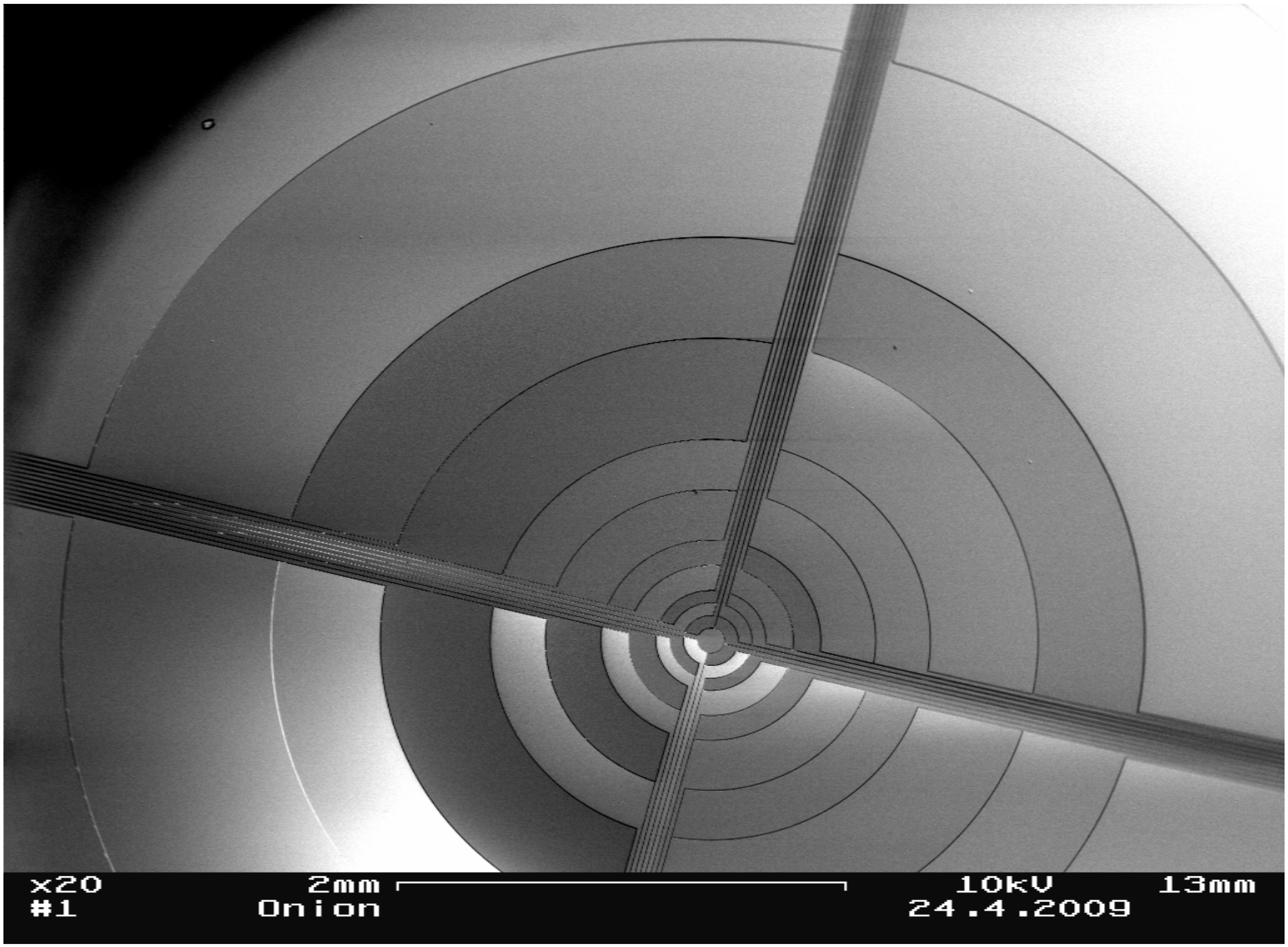

# Multiple single particle traps on chip

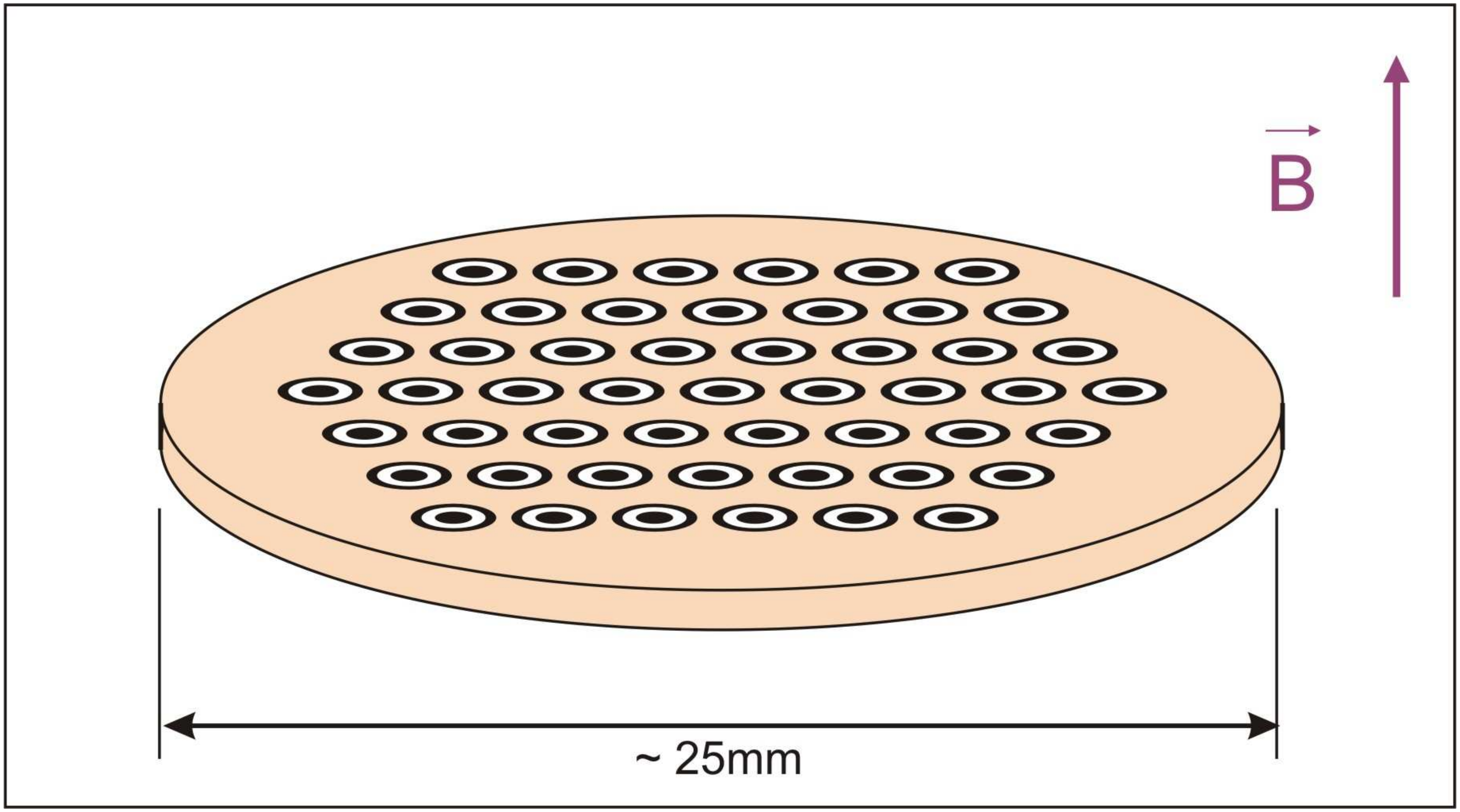

# Coupling of traps by induced image currents and superconducting wires

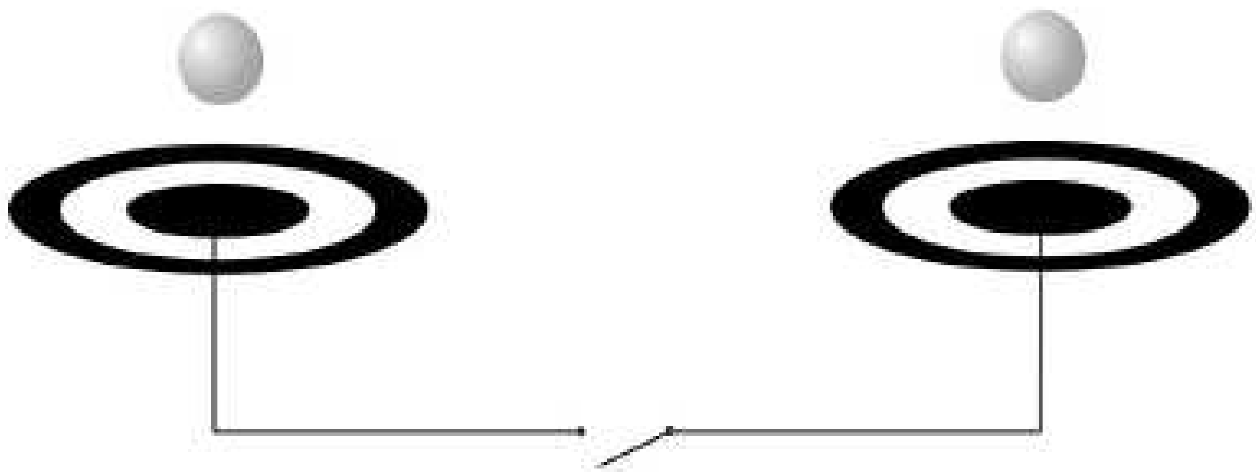

# Summary of Penning trap properties

- Storage time nearly infinit
- Non-destructive single ion detection
- Space charge limit in ion clouds ~ $10^6/cm^3$
- Instability by background gas collisions
- Ion centering by mode coupling
- Instability by trap imperfections
- Non-neutral plasma effects